AFRL-AFOSR-UK-TR-2012-0026

Effect of chromate and chromate-free organic coatings on corrosion fatigue of an aluminum alloy

Dr. Vasyl Pokhmurskii

Karpenko Physico-Mechanical Institute
National Ukrainian Academy of Sciences
5, Naukova Str.
Lviv, Ukraine 79601

EOARD STCU 06-8007

Report Date: February 2012

Final Report from 01 February 2009 to 31 January 2012

Air Force Research Laboratory
Air Force Office of Scientific Research
European Office of Aerospace Research and Development
Unit 4515 Box 14, APO AE 09421

REPORT DOCUMENTATION PAGE

Form Approved OMB No. 0704-0188

1. REPORT DATE *(DD-MM-YYYY)*	2. REPORT TYPE	3. DATES COVERED *(From – To)*
20 February 2012	Final Report	1 February 2009 – 31 January 2012

4. TITLE AND SUBTITLE

Effect of chromate and chromate-free organic coatings on corrosion fatigue of an aluminum alloy

5a. CONTRACT NUMBER

STCU Project P-340

5b. GRANT NUMBER

STCU 06-8007

5c. PROGRAM ELEMENT NUMBER

6. AUTHOR(S)

Dr. Vasyl Pokhmurskii

5d. PROJECT NUMBER

5d. TASK NUMBER

5e. WORK UNIT NUMBER

7. PERFORMING ORGANIZATION NAME(S) AND ADDRESS(ES)

Karpenko Physico-Mechanical Institute
National Ukrainian Academy of Sciences
5, Naukova Str.
Lviv, Ukraine 79601

8. PERFORMING ORGANIZATION REPORT NUMBER

N/A

9. SPONSORING/MONITORING AGENCY NAME(S) AND ADDRESS(ES)

EOARD
Unit 4515 BOX 14
APO AE 09421

10. SPONSOR/MONITOR'S ACRONYM(S)

AFRL/AFOSR/RSW (EOARD)

11. SPONSOR/MONITOR'S REPORT NUMBER(S)

AFRL-AFOSR-UK-TR-2012-0026

12. DISTRIBUTION/AVAILABILITY STATEMENT

Approved for public release; distribution is unlimited.

13. SUPPLEMENTARY NOTES

14. ABSTRACT

Effect of chromate and chromate-free and their compositions on the protective properties of organic coatings on cyclically stressed aluminum alloys was studied. Strontium chromate pigment, zinc phosphate pigment, calcium ion exchange silica pigment, natural bentonite, natural zeolite and Ca-ion exchanged and Zn-ion exchanged zeolites were studied as aluminum alloy corrosion inhibitors in organic coatings. Experimental methods included electrochemical impedance spectroscopy method (EIS), DC polarization, optical microscopy and scanning electron microscopy (SEM) with EDX analysis, corrosion fatigue and tribocorrosion tests.

15. SUBJECT TERMS

EOARD, aluminum alloys, corrosion, corrosion fatigue, corrosion inhibitors, organic coatings

16. SECURITY CLASSIFICATION OF:			17. LIMITATION OF ABSTRACT	18, NUMBER OF PAGES	19a. NAME OF RESPONSIBLE PERSON
a. REPORT	b. ABSTRACT	c. THIS PAGE			RANDALL POLLAK, Lt Col, USAF
UNCLAS	UNCLAS	UNCLAS	SAR	96	19b. TELEPHONE NUMBER *(Include area code)* +44 (0)1895 616 115

Effect of chromate and chromate-free organic coatings on corrosion fatigue of an aluminum alloy

Project manager: ***Vasyl Pokhmurskii***
Ph.D. & Sc.D., professor, head of department
Phone: *(+380 32) 263 15 77, Fax: (+380 32) 263 15 77,*
E-mail : pokhmurs@ipm.lviv.ua; zin@ipm.lviv.ua
Institution: Karpenko Physico-Mechanical Institute
of National Ukrainian Academy of Sciences
Financing party: United States of America
Project duration: 3 years.
Project technical area: Materials Science

Final report

Reported period: February 2009 – January 2012

Table of Content

SUMMARY

Effect of chromate and chromate-free and their compositions on the protective properties of organic coatings on cyclically stressed aluminum alloys was studied. Strontium chromate pigment, zinc phosphate pigment, calcium ion exchange silica pigment, natural bentonite, natural zeolite and Ca-ion exchanged and Zn-ion exchanged zeolites were studied as aluminium alloy corrosion inhibitors in organic coatings. It was used electrochemical impedance spectroscopy method (EIS), DC polarization, optical microscopy and scanning electron microscopy (SEM) with EDX analysis, corrosion fatigue and tribocorrosion tests.

Addition of strontium chromate to acid rain solution increases resistance of aluminum alloy D16T to corrosion fatigue destruction. Fatigue limit of the alloy in inhibited by chromate corrosion environment reaches nearly about 160 MPa after $5.5 \cdot 10^6$ cycles.

Chromate decreases probability of pits initiation, however it accelerates cathodic reaction on mechanically activated surface of aluminum alloy. Chromate layer on aluminum alloy is less strong and less wear resistant than aluminum oxide and zinc phosphate films. Zinc phosphate in contrast to strontium chromate decreases tribocorrosion aluminum alloy in acid rain in 1.5-2 times.

Corrosion current and charge transfer resistance decrease in one-two orders of magnitude for aluminum alloy in acid rain solution with addition of inhibiting composition on basis zinc phosphate and zeolite. The composition significantly inhibits aluminum alloy corrosion under fatigue loading.

The synergism of protective action of the couple "phosphate/ion exchange pigment" is possibly caused by the ion exchange pigment collecting of some undesirable ions from the corrosion solution and releasing of calcium ions, which can than react with phosphate ions.

Investigations of alloy AA7075 corrosion in acid rain solution, inhibited by chromate-free blends of zinc phosphate with bentonite, zeolite and calcium containing pigment have revealed significant increase of an inhibiting effect at combined use of phosphate and other pigments, able to Ca-ion exchange with solution components. Single use of zinc phosphate and these ion exchanged pigments for corrosion inhibition do not provide desired effect.

Charge transfer resistance of aluminum alloy D16T with artificially damaged polyurethane coating inhibited by zinc phosphate/zeolite pigments blend is close to the resistance of aluminum alloy samples with chromate containing polyurethane coatings. This testifies about significant anticorrosion effect from addition of the phosphate/zeolite pigment composition to polyurethane coating and confirms the possibility of chromate substitution in the primer paint layer.

Corrosion fatigue and impedance study of samples of aluminum alloy with polyurethane coatings has showed that the presence of chromate inhibitor slows down degradation of polyurethane coating under cyclic loading in acid rain solution and increases its protective properties. Impedance module of inhibited coating over the entire range of frequencies was greater by 5-8 times compared with uninhibited samples after 24 hours of cyclic load.

Polarization characteristics of the alloy D16T in acid rain solution with added natural zeolite and mixtures of zinc phosphate/calcium modified zeolite and zinc phosphate/zinc modified zeolites were studied. It was established that largest inhibiting effect has the pigment blend containing phosphate and Ca-ion exchanged zeolite.

It was established that addition of phosphate/Ca-zeolite pigment blend improves protective properties of polyurethane coatings at conditions of cyclic loading by inhibition of under paint corrosion of aluminum alloy.

Alloy samples with chromate containing polyurethane coatings had corrosion endurance under cyclic stress level of 150 MPa in about 7.5 times greater than unprotected samples. Polyurethane coating inhibited by phosphate/Ca-zeolite mixture increased endurance of the alloy for the stress level approximately in 7.0 times.

1. LITERATURE REVIEW

1.1. Introduction

Aluminum alloys are widely used as structural materials in the aerospace industry due to their low density, high strength and good corrosion resistance. Their resistance to corrosion is attributed to a stable oxide film that is rapidly formed in exposure to air. However, in the presence of aggressive anions, particularly halides, aluminum alloys are subject to localized corrosion [1, 2]. On high-strength aluminum alloys, corrosion tends to initiate at intermetallic phases, such as Al_2Cu, Al_7Cu_2Fe and Al_2CuMg that are present as strengthening components in the alloys. It is generally accepted that copper-rich precipitates act as preferential cathodes for the reduction of oxygen, relative to the matrix. The cathodic reaction at such sites generates OH^- ions, resulting in dissolution of the surrounding protective oxide layer [3, 4]. Enriched Cu sites drive corrosion at anodic sites, including anodic intermetallic sites, matrix sites, and crevices, which exist in airplanes at, for example, lap joints. The localized corrosion can be in the form of pitting, crevice, intergranular, exfoliation, or filiform corrosion. These forms of corrosion can initiate stress corrosion or corrosion fatigue cracks under service conditions. Clearly, corrosion-induced crack propagation in airplanes can cause irreplaceable human and very large financial losses.

1.2. General overview of corrosion mechanisms on aluminium alloys

Passivity of aluminum. From a purely thermodynamical point of view aluminum is active. However, in oxygen containing environment, aluminum is rapidly covered with a protective oxide layer [5]. The oxide layer is essentially inert, and prevents corrosion. The thickness of the layer may vary as a function of temperature, environment and alloy elements. Oxide films formed in air at room temperature are 2-3 nm thick on pure aluminum. Heating to 425°C may give films up to 20 nm [6]. If the oxide film is damaged, e.g. by a scratch, new oxide will immediately form on the bare metal [7]. In such way aluminum is given excellent corrosion protection.

Corrosion mechanisms.

a) Oxide destabilization.

The following factors may affect the stability of the aluminum oxide and thereby cause corrosion:

• The oxide is not stable in acidic (pH < 4) or alkaline (pH > 9) environments [5].

• Aggressive ions (chlorides, fluorides) may attack the oxide locally.

• Certain elements (Ga, Tl, In, Sn, Pb) may become incorporated in the oxide and destabilize it [8].

b) Micro galvanic coupling.

Most commercial alloys contain several types of intermetallic phases. Corrosion on aluminum alloys is essentially a micro galvanic process between these phases and the matrix alloy [8, 11]. While the phases often act as local cathodes because of their Cu or Fe content, the surrounding aluminum matrix undergoes localized attack (figure 1). In addition the following phenomena may become important:

• An active phase(s) may corrode preferentially.

• A corroding phase may serve as a sacrificial anode and provide cathodic protection to the surrounding material.

• Due to the electrochemical reactions at the corroding sites and the cathodes, the composition and pH of the electrolyte adjacent to the reaction sites may become different from the bulk electrolyte.

• Active components of the matrix alloy and the intermetallic phases may corrode selectively (dealloying), resulting in changed corrosion properties.

The cathode to anode area ratio is also important in case of the micro galvanic corrosion.

c) Pitting.

Pitting is a highly localized type of corrosion in the presence of aggressive chloride ions. Pits are initiated at weak sites in the oxide by chloride attack [8, 9, 11]. Pits propagate according to the reactions

$Al = Al^{3+} + 3e^-$ (1)

$Al^{3+} + 3H_2O = Al(OH)_3 + 3H^+$ (2)

while hydrogen evolution and oxygen reduction are the important reduction processes at the intermetallic cathodes, as sketched in figure 1:

$2H^+ + 2e^- = H_2$ (3)

$O_2 + 2H_2O + 4e^- = 4OH^-$ (4)

As a pit propagates, the environment inside the pit (anode) changes. According to reaction 2 the pH will decrease. To balance the positive charge produced by reaction 1 and 2, chloride ions will migrate into the pit. The resulting HCl formation inside the pit causes accelerated pit propagation.

propagation. The reduction reaction will cause local alkalinisation around cathodic particles. As previously mentioned aluminum oxide is not stable in such environment, and aluminum around the particles will dissolve (alkaline pits). The active aluminum component of the particles will also dissolve selectively, thereby enriching the particle surface with Cu and increasing its cathodic activity. Etching of the aluminum matrix around the particles may detach the particles from the surface, which may repassivate the alkaline pits. This may also reduce the driving force for the acidic pits causing repassivation of some in the long run.

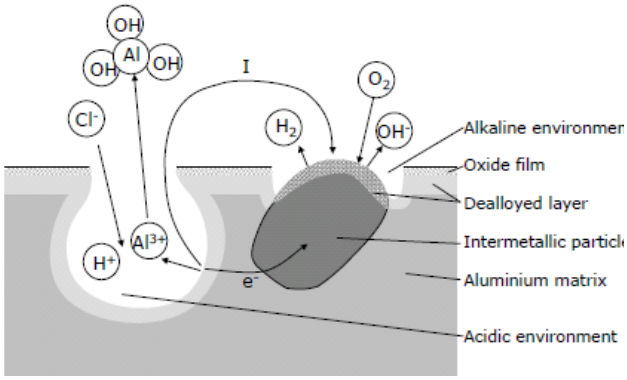

Figure 1. Generalized illustration of pitting corrosion of aluminum alloys [7].

d) Intergranular corrosion.

Intergranular corrosion (IGC) is the selective dissolution of the grain boundary zone, while the bulk grain is not attacked [10]. IGC is also caused by micro galvanic cell action at the grain boundaries. The susceptibility to IGC is known to depend on the alloy composition and thermo mechanical processing. Grain boundaries are sites for precipitation and segregation of intermetallic particles, which makes them physically and chemically different from the matrix. Precipitation of e.g. noble particles at grain boundaries depletes the adjacent zone of these elements, and the depleted zone becomes electrochemically active. The opposite case is also possible; precipitation of active particles at grain boundaries would make the adjacent zone noble. These two cases are illustrated in figure 2 [11].

Intermetallic compound CuA_2 is deposited on matrix grain boundaries of duralumin alloy during its ageing. As a result of copper diffusion from the matrix grain into $CuAl_2$-phase, neighboring parts of matrix became copper depleted. These parts mostly contain aluminum. Pure Pure aluminum can be an anode both for grain body and the intermetallide. It was supposed that duralumin locally corrodes due to the aluminum dissolution. However, there are questions. It is not so clear concerning duralumin corrosion. Golubev writes [12], that $CuAl_2$ phase serve as

complex cathode, which consists simultaneously cathodic and anodic parts. Cathodic parts of the intermetallic only to some extent work for matrix aluminum, mainly they interact with the aluminum, located right in the intermetallic, because of distance between cathodes and anodes in the intermetallide is much less. Al from the intermetallic will dissolve in a greater degree than contacting aluminum. Finally Golubev concluded: 1) intergranular corrosion of duralumin is not caused by dissolution of aluminum near intermetallic, but mainly by dissolution of aluminum from intermetallic itself; 2) intermetallides, like $CuAl_2$, $CuMg_2$, Al_3Mg_4 and others, behave in solutions as complex phases and are destroyed due to transfer into solution of the component which has more electronegative potential [12].

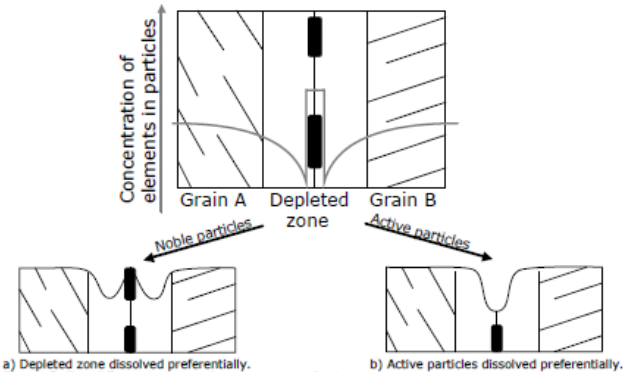

Figure 2. Two different intergranular corrosion mechanism

1.3. Corrosion fatigue of aluminum alloys

Aluminum alloys can be under risk of corrosion fatigue, especially in chloride solutions. Availability on alloy surface corrosion damages decreases its fatigue durability.

Corrosion pitting has a strong effect on fatigue life of structural Al alloys [13, 14]. Under the interaction of cyclic load and the corrosive environment, cyclic loading facilitates the pitting process, and corrosion pits, acting as geometrical discontinuities, lead to crack initiation and propagation and then final failure. The presence of localized corrosion pits modifies the local stress and may ultimately shorten fatigue life and lower the threshold stress for crack initiation and propagation.

The effect of pre-existing corrosion pits, produced by prior immersion in 3.5 wt% NaCI solution for various durations, on fatigue behavior of aluminum alloys in very long life range and in the near threshold regime was investigated by using piezoelectric accelerated fatigue test at 19.5 kHz [13].

It was established, that fatigue properties are significantly affected by the pre-existing corrosion pits, specially, crack initiation in the very long life range. Extensively developed corrosion pitting due to longer exposures accelerates crack initiation in the very long life range. The experiment results shows that fatigue crack growth (FCG) rates of small cracks in the aluminum alloy are greater than those of large cracks at almost the same stress intensity factor range, ΔK [13].

In the work [14] corrosion fatigue of aluminum coated alloy (Alcald 2024-T3) was studied. Authors suggest that corrosion fatigue in Alclad 2024-T3 involves two competing crack nucleation mechanisms ─ hydrogen effects in the cladding and pitting at constituent particles in the core alloy. In a given situation, the mechanism which dominates depends on environment (particularly pH) and (weakly) on specimen orientation. Cracks do not necessarily nucleate at the largest corrosion pit, suggesting that the main effect of a pit is not to raise the local stress. Rather, a high local hydrogen concentration associated with accelerated corrosion at a pit causes cracking in a nearby favorably oriented grain. Propagation rates of short cracks were slightly higher in acidic environments and in specimens with painted surfaces, but were unaffected by material orientation and surface roughness. Some results of the work [14] are summarized below.

Crack nucleation.

More crack nucleation sites were produced in pH 2 and pH 10 solutions of 0.5 M NaCl than in the pH 6 environment. This trend could be a result of the low solubility of corrosion products in pH 6 solutions, which enables an effective protective layer to form that retards the corrosion process.

Crack nucleation in the Alclad layer was observed to have a weak dependence on material orientation; the horizontal orientation had a lower crack nucleation rate. There were no indications of microstructure directionality, but traces of a rolling pattern on the surface of the sheet were visible. This pattern might be responsible for the orientation dependence.

Crack nucleation was greater on surfaces of higher roughness. Possibly, high surface roughness accelerates crack nucleation by promoting hydrogen ingress, which in turn enhances cracking susceptibility.

Crack nucleation in bare material without cladding or painting was slower than crack nucleation in cladded material. The mechanisms of crack nucleation were substantially different in these two cases: in bare material, cracks nucleated at constituent particles, whereas in clad material, cracks usually nucleated at or near crystallographic pit colonies. Low pH tended to promote crack nucleation at constituent particles in clad material.

Crack propagation.

The low pH environment produced a slightly higher crack growth rate than did the pH 6 or pH 10 environments. Similar observations by other investigators indicate enhanced cathodic reactions in acidic solutions as the cause of faster crack growth rate.

Specimen orientation and surface roughness had no effect on crack propagation rate. The crack propagation rate was slightly higher in skin material in the as received condition (i.e., with painted surfaces). This could be due to the tendency of the paint to limit fluid flow from the mouth of a crack and to develop an occluded (i.e., acidic) environment within.

The corrosion-fatigue experiments on Alclad 2024-T3 skin material suggest two competing mechanisms for crack nucleation: crack nucleation in the clad due to hydrogen effects and crack nucleation in the core material as a result of pitting at constituent particles. In the clad material, hydrogen has been shown by several investigators to enhance cracking by enhancing localized plasticity. Pitting at constituent particles is believed to form local stress risers that lead to crack formation [14].

Hydrogen can has significant influence on aluminum alloy cyclic life in a corrosion environment. For B95T1 and D16T Russian commercial alloys, the hydrogenation of the vicinity of the tip of corrosion crack, as well as the hydrogen-induced transgranular chippings on the fracture surfaces, is experimentally revealed. It was found that hydrogen can play both a negative role through weakening the intergranular bonds and a positive role, promoting the change from intergranular to transgranular type of fracture [15].

Vasil'ev et al [16] have found that character of changing of aluminum alloy D16AT corrosion stability depends not only on the number of loading cycles but also on the load. They explained the changes in the corrosion stability of aluminum alloys by the after decomposition of solid solution, formation of metastable phases, and segregation of Cu, Fe, Ca, and S [16].

High-strength, precipitation-hardened aluminum alloys, such as 7075, are used extensively in primary wing and fuselage structures in many Navy and commercial aircraft. These commercial-grade alloys contain numerous constituent particles of various sizes, which may have have electrochemical potentials different from those of the surrounding matrices. Because of the Navy's special service environments, these aircraft are subjected to prolonged periods of salt water spray and/or salt fog. In the presence of salt water, electrochemical reactions are possible and corrosion pits are readily formed at or around the constituent particles in 2000- and 7000-series aluminum alloys. Many such corrosion pits were observed in wing teardown analyses of Navy aircraft. These corrosion pits, once formed, act as stress concentration sites and can

facilitate crack initiation under both cyclic and sustained loading. However, only limited studies of the effects of pre-existing pits on fatigue crack initiation in aluminum alloys have been performed. Additionally, many of these studies used smooth specimen geometry and results could not be easily translated to more complex aircraft structural configurations, such as rivet holes. In the investigation of Pao et al [17], the influence of pre-existing corrosion pits, produced by prior immersion in 3.5 wt% NaCl solution, on fatigue crack initiation in 7075-T7351 aluminum alloy was studied using blunt-notch wedge-opening-load (WOL) type fracture mechanics specimens. It was established [17]:

1. The presence of pre-existing corrosion pits, produced by immersion in 3.5 wt% NaCl solution for 336 hrs, in 7075-T7351 aluminum alloy shortens the fatigue crack initiation life in air by a factor of two to three and decreases the fatigue crack initiation threshold, $(\Delta K/\sqrt{\rho})_{th}$, by about 50 percent.
2. Fatigue cracks in polished blunt-notched specimens often initiated from large constituent particles located on the notch root surface. For specimens that contained pre-existing corrosion pits, fatigue cracks always initiated from these corrosion pits.

Corrosion pits were identified as crack origins in all corroded 2024-T3 aluminum alloy specimens used in the study of Jones and Hoeppner [18]. Multiple fatigue cracks originating at different pits often contributed to final specimen fracture. Large pit surface areas contributed to crack formation in a low number of cycles. Fractographic analysis frequently indicated that cracks originated from deeper pits than those measured from the surface before fatigue experimentation occurred, indicative of sub-surface pit growth. The combined effects of pit depth, pit surface area, and proximity to other pits were found to substantially reduce fatigue life [18].

In order to understand the mechanism of corrosion and corrosion fatigue of aluminum copper alloys, the morphological changes of a 2024-T3 aluminum alloy have been studied in different concentration of hydrochloric acid by in situ atomic force microscopy [19]. This aluminum copper alloy has been found to be susceptible to intergranular corrosion in hydrochloric acid solutions. Severe intergranular damage is a result of a difference between the dissolution rates of copper depleted regions in the vicinity of second phase precipitates along grain boundaries and grain bodies.

The mechanism of corrosion fatigue of this alloy during cyclic fatigue in distilled water and 0.1 M HCl has also been investigated during free corrosion and under cathodic polarization. Both

Both anodic dissolution and hydrogen embrittlement mechanisms appear to cooperate and result in a significant reduction of the observed cycle life as compared to that observed in air. Intergranular cracking is observed in early stages of crack nucleation and propagation, and transgranular fracture in the later stages.

In order to investigate the role of hydrogen during fatigue of the 2024-T3 aluminum alloy in hydrochloric acid media, fatigue cycling has been performed in 0.1 M HCl solutions containing either a hydrogen combination poisoning agent, arsenic, or a copper complexing agent, ammonium chloride [19]. Shortening of cycle life in these solutions as compared to that observed in 0.1 M HCl with no additives clearly shows that the 2024-T3 aluminum alloy is susceptible to hydrogen embrittlement and that the most important factor controlling the hydrogen uptake by this alloy is the presence of metallic copper in a surface layer formed during the corrosion experiments.

Metallic copper acts as a preferential site for proton reduction during corrosion fatigue; however, due to very low hydrogen diffusivity in copper, hydrogen ions reduced at these sites do not contribute to hydrogen embrittlement. When copper is complexed by solution ions and is not present in its metallic form at the surface film, e.g., in a solution containing arsenic or ammonium ions, the hydrogen uptake is enhanced and significant reduction of cyclic life is observed. The significant role of re-deposited metallic copper in this alloy and its role in hydrogen embrittlement/fatigue is emphasized by a series of investigations performed on pre-corroded specimens from which the copper-containing film, formed during pre-exposure, either remained on or was removed from the sample surface prior to the corrosion fatigue experiments [19].

Metal corrosion potential changes during corrosion fatigue destruction under stress influence [20, 21, 22]. For instance, a potential of aluminum alloy D16 in 3% NaCl decreases proportionally to deformation level [20, 21]. However, mechanical factor is not so important in more aggressive environment, where surface films are less protective. During the same tests in H_2SO_4 acid solution the potential shift was only 6-7 mV.

Corrosion potential variation of metal under cyclic loading can be caused by [21, 23] : 1) change of metal physical state, owing to decrease of work of metal ion output in solution, 2) micro ruptures in surface films, 3) environment component adsorption and decrease of metal surface strength.

Apart of this, Gerasymov has found that open circuit potential can be decreased up to 0.1 V on aluminum alloys in the area of plastic deformation [24].

Generally, main effect of cyclic loading consists in an increase of local corrosion at places of protective film destructions and stress concentrators [21], that can makes a significant contribution for decrease of corrosion-fatigue durability of metals.

Al alloy endurance greatly depends from solutions composition (kind of anions and their concentration), depolarizer concentration, value of pH, and also from concentration of corrosion inhibitors. Factors, which increase corrosion rate, as usually decrease metal resistance to corrosion fatigue. Ions Cl^- i SO_4^{2-} are most danderous relatively to corrosion fatigue, which can be explained by their strong depassivation ability. The dependence of corrosion and electrochemical behavior, and also corrosion fatigue of aluminum alloys A1 - Cu - Mg, A1 - Cu - Mg - Si and A1 - Zn - Mg from chloride ions concentration and solution pH has been shown in works [20, 25-28]. The alloys A1 - Zn - Mg and A1 - Cu - Mg have maximal resistance to corrosion fatigue in electrolyte with pH = 8-10, and commercial alloy B95 – in pH interval 4-10. Corrosion fatigue life of the alloys decreases after pH leaving the interval.

1.4. Prevention of aluminum alloy corrosion with inhibited organic coatings

Traditional anti-corrosion strategies for aluminum alloys involve, firstly: an initial alloy surface treatment (for instance formation of conversion chromate or phosphate coatings) aimed at 'strengthening' the air-formed film; and, secondly: the use of a high-performance protective organic coating (paint). Organic coatings form an important part of the whole anti-corrosion system for aluminum alloys. The main anti-corrosive function of the organic paint layer is generally contained within the base primer coating and is formulated to prevent or control the various failure modes of paints: e.g. cathodic disbonding, blistering and especially filiform corrosion. All successful coating formulations for aerospace alloys rely on hexavalent chromium to provide corrosion inhibition. Modern coatings use the sparingly soluble species, strontium chromate, from which chromate is slowly leached, accumulating at local areas of high moisture content, such as paint defects or at delaminated areas at the coating-substrate interface [29, 30], where it can act as a classical corrosion inhibitor. However, chromates are carcinogenic, expensive to handle, and create disposal problem. The use of chromates might soon be tightly restricted by environmental regulation. Some environment-friendly replacements for the chromates have been developed, but none currently pass the qualifying tests for aerospace alloy corrosion.

There are several reasons why chromate is an extremely effective corrosion inhibitor for Al alloys [31]:

1. Chromate can be stored in conversion coatings and as a pigment in paints.
2. Chromate is released from these coatings, particularly when they are scratched to refresh the coating area. The released chromate is in equilibrium with the chromate in the coatings, and higher pH favors CrVI release.
3. Chromate is mobile in solution and migrates to exposed areas on the Al alloy surface.
4. Chromate adsorbs on the active sites of the surface and is reduced to form a monolayer of a CrIII species.
5. This layer is effective at reducing the activity of both cathodic sites (Cu-rich intermetalic particles) and anodic sites in the matrix or at S phase particles. The anodic inhibition is related to the initiation stage of localized corrosion and not propagation.
6. The combined properties of storage, release, migration, and irreversible reduction provided by chromate coatings underlie their outstanding corrosion protection.

Chromate is able to act simultaneously as both an anodic and a cathodic inhibitor. Also, it has activity at high concentrations and at ppm levels. It is reasonable to expect that replication of the protective characteristics of chromate using other inhibitor is necessary to successfully replace chromate. In particular, inhibition of the oxygen reduction reaction at intermetallic particle sites that are cathodic to the aluminum matrix is an important part of the overall corrosion inhibition mechanism. A possible replacement for the strontium chromate is also keenly sought for the organic coating (paint) primer. Some approaches consist in incorporation of of inorganic inhibitors including cerium(IV), molybdenum (VI), manganese (VII), silicate, molybdate, phosphate, [32] ion exchange pigments [33-36].

Inhibitor characteristics of different compounds as possible replacements for chromate pigments in aerospace paints were investigated in the work [32]. These compounds were tested and screened in solution and not as actual paint additives. In initial testing, aluminum alloy 2024-2024-T3 samples were exposed to 0.6 M sodium chloride (pH adjusted to 7, T = 23°C) with 3.4 mM of the candidate compound dissolved in solution. Corrosion inhibition characteristics were assessed via electrochemical impedance spectroscopy (EIS) performed over 10 days, and the statistical analysis of pit depths was analyzed at the conclusion of each exposure. Promising candidates then were exposed to more extreme environments to simulate possible service-life conditions. These environments included unbuffered 0.6 M NaCl initially adjusted to pH 3, T = 23°C and pH 10, T =23°C. Several candidate inhibitors appeared promising: barium metaborate,

cerium chloride, cerium oxalate, lanthanum chloride, and sodium metavanadate. Under the conditions of these tests, sodium metavanadate consistently displayed the best performance. EIS data indicated the corrosion performance of sodium metavanadate was within an order of magnitude of sodium chromate (Na_2CrO_4), while pit depth values for metavanadate were comparable to those observed for Na_2CrO_4.

It was also underlined in the paper of Cook and Taylor [32], that the effectiveness of an inhibitive pigment is, at a minimum, a balance between the solubility of the compound within the binder and the inhibitor efficiency. A highly soluble pigment, even though efficient from the standpoint of preventing corrosion, will not be a good additive to an organic coating.

Kendig et al [37] established that barium metaborate has a potential inhibiting power that exceeds that for the hexavalent chromium-containing inhibitor zinc chromate for the bulk 2024-T3 alloy in deaerated 0.01 *M* NaCl. The metaborate releases levels of ionic species comparable to the zinc chromate. Hence, even on a per mole basis, the corrosion inhibition by species produced by the solid barium metaborate remains substantially greater than the chromates in the deaerated, dilute chloride (0.01 M) environment. This may not be the case for aerated dilute chloride environments. However, this result remains significant for solid inhibitors used in paints and sealants where they must act in relatively oxygen-depleated conditions (under coatings and in crevices for example). Barium metaborate inhibits the corrosion of phase CuAl2 intermetallic in aerated 0.01 *M* NaCl. Species released from barium metaborate appear to slow the anodic dissolution of this intermetallic phase as do the species released from zinc chromate. There appears to be a fundamental interaction of the barium metaborate with the Cu-rich intermetallics which determine the corrosion rate of the alloy. This work [37] indicates that barium metaborate is a good substitute for hexavalent chromium compounds when properly formulated into paints and sealants.

Phosphate pigments can be used as a non-toxic alternative to chromate pigments. They have been shown to provide corrosion inhibiting properties when incorporated into a primer coatings and paints for iron and steel [38-40].

Regarding the mechanism of inhibition zinc phosphate containing primer it has been suggested that it slowly phosphates the metal surface thus rendering it passive [40]; that tribasic zinc phosphate may be converted into a more soluble form by reaction with atmospheric acids or by ion exchange with carboxyl groups present in the polymer [41].

Highly insoluble pigments such as zinc phosphate rely on hydrolysis or reaction with acid contaminants to release the anticorrosive species. This process is essentially fortuitous and likely

to be slow, although hydroxide from the cathodic corrosion reaction may aid hydrolysis [42].

R.Romagnoli and V.F.Vetere concluded [43], that the presence of phosphate anion induces the formation of a compact oxide layer and the thickness of the layer is depended on the solubility of the phosphate, but the corrosion rate is relatively high for steel in zinc phosphate suspensions (not for steel with organic coatings pigmented by zinc phosphate). The pigment performs well in industrial environments - because the solubility of phosphates increases as pH decreases in such environments [43].

J.A.Burkill and J.E.O.Mayne have found by using immersion tests of mild steel specimens in distilled and sea water that the zinc phosphate extracts had no inhibitive properties [44]. It was concluded that the solubility of zinc phosphate in pH range 6.6-8.0 was too low for it to have inhibitive properties. It was established that in phosphoric, sulfuric and sulfurous acids solutions with pH 3.7-3.8 zinc phosphate was much more soluble. It was concluded that tribasic zinc phosphate has a very low solubility in water, but that it readily dissolves in acids, being more soluble in sulfuric and sulfurous acids than phosphoric acid. In industrial and urban areas, where the pH of the rain may be in the region of 4, it is suggested that the tribasic phosphate may be converted into the more soluble monohydrogen phosphate.

The possible mechanism for inhibition by zinc phosphate is proposed by H.F.Clay and J.H.Cox [45]. There is a greater tendency for steel to polarize both anodically and cathodically in extracts from zinc phosphate than in extracts from blanc fixe, and it is assumed that zinc phosphate is sufficiently soluble to cause polarization effects. It could be that, under a paint film, the active anodic areas are small and the current concentrated, so that the observed anodic polarization effect becomes of practical importance [45].

Zinc phosphate pigment show itself to be a “non-toxic” alternative to chromates. According to the experimental results obtained, the anticorrosive properties of coatings with zinc phosphate are not only equal, but on numerous occasions exceed the protection provided by the conventional anticorrosive pigments of red lead and zinc chromate [46]. A.Amirudin and others established [46], although the solubility of zinc chromate and zinc phosphate pigments in 0.5M NaCl solution increased on both sides of the neutral range, it was far more pronounced in the acidic range. However, this increased solubility did not result in an increased efficiency of either pigment. In contrast to the chromate, excess acids do not seem to affect so much the inhibition efficiency of the phosphate as the latter does seem to passivate steel in addition to functioning as a cathodic inhibitor. The passivating action of phosphate is superior to that of chromate even in alkaline media. They concluded that, the major limitation of zinc phosphate as an inhibitive

pigment is its poor solubility [46].

L.Fedrizzi and others [47] studied epoxy type primer containing strontium chromate and strontium phosphate as pigments. The characterization of the complete system (pretreatment and primer) in the sodium sulfate solution clearly showed the different water uptake behavior of the two different primers, which highlights the better barrier properties of the one containing phosphate. However the corrosion protection of the chromates containing primer is also due to the inhibitive action of the chromates. Hence a such type of primer better withstands the presence of defects in the coating.

Current strategies generally focus on identifying a single chemical species that provides the chromate performance required. However, it seems now unlikely that this will be successful and anti-corrosion synergies with several compatible inhibitors may be required. Also it would be interesting to create an protective system where inhibitor release could be caused or accelerated by corrosion event.

Recently an attempt was made to find effective synergistic combination of chromate-free pigments for AA2024 alloy corrosion inhibition. It was found that the combination of zinc phosphate/molybdate and calcium ion exchange silica pigment (Shieldex) has significant anticorrosion effect for aluminum alloy AA2024-T3 in an artificial acid rain [48]. Solution analysis indicates that the species present in the extract are dominated by phosphate, zinc and calcium ions. The charge transfer resistance of the alloy in artificial acid rain solution saturated with the mixed pigment extracts has the same values as in strontium chromate pigment extract. Thus, the inhibitive efficiency in this condition appears to be equivalent to chromate. Mechanistically, this is a mixed inhibitive effect, due to deposition of protective films on aluminum (anode) and on the intermetallic 2^{nd} phases (cathode). Analytical microscopy established that the use of the pigment blend extract leads to the development on the aluminum alloy surface of a macroscopic, but relatively thin, film containing aluminum, copper, calcium, zinc, phosphorus, silicon and oxygen atoms. An XPS study has showed that at open circuit potential conditions the surface film is a mixed calcium/zinc phosphate with admixture of hydroxides. Mainly zinc phosphate and zinc hydroxide with admixtures of calcium phosphate are present on cathodically polarized surface of the alloy. At anodic potentials, it likely contains zinc and aluminum phosphates.

1.5. Control of aluminum alloy corrosion fatigue with inhibitors in organic coatings

During service, airplane constructions protected by organic coatings are subjected to the influence of ultra-violet radiation, wind, temperature cycles, humidity cycles, acidic atmospheric precipitation etc. The predominance of research is related to study of an influence of their impact on the service-life of organic coatings. However, another extremely relevant parameter that could also influence the protective properties of the coating is that of mechanical stress. These stresses could arise as residual stresses from the production process (e.g., welding, punching, flexion, mechanical operation, and torsion), or could be a result of operational conditions (e.g., static and dynamic loading). It is logical to assume that mechanical stress decreases the service-life of an organic coating. The effect of the stress on coating is strengthened by an influence of a corrosion environment.

From other side, an effective protective coating could be able to extend service life of cyclically loaded in corrosion environment aluminum alloy constructions. However the influence of inhibiting chromate and chromate-free pigments and whole organic coating on Al alloys protection from environmental assisted cracking is not studied enough.

Mainly the influence of different polymer coatings on the corrosion endurance limit of steels has been examined in a number of studies [49-51]. It can be generally concluded that the presence of a coating has essentially no effect on the endurance limit of steel substrates in air, but but the coating can significantly increase service life of steel under fatigue conditions in a corrosive environment. It has been observed that a combination of corrosion protection strategies, strategies, e.g., coating and another corrosion mitigating method (e.g., inhibitors), were needed for the optimal improvement in corrosion fatigue-life of these substrate materials.

Preliminary corrosion fatigue tests revealed [52], that time to crack initiation in mild steel samples increases and rate of crack propagation decreases in inhibiting pigment extracts. This effect is more marked on early stage of crack propagation. At K_I values less than 30…35 $MPa \cdot m^{1/2}$ effectiveness of slowing down of crack propagation is substantial in corrosion solutions inhibited with chromate and zinc phosphate/ion exchange pigment blend. Inhibiting additives can to change electrochemical conditions and intensity of electrochemical processes at crack tip and to influence metal dissolution rate, hydrogen evolving and its adsorption on metal. Electrochemical activity of loaded metal surface increases as result of local galvanic elements development. In inhibiting pigment-containing environment cathodic and anodic reactions of micro galvanic couples are slowed down as a result of passivation of metal surface (chromate solution) or protective phosphate film deposition (chromate-free solution). Thus, in both cases local anodic dissolution of metal decreases significantly and time to crack initiation increases.

Hopefully similar pigment combinations could have positive effect in corrosion inhibition of mechanically loaded aluminum alloys.

In the book of Davis [53] is described, that paint coating (chromate etch primer pus two-component aluminum pigmented epoxy topcoat) increases corrosion fatigue life of aluminum alloys (6061-T6 and 5083-H31) and the highest corrosion fatigue life is achieved by application of the inhibited paint coating after shot peening pretreatment. However the results are not full and further work is necessary.

In US patent N 4,327,152 [54] it is claimed a protective coating to retard crack growth in aluminum alloy. The coating consists an epoxy polyamide primer with inhibitor on basis of reaction product of hexafluoroisopropanol and ceclohexylamine and a low-permeability organic film topcoat. Epoxy polyamide composition can be used for primer, and polyurethane for topcoat. In this case mechanism of protection under cyclic loading of the aluminum alloy in a corrosion environment is not understood well. It is not clear whether corrosion inhibition or isolation from solution prevails.

Wim J. van Ooij et al [55] have made an attempt to use of organofunctional silanes to protect aluminum or other metals against corrosion fatigue cracking. It was developed a novel water-based organic coating that is chromate-free and obliterates the need for a conversion coating pretreatment. This coating is called super primer [56]. In this paper it was reported the first super primer performance against corrosion fatigue cracking under a commercial polyurethane topcoat. As a control, they used samples of chromated AA2024-T3 and AA7075-T6 samples which were coated with a commercial chromate-containing primer and topcoated with a military polyurethane topcoat, DESOTHANE HS.

The estimated fatigue life of the alloys AA2024-T3 and AA7075-T6 alloys was found to be 65.44 x 10^3 cycles and 25.11 x 10^3 cycles, respectively. The chromated samples gave a fatigue life of 65.16 x 10^3 cycles for the AA2024-T3 alloy and 23.15 x 10^3 cycles for the AA7075-T6 alloy. The AA2024-T3 and AA7075-T6 alloy coated with a superpimer followed by a polyurethane topcoat gave a corrosion fatigue life of 35.53 x 10^3cycles and 21.77 x 10^3 cycles, respectively. The control specimens, i.e., the commercially available system gave a corrosion fatigue life if 46.92 x 10^3 cycles and 24.43 x 10^3 cycles for the AA2024-T3 and AA7075-T6 alloys, respectively. Thus, the super primer-based system resulted in a decrease of 11.39 x 10^3 cycles and 2.66 x 10^3 cycles for the AA2024-T3 and AA7075-T6 alloy, respectively, when compared with the commercial system. This decrease can be attributed to the poor topcoat adhesion to the super primer [55]. This problem of topcoat adhesion deficiency has been sorted out by varying the curing procedure of the super primer.

Further tests will be conducted for investigating the performance of the new modified super primer.

The fatigue crack growth rates of 7075-T76 aluminum alloy were measured in 3.5%NaCl solution with the presence and absence of corrosion inhibiting pigments, including chromate, phosphate, and a kind of nontoxic compound pigment, which was composed of phosphate, molybdate, citrate, and thiazole/imidazole derivatives (MBTZ). Microscopic features of fracture morphology were analyzed with scanning electron microscopy. In order to study the inhibition of these pigments, electrochemical polarization curves were measured in 3.5%NaCl (pH 6.2 and 3) solution with and without these pigments. The results showed that these pigments slowed down the fatigue crack growth rate of aluminum alloy mainly at the early propagation stage, and the retardation was related closely to the inhibition mechanism of the pigments, respectively. Thus it was concluded:

1. The studied pigments could retard crack growth of high strength aluminum alloy at the early propagation stage.

2. The nontoxic compound pigment, phosphate/ molybdate/citrate/MBZT, made crack growth rate to remain at a low level at low K values leading to an increase in life, and would be a promising substitute for hazardous chromate to inhibit CF of aluminum alloy [57, 58].

Molybdate MoO_2^{-4} effectively inhibits environmentally assisted fatigue crack (EFCP) propagation in 7075-T651 alloy during loading in chloride solution. It decreases negative influence of hydrogen environment following film rupture. MoO_2^{-4} enhanced aluminum passivity reduces hydrogen production and uptake at the crack tip. Inhibition is governed by the balance between crack tip strain rate and repassivation kinetics which establish the stability of the passive film. The inhibition is promoted by a reducing of loading frequency and stress intensity range, increasing crack tip MoO_2^{-4} concentration, and is more strong at potentials from anodic to free corrosion. The inhibiting effect of MoO_4^{2-} parallels that of CrO_4^{2-}, but molybdate effectiveness is shifted to a lower frequency regime suggesting the $Al_xMo_yO_z$ passive film is less stable against crack tip deformation. For high R loading at sufficiently low frequencies MoO_4^{2-} fully inhibits EFCP, quantified by reduced crack growth rate to that typical of ultra-high vacuum, reduction in crack surface facets typical of hydrogen embrittlement, and crack arrest. Chromate did not produce such complete inhibition. Methods exist to incorporate molybdate or Mo in self-healing coating systems, but the complex effects of mechanical and electrochemical variables must be understood for reliable-quantitative fatigue performance enhancement [59].

In the work [60] it has been demonstrated that the addition of 10,000ppm of CeCl3 to the medium inhibits the stress corrosion cracking of 8090 alloy by precipitation of cerium oxides/

hydroxides. The deposition of these compounds on the alloy surface decreases the pit density and and slows the crack growth through the grain boundaries by hindering the anodic dissolution of T T phases.

1.6. Conclusions

○ Aluminum alloys are inclined to local corrosion, which can occur accordingly to different mechanisms (oxide destabilization, microgalvanic coupling, pitting, intergranular corrosion). However, main driving force of such corrosion destruction of aluminum alloys is electrochemical interaction of aluminum matrix and intermetallic inclusions.

○ Local corrosion of aluminum alloys decreases their fatigue life and it can cause substantial economical and human losses. The alloys durability can be reduced by prior corrosion during storage of vehicles, machines, equipment and materials or can be decreased directly during exploitation by combined action of an environment and fatigue loading.

○ The durability decrease of aluminum alloys is observed both on stages of crack initiation and crack propagation.

○ A wide variety of chromate-free inhibitors and inhibiting pigments, which are proposed or already used for steel and aluminum alloys protection, exists. The inhibitors have protective properties both at usual corrosion and under corrosion fatigue. But they are less effective then chromate compounds. Compositions of chromate-free inhibiting pigments can be prospective candidates for chromate replacement.

○ In general, not much data present in literature about effectiveness and mechanism of protection of aluminum alloys by uninhibited and inhibited organic coatings from corrosion fatigue. Many papers and reports refer to corrosion protection of steel. However the possibility of improvement of corrosion fatigue life of aluminum alloys by use of organic barrier coatings and inhibited coatings, which contains anticorrosion pigments, also exists. From this point of view a composition on basis phosphate and ion exchange pigments is perspective for use.

The aim of the study was investigation of influence of epoxy and epoxychromate coatings on corrosion endurance of aluminum alloy D16T in artificial acid rain solution. It was interesting to reveal protection mechanism and corrosion inhibition properties of chromate containing organic coating on cyclically loaded aluminum alloy in order to obtaine input data for further search of chromate replacements.

2. EXPERIMENTAL PART

2.1. Materials and samples

D16T aluminum alloy (analogue of AA2024) was used as base material for samples of corrosion and corrosion fatigue tests (Table 2.1) [61].

Table 2.1

Composition of D16T alloy

Alloy	Element content, mass. % *					
	Cu	Mg	Mn	Fe	Si	Zn

Д16Т	3,8-4,9	1,2-1,8	0,3-0,9	<0,5	<0,5	<0,3

*Note: Al makes up a balance.

Alloy plates with a thickness of 5 mm and rods with 16 mm diameter in a state of supply were used for experiments. If necessary, the aluminum clad layer from specimens was removed by grinding machine.

Specimens for fatigue testing were made at Karpenko institute machine shop. It was prepared two kinds of specimens: flat and round (fig. 2.1,2.2, 2.3, 2.4).

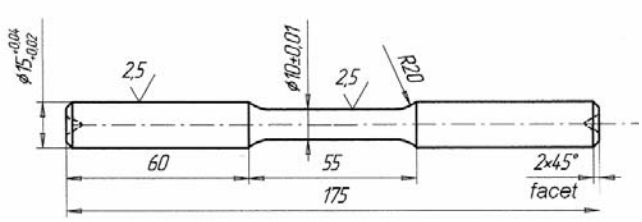

Fig. 2.1. Design drawing of round specimens for corrosion fatigue tests.

Fig. 2.2. Photo of round fatigue specimen

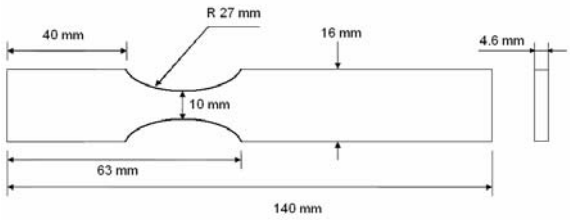

Fig. 2.3. Design drawing of flat specimen for corrosion fatigue tests.

Fig. 2.4. Photo of flat specimens for corrosion fatigue tests.

Additionally, inhibition of AA7075 aluminum alloy corrosion was studied in pigment blend extracts (filtrates) in acid rain solution. The pigment blends included 0.66 g/l phosphate pigment Actirox 106 plus 0.34 g/l bentonite or 0.34 g/l Ca-ion exchange pigment Shieldex CP-4

4 7394 or 0.34 g/l zeolite. Alloy plates with a thickness of 2 mm in a state of supply were used for experiments.

Aluminum 99.8% Al (AA1080A) and specially synthesized intermetallic compound Al_2Cu were studied as well. The intermetallic compound Al_2Cu was synthesized by alloying of initial components Al and Cu at their stoichiometric ratio in an electro-arc furnace with a tungsten electrode (cathode) on a copper water-cooled base (anode) in a pure argon atmosphere under a pressure of 105 MPa.

2.2. Corrosion solution

Synthetic acid rain was used as corrosion solution (table 2.2).

Table 2.2. Composition of acid rain solution [67].

Artificial acid rain	Chemical species	Concentration, $mg \cdot dm^{-3}$
(pH was adjusted to 4.5 with Na_2CO_3)	H_2SO_4 (98%)	3.185
	$(NH_4)_2SO_4$	4.620
	Na_2SO_4	3.195
	HNO_3 (70%)	1.575
	$NaNO_3$	2.125
	NaCl	8.483

2.3. Inhibitive pigments

Strontium chromate pigment (A Johnson Matthey Company, England), modified zinc phosphate pigment (Actirox 106, Nubiola Inorganic Pigments), calcium ion exchange silica pigment (Shieldex CP-4 7394, Grace Davison), bentonite (Sphere 7 Trade Company, Ukraine), natural zeolite (Sokyrnyanske deposit, Ukraine) and Ca-ion exchanged and Zn-ion exchanged zeolites were studied as aluminum alloy corrosion inhibitors in polyurethane coatings.

2.4. Epoxy coatings composition

Two component epoxy composition was choosed as base for organic coating on aluminum alloy D16T. The composition included epoxy resin ED-20, polyethylene polyamine hardener (PEPA), plasticizer and organic solvent. Epoxy coatings have been applied onto aluminum alloy specimens in two layer, primer and top. Two primer compositions were studied: first without an

inhibitor and second containing 3 mass % of strontium chromate. Mildly alkaline degreasing composition Alficlean 158/3 from Alufinish-Ukraine Ltd was used for aluminum alloy surface degreasing. Directly before before painting surface of samples was treated by Vienna lime. The epoxy coating thickness was 150…200 μm. The working area of epoxy coated sample was 8 cm^2.

2.5. Polyurethane coatings composition

- Acryl/polyurethane basis - Temadur Clear from Tikkurila Coatings;
- Aliphatic isocyanate - Hardener 008 7590 from Tikkurila Coatings;
- Solvent 1048.
- Inhibiting pigment blend at 3 vol. %.

It has been studied inhibition effects of chromate-free pigment blends – zinc phosphate/Ca-ion exchanged silica, zinc phosphate/zeolite, zinc phosphate/Ca-ion exchanged zeolite and zinc phosphate/ Zn-ion exchanged zeolite. In order to reveal protective action the inhibitors, through defects have been made in polyurethane coatings.

Before painting, samples surface was treated by Vienna lime and special phosphate composition for obtaining conversion coating. Polyurethane coatings have been applied onto aluminum alloy specimens in two layer, primer and top. The two layer polyurethane coating thickness was 120…150 μm. The working area of coated round sample was 4 cm^2 and coated flat sample – 10 cm^2. Through defects, 1 cm long, have been made in polyurethane coatings on flat samples to reveal of inhibiting pigments effect. Photos of test samples with inhibited coatings are presented in Fig. 2.5.

2.6. Electrochemical impedance spectroscopy

The corrosion behavior of coated and bare aluminum alloys was investigated using electrochemical impedance spectroscopy (EIS). The measurements were carried out in a synthetic acid rain solution (table 2.2), using a three-electrode electrochemical cell with a platinum auxiliary electrode (AE) as a counter and saturated calomel (SCE) as reference electrode (RE). The EIS measurements were carried out close to the corrosion potential using an Gill AC Potentiostat/Frequency Response Analyzer in the 10000 to 0.01 Hz frequency range. The signal amplitude was 30 mV. The impedance spectra were interpreted with The EIS Spectrum Analyzer program (beta version) (http://www.abc.chemistry.bsu.by/vi/analyser) [83].

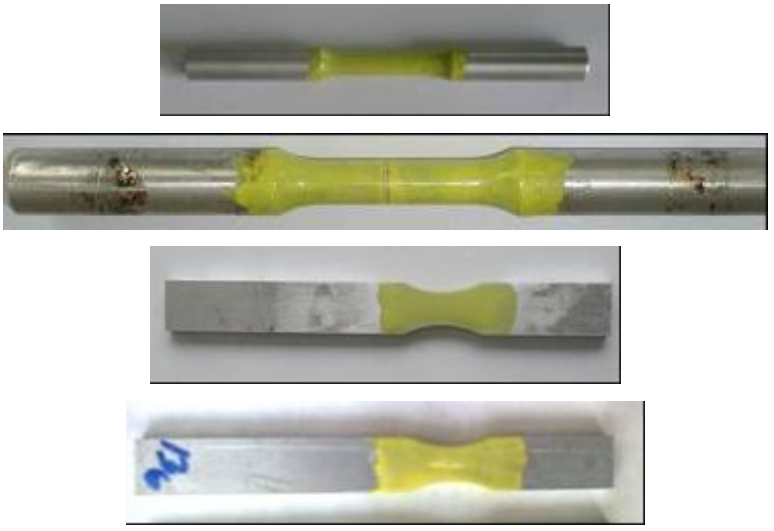

Fig. 2.5. Photos of round and flat test samples with inhibited coatings.

2.7. Surface study

Scanning electron microscopy EVO-40XVP (Carl Zeiss) with an INCA Energy 350 Microanalysis System (Oxford Instruments) was used for study of alloy surface after mechanical activation.

Surface of AA7075 alloy after exposure to corrosion solution with pigment blend filtrates was studied using Carl Zeiss Stemi 2000 Stereomicroscope.

2.8. DC polarization

DC polarization study of bare aluminum alloy samples in inhibited acid rain solutions were carried out using ACM potentiostat AUTOTAFEL, saturate silver chloride reference and platinum counter electrodes. Potential scanning rate was 1 mV/s. Corrosion currents of aluminum alloy in different inhibited solutions were obtained by graphical extrapolation of Tafel slopes of polarization curves. The working area of bare aluminum alloy samples for polarization experiments was 1 cm^2.

2.9. Corrosion fatigue tests

Aluminum alloy round samples with inhibited coatings were cyclically loaded with simultaneously corrosion solution spraying with use of a fatigue machine with general scheme presented on Fig. 2.6. Here a test specimen is deformed in pure bending mode at loading frequency 50 Hz.

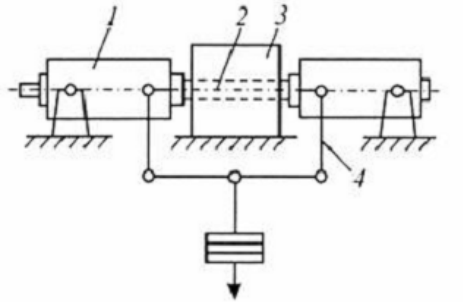

Fig. 2.6. General scheme of corrosion fatigue testing machine: 1 – drum; 2 – round specimen; 3 – spraying camera; 4 – loading device

A testing machine, which can provide cyclic deformation of flat sample in a special corrosion cell, was used in the experiment as well (Fig. 2.7). OCP potential and electrochemical impedance spectra of coated samples were obtained after certain number of loading cycles using potentiostat Gill AC, a SCE reference electrode and platinum counter (AE) electrodes connected to the cell. Cantilever bending of flat samples of aluminum alloy with frequency 10 Hz was used in this experiment (Fig. 2.8).

Fig. 2.7. Photos of machine for corrosion fatigue test by cantilever bending. The eccentric shaft can rotate at 10…50 Hz and imparts a vertical deflection to the higher end of the specimen via the pivot arm. The lower end of the specimen is pressed in the fixed clamp. The specimen is calibrated for each deflection by using an indicator. The eccentric shaft rotation speed can be modified by changing rotation speed of direct current electric motor. The working loading frequency was 10 Hz.

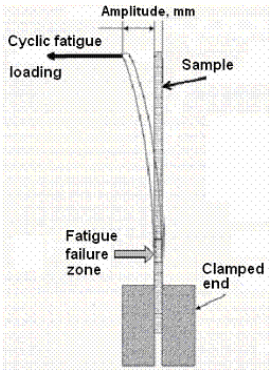

Fig. 2.8. Scheme of flat specimen cyclic loading.

2.10. Aluminum alloy corrosion study under surface activation

A special installation (fig. 2.9, 2.10) was used for study of aluminum alloy corrosion under surface mechanical activation. The installation works accordingly to the friction scheme "ball-plane" and consists frame 1 with bearings 4, which support straight movement of stage 2. The stage is put in motion by way of worm-gear from electric motor placed in the frame 1.

Sample 11 is fixed to frame together with corrosion cell 3. The cell is pressed with rubber seal to the sample and simultaneously strengthens the sample. Load of the sample is realized by weights 8, which are placed on top of indentor 9, adjusted by level 6 for providing of its perpendicularity with surface of sample 11. Samples of 50×40×5 mm size were prepared from aluminum alloy D16T. Tests were carried out in acid rain without and with addition of 1 g/l strontium chromate. Measurements of open circuit potential were carried out and polarization curves were recorded during mechanical activation of D16T alloy in corrosion solutions with use of potentiostat PI-50-1, silver chloride reference electrode and platinum counter electrode. At the same time friction torque was recorded. Constant of friction was estimated on basis friction torque value. All data were collected on PC connected to the potentiostat.

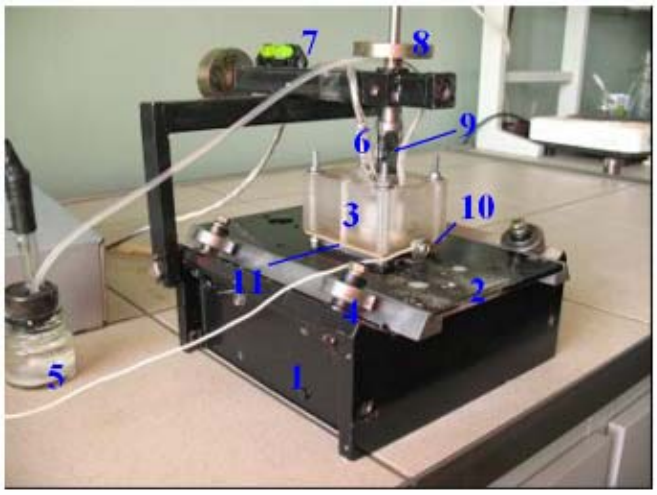

Fig. 2.9. Installation for electrochemical investigation of alloy samples during their surface activation in corrosion solution: 1– frame; 2 – stage; 3 – corrosion cell; 4 – bearing; 5 – silver-chloride reference electrode; 6 – platinum counter electrode; 7 – level; 8 – load; 9 – indentor; 10 – contact assembly; 11 – sample.

The roughness of surface of aluminum alloy samples after their corrosive wear was studied using a profilograph-profilometer "Kalibr C-265". The surface was washed by ethyl alcohol

before the measurement.

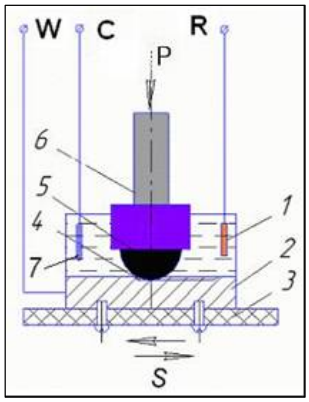

Fig. 2.10. The scheme of open circuit potential measurement during mechanical activation of D16T alloy surface: R – reference electrode, W – working electrode, P – loading, 1 – reference electrode tip; 2 – aluminum alloy sample; 3 – movable table; 4 – contact zone; 5 – counter body (corundum wheel ball, d=9 mm); 6 – indentor with strain sensors; 7 – platinum counter electrode

3. STUDY OF ALUMINUM ALLOY CORROSION FATIGUE

3.1. Corrosion fatigue of epoxy coated aluminum alloy in acid rain solution

Cyclic deformation of aluminum alloy in corrosion environment practically do not influence rate of its general electrochemical corrosion, and causes predominantly development of local corrosion, which depends from loading value, from time of deformed material exposition to corrosion environment and from peculiarities of the environment action on the material.

It was established (fig. 3.1), that fatigue limit (the stress below which a material can be stressed cyclically for an infinite number of times without failure) of round polished samples from alloy D16T in air is equal σ_{-1} = 175 MPa, while it decreases to σ_{-1c} = 125 MPa in acid rain solution at $5 \cdot 10^7$ cycles. Epoxy coating, due to surface shielding, causes an increase of corrosion fatigue limit of alloy D16T from 125 MPa to 155 MPa, which make up about 20%.

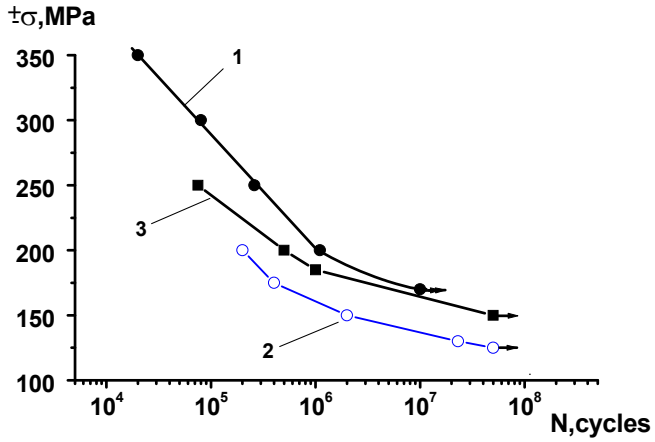

Fig. 3.1. Fatigue curves of alloy D16T samples:
1 – in air, 2 – in acid rain solution,
3 – epoxy coated in acid rain solution.

Time dependencies of open circuit potential (OCP) of aluminum alloy samples with epoxy coatings in unloaded state and under cyclic loading of 180 MPa in acid rain solution are shown on fig. 3.2. Corrosion potential of unloaded sample moves to more positive values and after 200..250 thousands cycles reaches the level of -380 mV, which are characteristic for bare alloy in acid rain solution. At the same time the potential of loaded sample goes to the same level already after about 9..12 thousand cycles of deformation. Such dependence of potential testifies about acceleration of electrolytic solution penetration through polymer layer to metal substrate under influence of cyclic deformation. Also a formation of microcracks in epoxy coating is possible. Despite of this, an availability of coatings on alloy surface ensures an increase its corrosion endurance (fig. 3.1).

Polarization dependencies (fig. 3.3, 3.4), obtained on aluminum alloy samples with epoxy coatings, testifies about significant influence of cyclic deformation on values of anodic and cathodic currents. The currents increase in about 10 times under loading. Thus cyclic loading facilitates both anodic and cathodic reactions on aluminum alloy. The anodic parts of polarization curves loaded sample of epoxy coated alloy looks interestingly (fig. 3.3, 3.4). It is possible that coated sample after some period of loading gives polarization response like bare aluminum alloy. There also we can see an anodic curve with some passivation plateau and after it a rapid rise of anodic current.

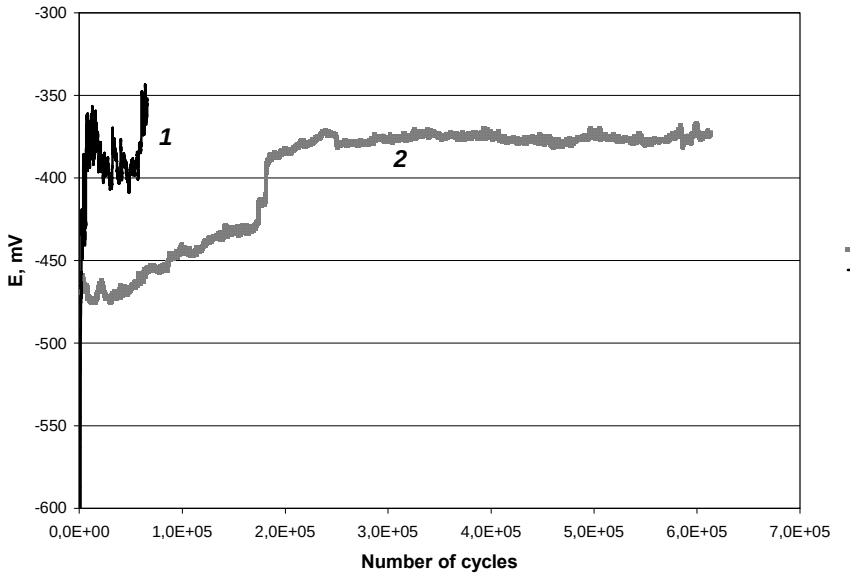

Fig. 3.2. Changes of OCP for epoxy coated sample of D16T aluminum alloy at $\pm\sigma = 180$ MPa (1) and without loading (2).

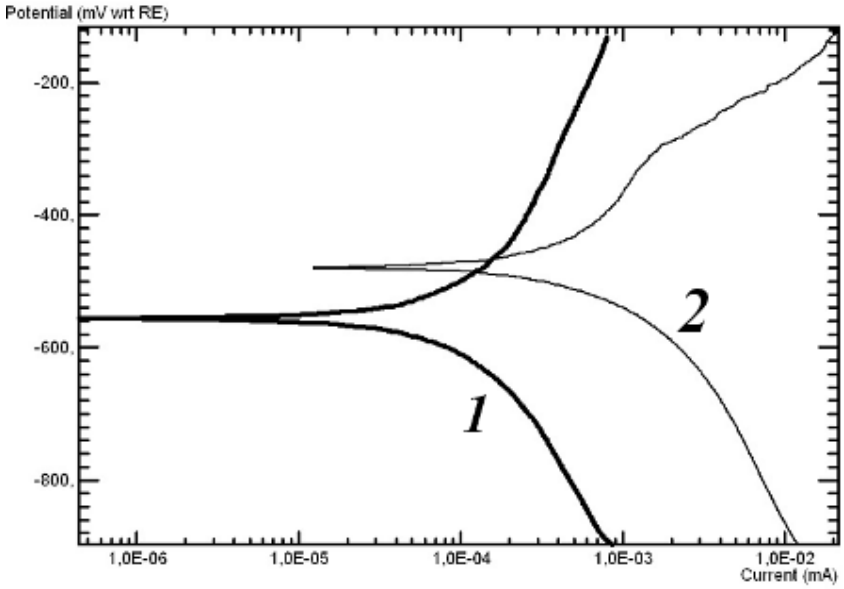

Fig. 3.3. Polarization dependencies of epoxy coated D16T alloy samples after 1728 thousands cycles in acid rain solution: 1- unloaded; 2 – $\pm\sigma = 180$ MPa.

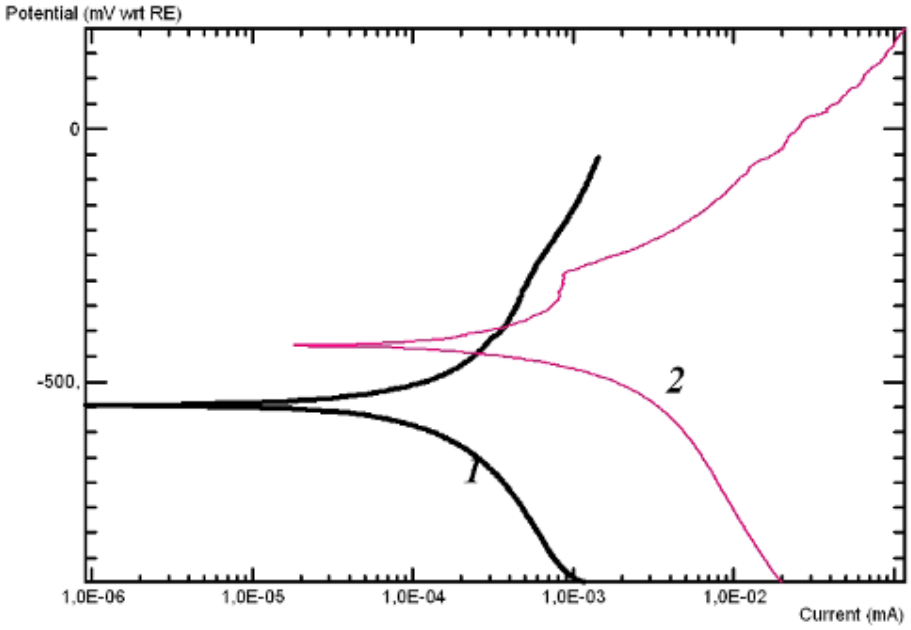

Fig. 3.4. Polarization dependencies of epoxy coated D16T alloy samples after 2592 thousands cycles in acid rain solution: 1- unloaded; 2 – $\pm\sigma = 180$ MPa.

Calculation of corrosion currents by method of extrapolation of Tafel slopes shows significant increase of substrate self-dissolution under epoxy coating in case of the sample cyclic loading at $\pm\sigma = 180$ MPa (fig. 3.5).

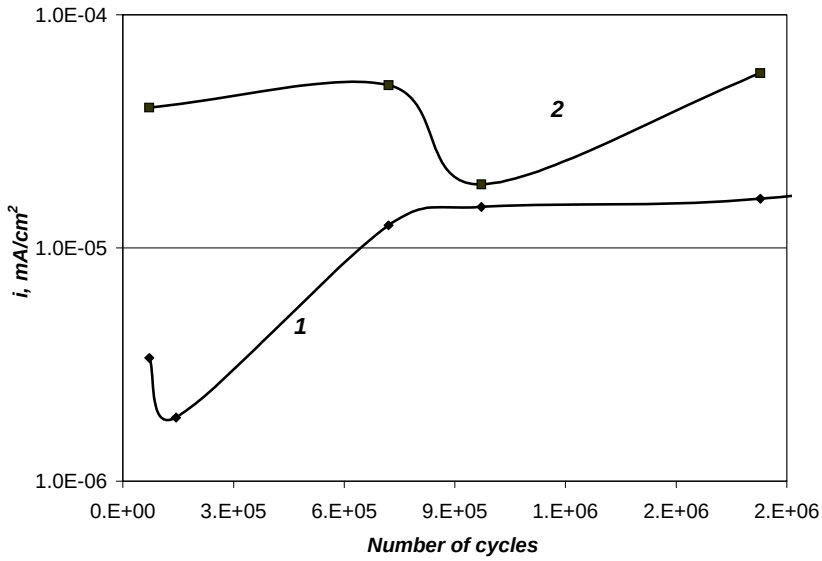

Fig. 3.5. Time dependence of corrosion current for epoxy coated D16T samples in acid rain solution: 1 – unloaded sample, 2 – $\pm\sigma = 180$ MPa.

Open circuit potential has been measured on D16 samples during cyclic deformation (fig. 3.6). The potential varies over the range of 350…400 mV. It seems that potential of epoxy coated aluminum alloy after short period loading is located in the same range as bare aluminum alloy. However, the corrosion endurance of epoxy coated sample is greater and makes up 4.8 million cycles at 180 MPa (fig. 3.6). The free corrosion potential changes rapidly in the period of metal cracking. Its value goes to about -700 mV. The effect is caused by crack developing in aluminum alloy sample, which is accompanied by formation of juvenile surfaces without oxide film.

Changes of polarization current on epoxy coated sample at OCP were studied by a method described in the work [66]. The method is that the potential of unloaded sample during corrosion fatigue tests in electrochemical cell is held at corrosion potential ($E_{pol}=E_{OCP}$). At that, current between sample and platinum counter electrode is equal zero. After next loading, potential of the sample moves to more negative values. On condition that $E_{pol}=E_{OCP}$ it causes anodic polarization of sample and appearance of polarization current (I_{pol}). In this situation changes of the current will be related mainly to its corrosion fatigue damaging. The study of polarization current revealed (fig. 3.7), that it rapidly rises during first 100 thousands cycles of loading and reaches the level of $2 \cdot 10^{-3}$ mA. Possibly an environment penetration through deformed epoxy coating to metallic substrate occurs during the period. Later, current increase becomes more slow and it can be interconnected with expansion of underfilm corrosion. The third period (fig. 3.7), where current increases rapidly, can be attributed to crack initiation and crack development in the epoxy coated aluminum alloy sample.

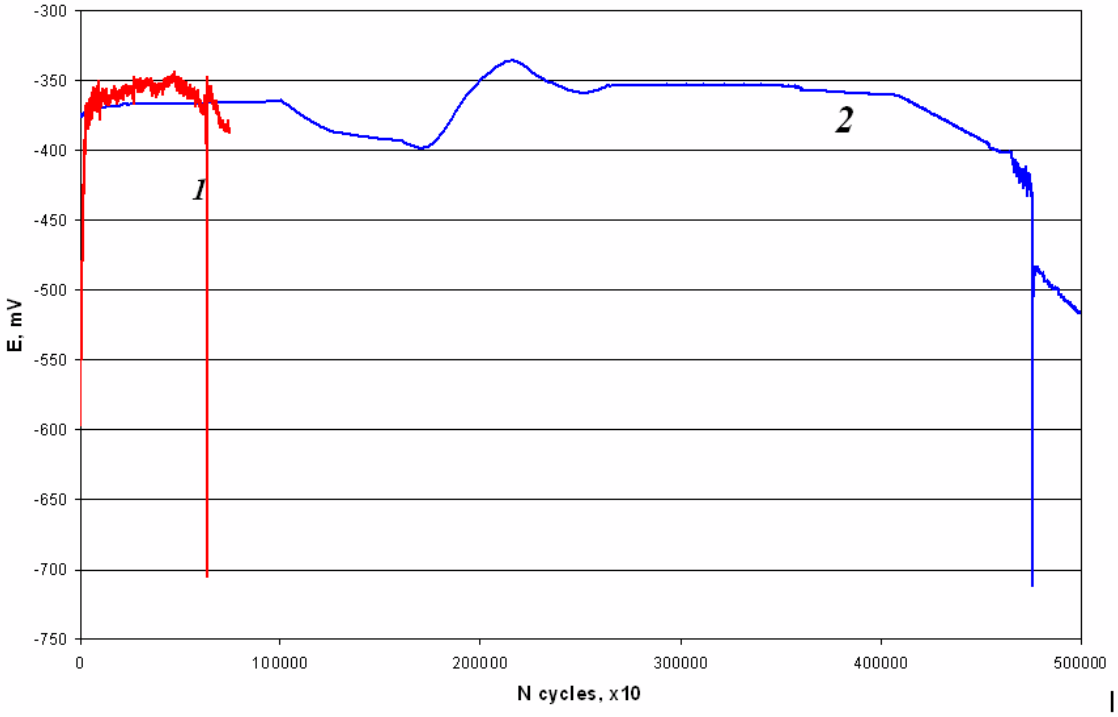

Fig. 3.6. Time dependence of corrosion potential for bare (1) and epoxy coated (2) D16T alloy sample ($\pm\sigma = 180$ MPa).

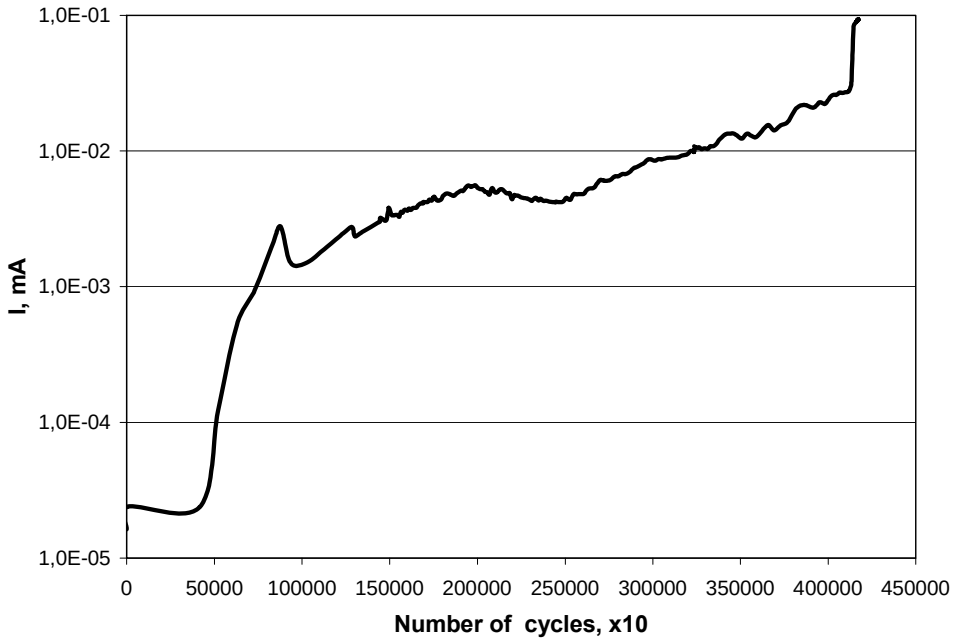

Fig. 3.7. Time dependence of polarization current at open circuit potential of cyclically loaded D16T sample with epoxy coatings in acid rain solution at $\pm\sigma = 180$ MPa.

3.2. Influence of strontium chromate on corrosion fatigue of aluminum alloy

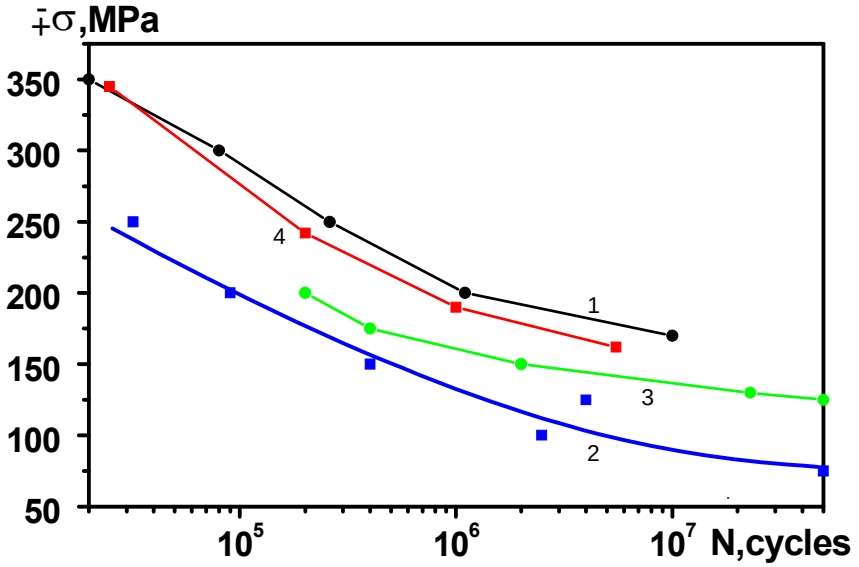

Fig. 3.8. Fatigue curves of D16T alloy round samples in: 1 – air, 2 – 3% NaCl, 3 – acid rain solution, 4 – acid rain with 1 g\l strontium chromate

It was established (fig. 3.8), that fatigue limit (the stress below which a material can be stressed cyclically for an infinite number of times without failure) of round polished samples from alloy D16T in air is equal σ_{-1} = 175 MPa, while it decreases to σ_{-1c} = 125 MPa in acid rain solution at $5 \cdot 10^7$ cycles. 3% sodium chloride solution, as more aggressive environment, decreases fatigue limit of the aluminum alloy to about 75 MPa. Addition of 1 g/l of strontium chromate to acid rain solution significantly increases the aluminum alloy corrosion resistance due to formation of on its surface a passive chromate film. This causes an increase of cyclic durability of alloy samples in the inhibited corrosion solution to about 160 MPa after $5.5 \cdot 10^6$ cycles. The main reason of it can be inhibition by chromate of pitting development on deformed local areas of aluminum alloy [27, 63].

Time dependencies of open circuit potential (OCP) of bare aluminum alloy, epoxy coated samples and epoxy chromate coated samples under cyclic loading of 180 MPa in acid rain solution are shown on fig. 3.9. Corrosion potential of bare aluminum alloy and epoxy coated samples moves to more positive values and after 150…200 thousands cycles reaches the level of -380…-350 mV. The potential of loaded sample with epoxy chromate coatings slowly moves into negative direction and finally after about 2 million cycles reaches the level of -750…-780

mV.

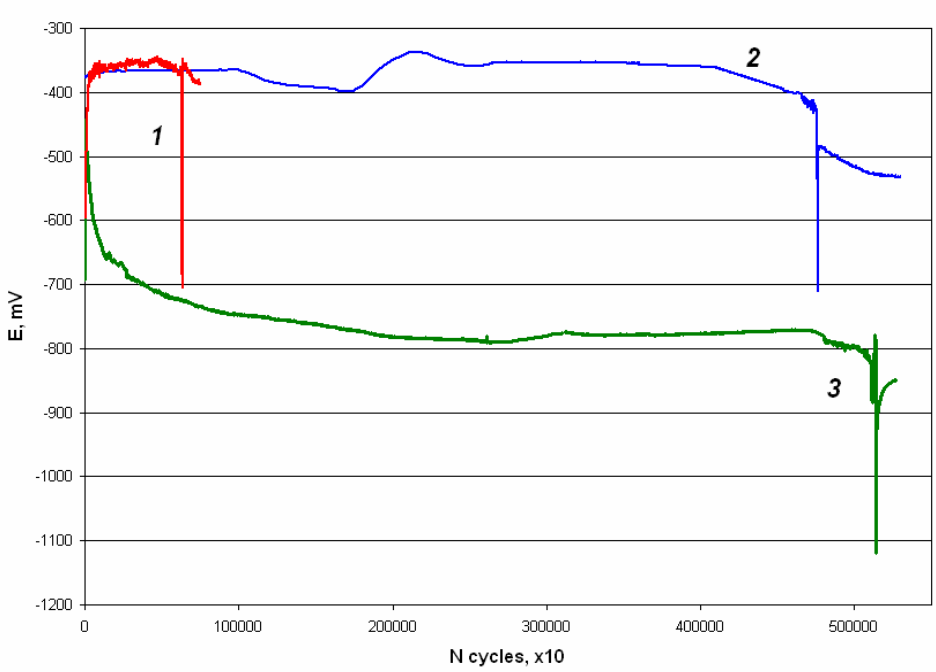

Fig. 3.9. Time dependence of corrosion potential for bare (1), epoxy coated (2) and epoxy chromate coated D16T alloy sample ($\pm\sigma = 180$ MPa).

Chromate could be released from paint, particularly when they are scratched or cracked. Higher pH favors Cr^{VI} release. Cathodic sites, which raise the local pH, may favor Cr^{VI} release [64]. Cracking of epoxy chromate paint can be caused by cyclic mechanical loadings during corrosion fatigue tests. As shown by polarization measurements [2], the presence of 15 ppm of chromate in chloride solution decreases the corrosion potential into the region where no pitting corrosion occurs; hence, the region of potential below the pitting potential is enlarged. This effect is probably caused by the increasing pH of the solution. For example, the pH of 1 M NaCl is 5.7 in the same solution with 100 ppm of chromate the pH is 7.4 [2]. This change in pH corresponds to a decrease of about 100 mV in the corrosion potential. An addition of about 0.01 M chromate increases the pH to 8.2 which corresponds to corrosion potential decrease of about 150 mV. Potential changes 50 mV for one unit of pH of the solution [2]. This explains the potential decrease of D16T alloy samples with epoxychromate coatings, which was observed during their cyclic loading in corrosion environment. Similar potential kinetic was observed in the work [65] on unloaded samples of alloy AA2024, protected by paint containing strontium chromate.

Polarization dependencies (fig. 3.10), obtained on aluminum alloy samples with epoxy

and epoxychromate coatings, testifies about significant influence of cyclic deformation on values of anodic and cathodic currents. The currents increase in about 10 times under loading. Thus cyclic loading facilitates both anodic and cathodic reactions on aluminum alloy. The anodic polarization curves of loaded epoxy coated alloy consists of two parts – more flat (looks like some passivation plateau) and more steep (fig. 3.10). A rapid increase of anodic current was observed at sample potential shift to positive direction on 150…180 mV from OCP. Such fast current increases can testifies about disposition towards pitting development on the metal. Significantly less anodic and cathodic currents are observed for alloy samples with epoxychromate coating under conditions of corrosion fatigue. The pitting potential on anodic polarization curve was not established for epoxychromate coated samples during about 2500…3300 thousands cycles of loading at 180 MPa. The situation took place only after 3300 thousands cycles (fig. 3.10).

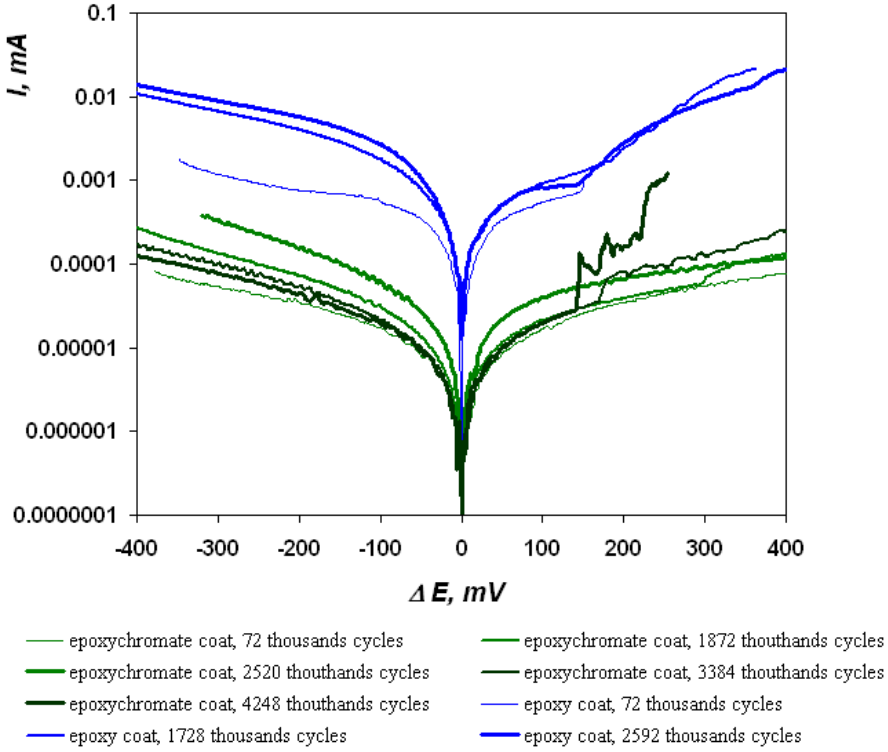

Fig. 3.10. Polarization curves of epoxy and epoxychromate coated D16T alloy samples under cyclic loading of 180 MPa in acid rain solution

Calculation of corrosion currents by method of extrapolation of Tafel slopes shows significant increase of substrate self-dissolution under epoxy coating in case of the sample cyclic loading at $\pm\sigma = 180$ MPa (fig. 3.11) if compare with alloy samples coated with epoxychromate coatings.

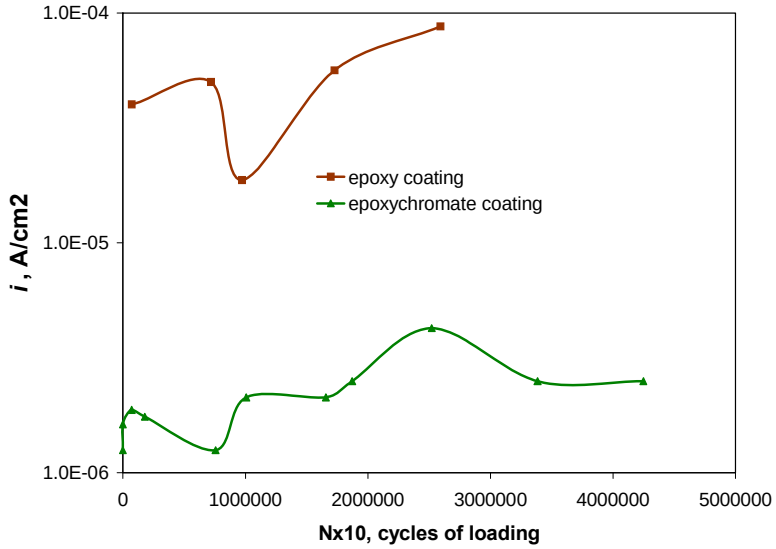

Fig. 3.11. Time dependence of corrosion current for epoxy and epoxychromate coated D16T samples in acid rain solution at $\pm\sigma = 180$ MPa.

3.3.Corrosion of aluminum alloy under conditions of surface mechanical activation

It was carried out a mechanical activation of aluminum alloy surface, as described in part 2, for understanding corrosion and corrosion inhibition of aluminum alloy under conditions of stress corrosion fracture in acid rain solution. Passive oxide film was removed continuously from alloy sample surface by ceramic ball. Open circuit potential and friction moment were recorded during the process. The samples were studied in artificial acid rain solution without and with addition of 600 ppm strontium chromate. Open circuit potential of unloaded samples in both control and inhibited solutions was situated in the range of -450 … -550 mV. The potential has rapidly moved to more negative values after beginning of ball cyclic movement (load weight - 1 N, length of scratch – 24 mm, ball sliding rate – 1.6 mm/sec) (fig. 3.12). Such negative potential values are close to potential of bare aluminum. The potential shift in negative direction is larger at presence of strontium chromate in corrosion solution. After shutdown of mechanical activation of alloy surface its potential in control solution rapidly, and in the solution with chromate more slowly returned to previous level. Potential kinetics of aluminum alloy during the wear testifies about more electrochemically active state in case of availability in corrosion solution of strontium and chromate ions. The experimental data of friction coefficient measurements for the couple “ceramic ball – aluminum alloy D16T” in uninhibited and inhibited solutions testifies that chromate film formed on alloy surface at scratch site has worse antifriction properties or it is less resistant to mechanical destruction (fig. 3.13).

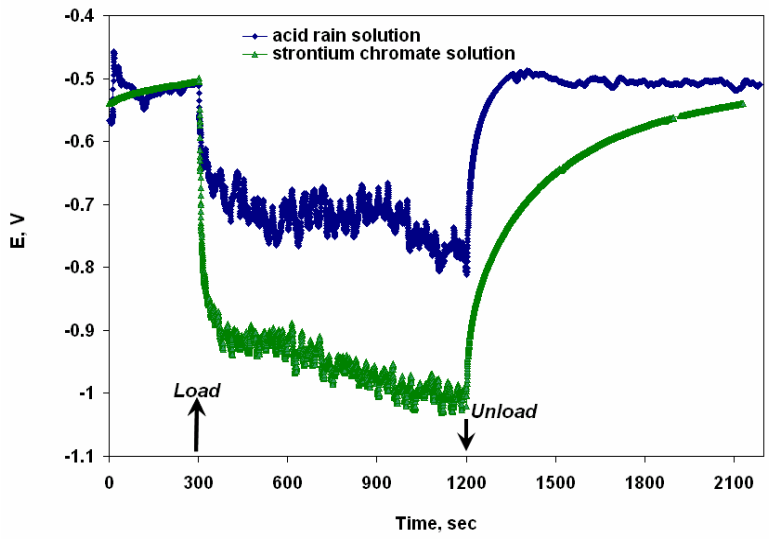

Fig. 3.12. Time dependencies of open circuit potential of aluminum alloy D16T during its surface mechanical activation in corrosion solutions.

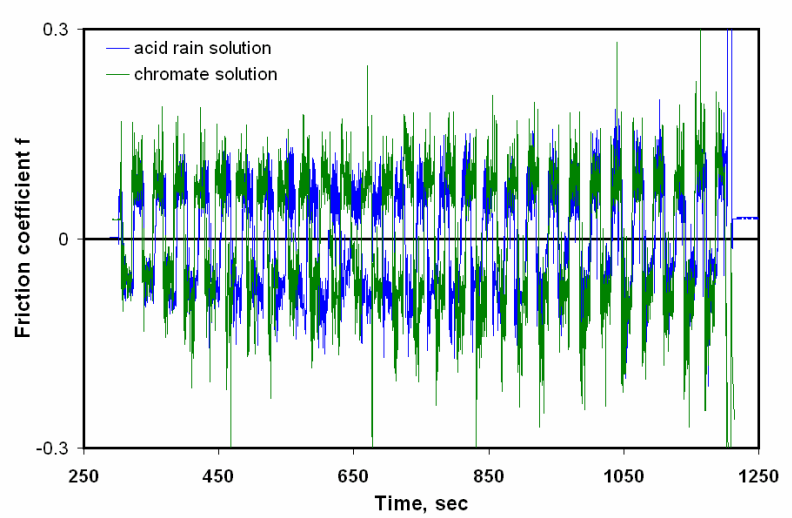

Fig. 3.13. Time dependencies of friction coefficient of the sliding couple - aluminum alloy D16T/ceramic ball in corrosion solutions (Load = 1 N)

Hence, wear of alloy surface by ceramic ball at mentioned loading conditions is larger in chromate solution. This is confirmed by results of scanning electron microscopy investigation (fig. 3.14). It can be seen, that width of wear track on aluminum alloy sample exposed to chromate solution is about 1.5 times bigger than in uninhibited environment.

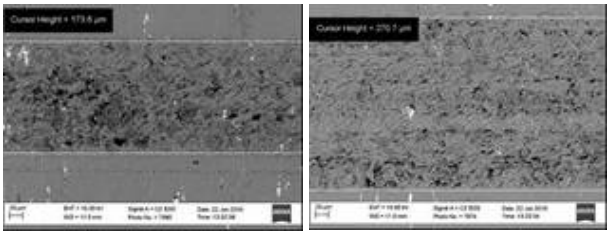

uninhibited solution (BSD, x 250) strontium chromate solution (BSD, x 250)

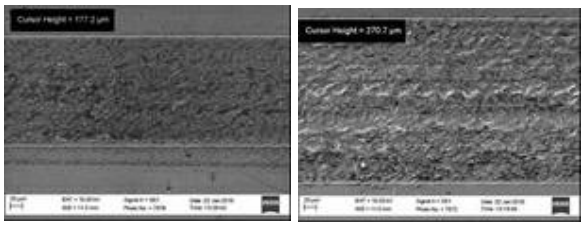

uninhibited solution (SE, x 250) strontium chromate solution (SE, x 250)

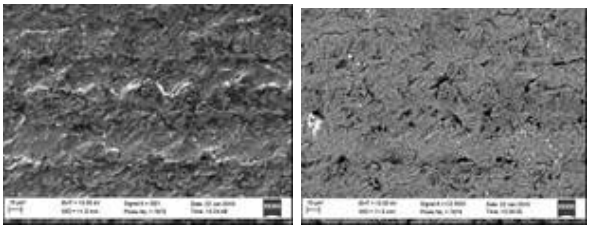

strontium chromate solution (SE, x 500) strontium chromate solution (BSD, x 500)

Fig. 3.14. Back-scattered and secondary electron SEM images of scratched alloy surface.

The form of polarization curves obtained on unloaded samples of D16T in acid rain solution and in inhibited acid rain solution has revealed, that strontium chromate reduces both electrode reactions, cathodic and anodic. At this situation anodic reaction is slowed down to larger extent (fig. 3.15). Some tendency of the metal to passivation could be discussed.

Polarization curves of aluminum alloy were changed significantly in case of mechanical activation of alloy surface (fig. 3.16, 3.17). Firstly, anodic and cathodic currents have risen essentially. Anodic plateau have became more apparent. The current rise typical for pitting development was observed at potentials of -400…-600 mV. This does not happen when chromate chromate is present in corrosion solution. Chromate inhibitor reduces anodic dissolution of activated surface (fig. 3.16, 3.17), however cathodic currents at its presence are increased

comparing with uninhibited solution. Chromate decreases probability of pits initiation, however it accelerates cathodic reaction on mechanically activated surface of alloy and increases wear of the metal. It is possibly that protective chromate film is less strong and less wear resistant than aluminum oxide film.

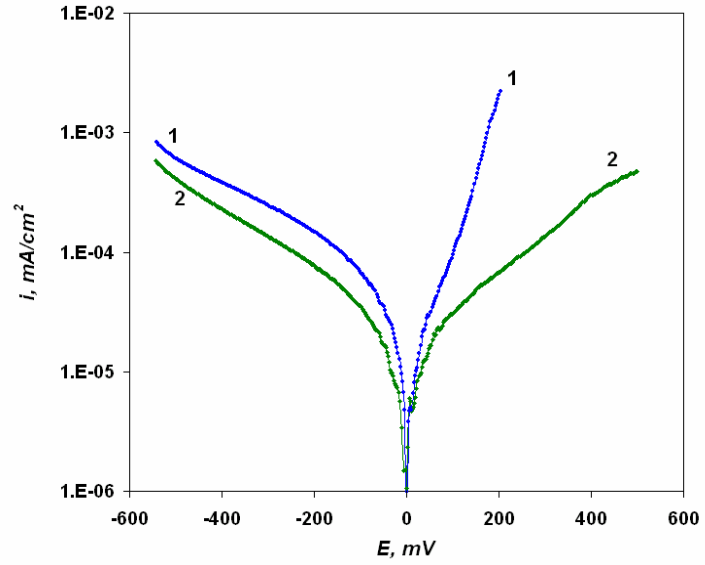

Fig. 3.15. Polarization curves of aluminum alloy D16T after 2 hours exposure in acid rain solution (1) and in acid rain inhibited by strontium chromate (2)

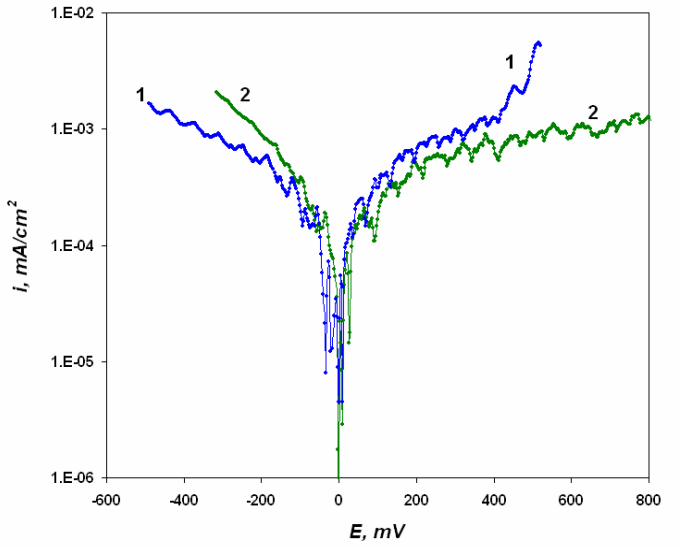

Fig. 3.16. Polarization curves of aluminum alloy D16T during mechanical activation in acid rain solution (1) and in acid rain inhibited by strontium chromate (2). (Values of polarization current are related to all sample surface)

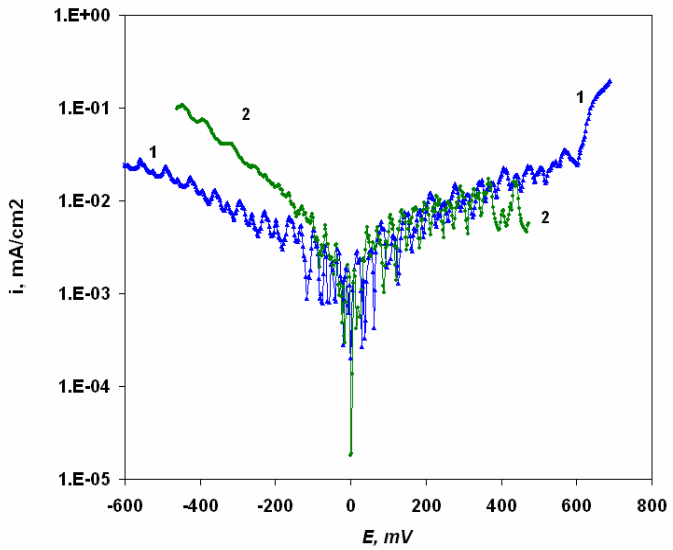

Fig. 3.17. Polarization curves of aluminum alloy D16T during mechanical activation in acid rain solution (1) and in acid rain inhibited by strontium chromate (2). (Values of polarization current are related to surface of scratch. The rest surface of the sample was isolated during experiment by polymer adhesive tape)

The open circuit potential behavior of the aluminum alloy D16T during its mechanical activation in the acid rain solution with and without addition of inhibitors is shown in Fig. 3.18. At the beginning, the corrosion potential of the unloaded sample in the uninhibited solution was on the level of -400 mV and reached nearly -600 mV in chromate and phosphate containing acid rain. Such difference of potentials can be explained by possible prevalence of cathodic control of the corrosion. Accordingly to Szklarska-Smialowska data [2], the negative shift of corrosion potential in the inhibited acid rain could be also caused by an increase of pH of the solution. One unit increase in pH corresponds to a decrease of about 50 mV in the potential [2].

Corrosion potentials of the aluminum alloy in all solutions after its surface mechanical activation have reached more negative values, typical for nonpassive state. The instantaneous drop in potential is due to the surface becoming active owing to a destruction of surface oxide film, thereby exposing the alloy. At that, the loading of ceramic ball was 1 N, the length of wearing track – 24 mm and the speed of sample horizontal movement relatively the indenter – 1,6 mm/sec. The negative shift of corrosion potential of D16T during its corrosive wear in the chromate containing acid rain was on 200 − 250 mV greater and in phosphate containing acid rain on 150-200 greater, than in the blank solution. The potential in the uninhibited solution has returned to starting values during about 500 sec after stopping of the alloy surface wear with the

ceramic ball due to the passive oxide film formation. Similar potential changes happened, but more slowly, in the inhibited solutions, which can be explained by taking part of inhibiting ions in the formation of surface film.

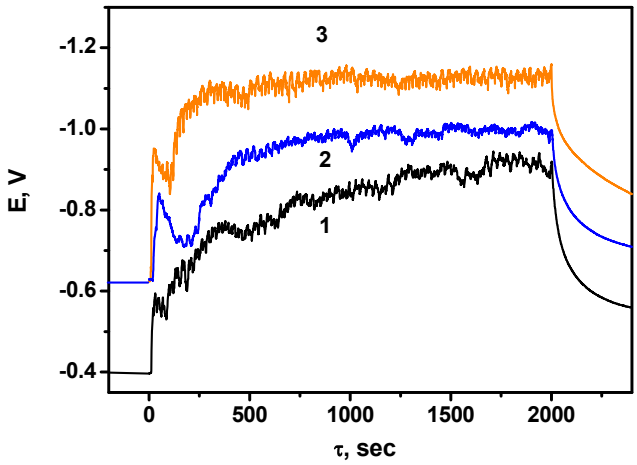

Fig.3.18. Time dependencies of corrosion potential of aluminum alloy D16T during its tribocorrosion in the acid rain: 1) uninhibited, 2) containing extract of phosphate pigment Actirox 106; 3) inhibited by strontium chromate.

Time dependencies of a potentiostatic polarization current on the aluminum alloy sample at corrosion potential (E_{pol} = E) can give useful information which related to the development of electrochemically active metal sites with the damaged passive film [67]. At absence of a mechanical loading the current value is equal to zero and the polarization current flow will be mostly determined by the destruction of protective films on the alloy surface. The measurements revealed (Fig. 3.19), that the polarization current on the aluminum alloy sample in the acid rain rapidly rises in the anodic side from 0 to about 0.0015 μA at the moment of loading and further slowly reaches the range of 0.0075 − 0.0100 μA, probably due to the oxide film destruction caused by the corrosive wear and an extension of electrochemically active surface of the alloy. The addition of strontium chromate to acid rain decreases the alloy polarization current in 2 − 3 times, indicating about an inhibition of anodic dissolution during the corrosive wear (Fig. 3.19). In contrast to strontium chromate, phosphate Actirox 106 greater decreases polarization current of alloy D16T during its wear in corrosion solution. Since phosphate inhibiting pigments are less effective than chromates [68, 69], the polarization current decrease could be explained by a high resistance of formed phosphate film to corrosion wear in acid rain. It is known the use of phosphate conversion coatings to enhance wear and corrosion resistance of metal [70]. At the same time, higher wear endurance of the alloy with deposited phosphate film results in a

development of smaller track width and in a reduction of integral polarization current.

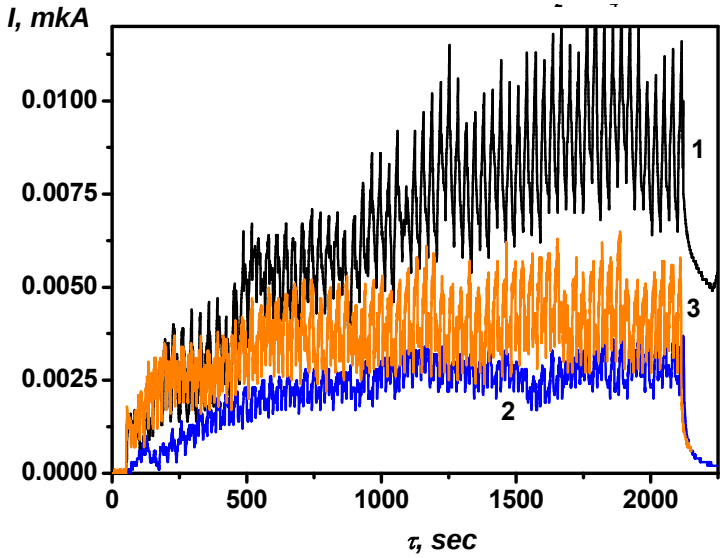

Fig.3.19. Time dependencies of polarization current for aluminum alloy samples during corrosive wear in the acid rain: 1) uninhibited, 2) containing extract of phosphate pigment Actirox 106; 3) inhibited by strontium chromate.

In Fig. 3.20, the friction data of the contacting couple D16T/ceramic ball under free corrosion conditions is presented. In this figure the friction coefficient is given as a function of sliding distance during the wear in corrosion solutions. The dependence of friction coefficient is cyclical, which is associated with the reciprocal sliding of the ceramic ball on the aluminum alloy surface. The coefficient conditionally changes its own sign depending on a direction of the ball movement (Fig. 3.20a). This is done for a better visual presentation of its dependence on the distance of displacement, in fact, the coefficient of can not be negative. As can be seen from the diagram, the friction coefficient approaches to zero value at the moment of ball stop, and it rises during ball sliding from one end of the scratch to another and its dependence gets a stochastic character. A comparison of the friction coefficient of the couple "ceramic ball – aluminum alloy" in blank and inhibited acid rain solutions shows, that chromate film has worse antifriction properties or is less resistant to mechanical damaging, than oxide one (Fig. 3.20(a,b)). Consequently, the wear of alloy surface by the ceramic ball in the chromate containing corrosion environment can be significantly larger. SEM analysis of the surface of alloy samples after their corrosive wear confirms the negative effect of chromate (Fig. 3.21). It can be seen, that the wear track width increases in the inhibited acid rain in 1.5 times compared to the blank solution.

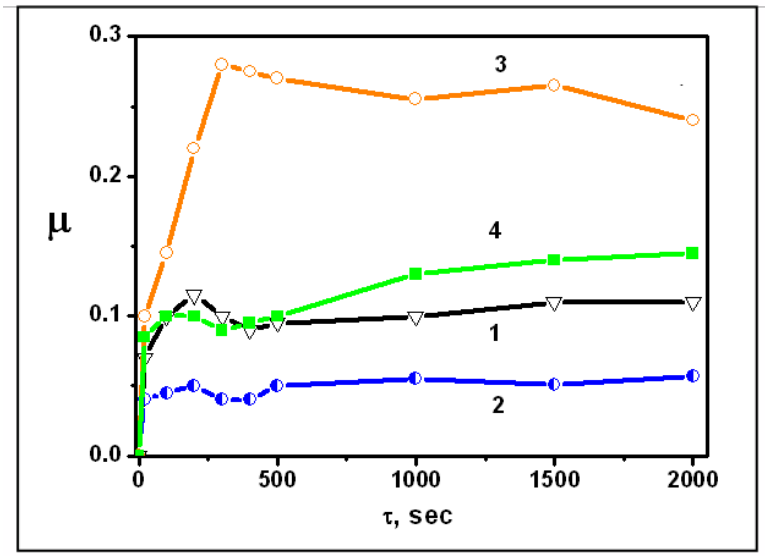

Fig. 3.20. The dependence of friction coefficient of the couple "ceramic ball – aluminum alloy" from sliding length:
1 – uninhibited corrosion environment; 2 – inhibited with phosphate;
3 – inhibited with chromate;
4 – air.

Oxidation of juvenile surfaces, formed in the acid rain on the alloy during its wear, takes place after each pass of the indenter. Products of the alloy wear are oxidized as well. As a result, amount of oxide on the aluminum alloy surface in the wear zone increases, which is confirmed by the X-ray microanalysis. A more thick oxide film, than usually, is formed under the moving indenter (Fig. 3.21). This, in turn, reduces the friction coefficient and the wear of the sample material. Based on the SEM photos, the sample of aluminum alloy is more wear out in the chromate solution, possible because of the surface film in the scratch are is amorphous and thinner, than in the uninhibited solution. Phosphate inhibiting pigment more decreases corrosion wear of aluminum alloy than chromate. Phosphate film remains on surface of aluminum alloy after wear in acid rain solution inhibited with phosphate Actirox 106 (Fig. 3.21). Such film accordingly to data of [71] has an excellent adhesion to metal, attributed to epitaxial growth. Heating of the film [71], consisting of interconnecting channels between the individual phosphate crystals, is decreased during corrosion wear due to penetration of an environment.

Roughness measurement results correlate with the SEM data (Fig. 3.22). The worn surface of D16T alloy in the chromate inhibited acid rain is rougher, and the depth and the width of track – larger, than in case of its corrosive wear in the blank acid rain and in the phosphate solution. The smallest dimensions of track wear are observed on sample of aluminum alloy after wear in the phosphate solution.

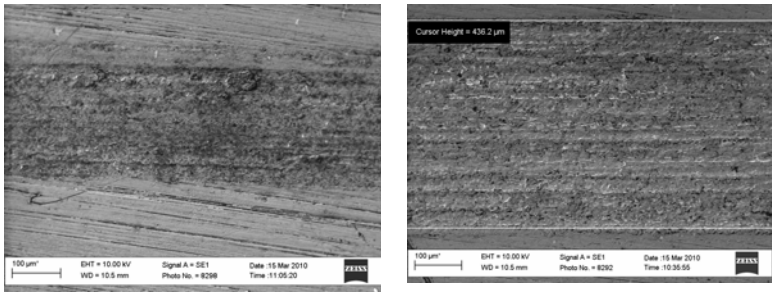

a) wear in air **b) wear in chromate solution**

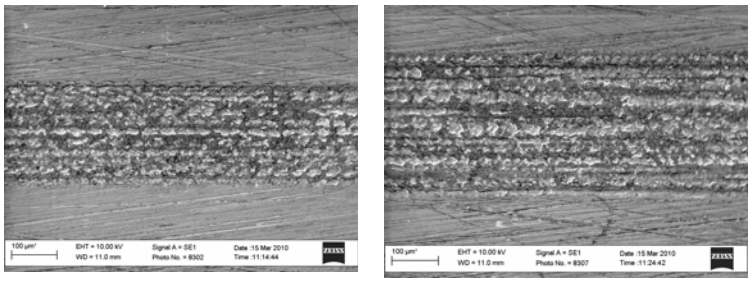

c) wear in phosphate solution **d) wear in uninhibited acid rain**

Fig. 3.21. The appearance of aluminum alloy surface after the corrosive wear: a) in air; b) in chromate solution; c) in phosphate solution; d) in uninhibited acid rain.

Despite of the control of electrochemical corrosion, total corrosive wear of the alloy in the chromate containing acid rain is greater, than in the conventional solution. Apparently, it happens due to worse antifriction properties and a lesser strength of the chromate layer on the aluminum alloy, than the oxide film. According to the work [72], chromate conversion coatings can be easily damaged in a wet environment and are not scratch and wear resistant. Thus, aluminum alloy products can be the subject of accelerated wear destruction at the presence of chromate ions in the corrosion environment, that should be considered during a development of technologies for their corrosion protection. In contrast to chromate inhibitor, modified zinc phosphate decreases corrosion wear of aluminum alloy D16T in acid rain solution due to better antifriction properties.

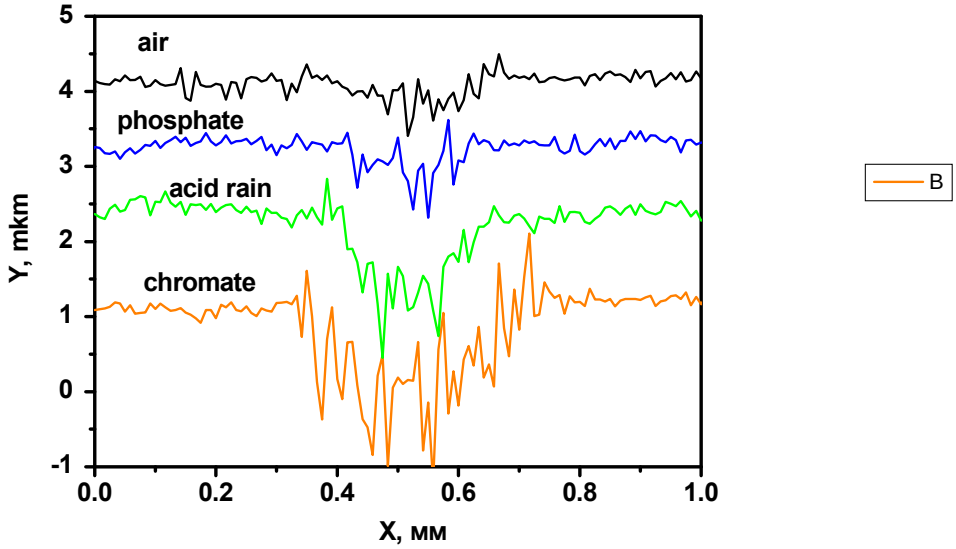

Fig. 3.22. Profilograms of aluminum alloy surface obtained across of track after corrosive wear tests in acid rain solutions.

4. STUDY OF AL ALLOY CORROSION INHIBITION

4.1. DC polarization study of D16T corrosion in acid rain solutions inhibited with single pigments

It was interested to study an influence of single inhibiting pigment extracts on corrosion of alloy D16T in acid rain. Potentiodynamic polarization curves of the alloy in acid rain solution with 1000 ppm of phosphate, chromate and bentonite were periodically recorded for this purpose. Action of zinc/iron phosphate (Actirox 213) and zinc phosphate, modified by 1% molybdate (Actirox 106), and also strontium chromate and calcium containing bentonite (Sphere 7 Trade Company, Ukraine) was studied. The investigations revealed, that largest polarization both cathodic and anodic reactions is observed in strontium chromate solution (fig. 4.1). Phosphate Actirox 213 very little inhibits cathodic and anodic reactions on the aluminum alloy. The positive effect from phosphate Actirox 213 becomes apparent only at anodic potentials, which exceed 100 – 150 mV. At that time anodic polarization current decreases in 5-10 times.

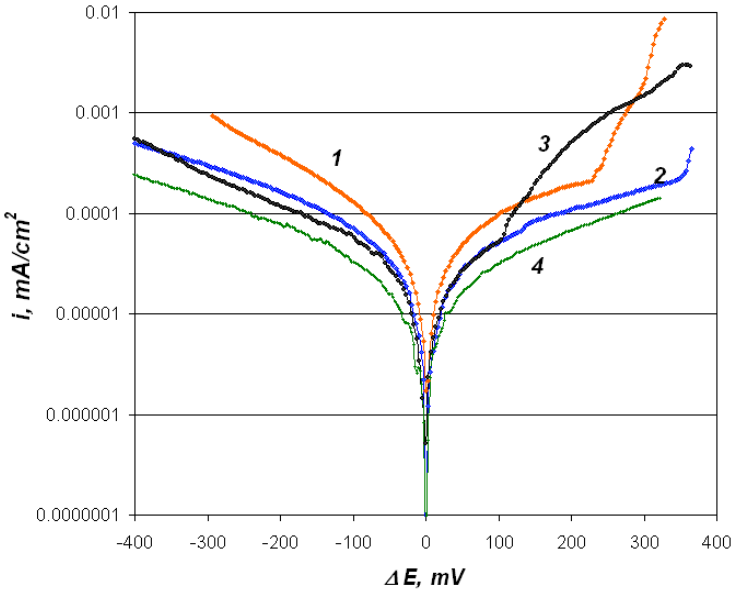

Fig. 4.1. Polarization curves of D16T alloy after 24 hours in acid rain solutions: 1) with bentonite, 2) with phosphate Actirox 213, 3) uninhibited, 4) with chromate.

The properties of bentonite (ion exchange, water absorption and swelling) make it a valuable material for a wide range of uses and applications. Bentonite is used in coatings, adhesives, oil drilling and as corrosion inhibitor [73]. In the presence of aggressive electrolyte, bentonite can release an inhibiting cation and simultaneously absorb and immobilize sodium or other cation available in the vicinity. Bentonite is hydrated alumino silicate clay primarily composed of the smectite class mineral montmorillonite [73]. The ideal formula for montmorillonite is $(Na,Ca)_{0.33}(Al_{1.67},Mg_{0.33})Si_4O_{10}(OH)_2nH_2O$. Cation exchange capacity of montmorillonite is 80 to 150 meq/100g. The composition of the bentonite used in this study is given in Table 4.1.

Table 4.1. The bentonite composition based on EDX analysis data.

Element	Weight, %	Atomic, %
O K	55.02	70.09
Na K	0.51	0.45
Mg K	0.63	0.53
Al K	9.42	7.12
Si K	25.00	18.15
K K	0.71	0.37
Ca K	0.50	0.26
Ti K	0.72	0.31
Fe K	7.49	2.72
Total	100.00	100.00

It was established that bentonite itself slightly accelerates aluminum alloy corrosion in acid rain. Anodic and cathodic currents of alloy D16T in acid rain inhibited with 1000 ppm bentonite rise in comparison to phosphate (Actirox 213) and chromate solution (Fig. 4.1). Time dependencies of corrosion current of aluminum alloy in inhibited solutions testify about significant decrease D16T dissolution during first six hours of exposure and further stabilization of the process (Fig. 4.2). The corrosion current in bentonite solution gradually increases and after 48 hours of exposure makes up 1.0E-4 mA/cm^2.

Polarization dependencies of the alloy D16T in acid rain inhibited with strontium chromate, bentonite and zinc phosphate/molybdate (Actirox 106) were recorded as well (Fig. 4.3). Chromate pigment mostly decreases anodic and cathodic currents of alloy D16T. The phosphate pigment is the second one for effectiveness. The alloy corrodes in the solution inhibited with bentonite about 10 times faster (Fig. 4.4).

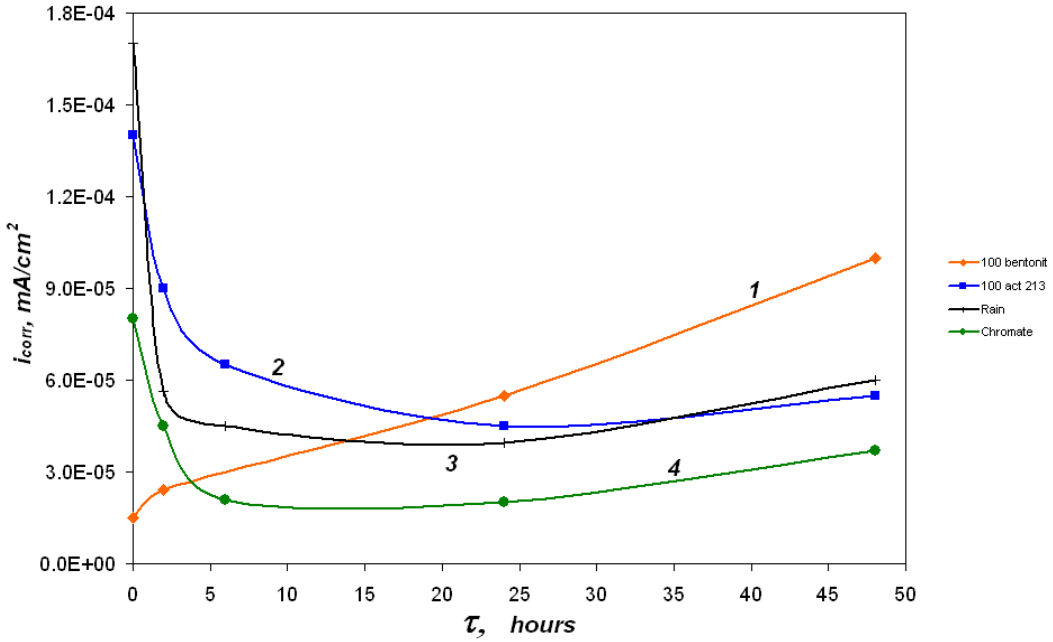

Fig. 4.2. Time dependencies of corrosion current of D16T alloy in acid rain solutions: 1) with bentonite, 2) with phosphate Actirox 213, 3) uninhibited, 4) with strontium chromate.

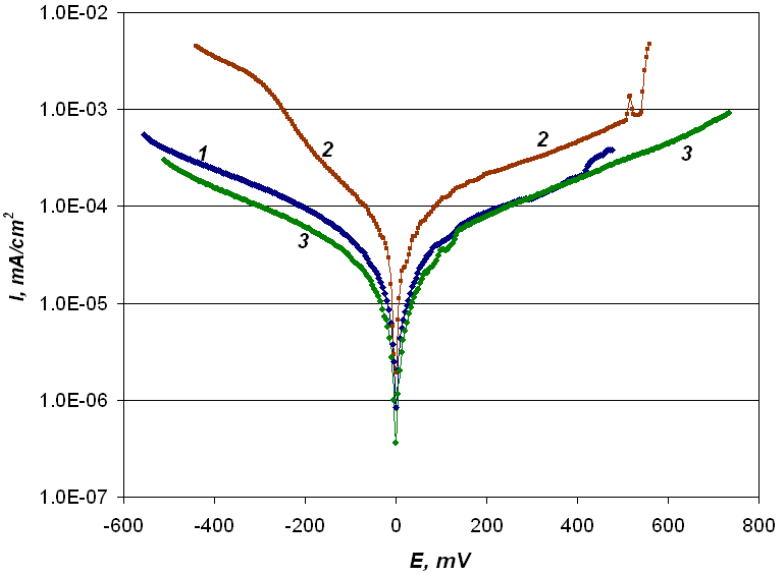

Fig. 4.3. Polarization curves of D16T alloy after 1 day exposure in acid rain solutions: 1) with phosphate Actirox 106, 2) with bentonite, 2) with chromate.

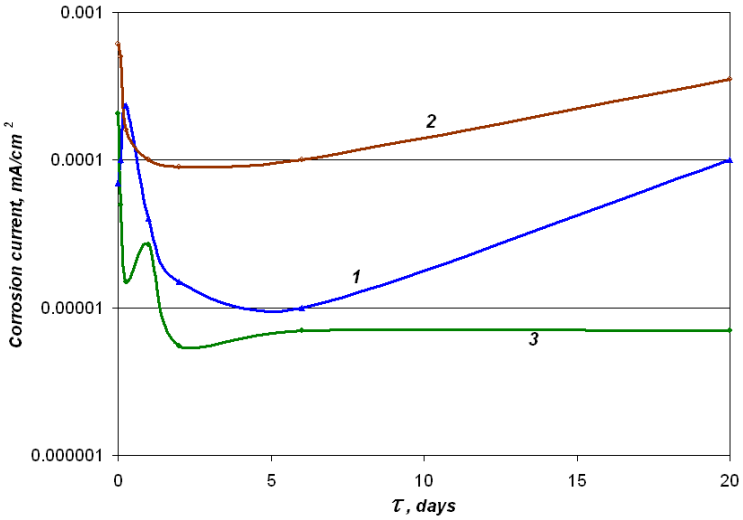

Fig. 4.4. Time dependencies of corrosion current of D16T alloy in acid rain solutions: 1) with phosphate Actirox 106, 2) with bentonite, 3) with chromate.

4.2. DC polarization study of D16T alloy, pure aluminum and Al_2Cu corrosion in acid rain solutions inhibited with pigment blend

The effect of inhibiting pigments and their blends on corrosion of aluminum alloy in acid rain solution has been studied. Polarization dependencies of aluminum alloy in blank and inhibited acid rain have been obtained with this aim (Fig. 4.5). Zinc phosphate pigment (Actirox

106) and strontium chromate were used as inhibitors. It was studied also bentonite clay, which contains 99% of montmorillonite. The reason of choosing bentonite as aluminum alloy corrosion corrosion inhibitor consists in ability of the material to adsorb from solution Copper and Hydrogen ions and in possibility of its use as multipurpose additives in organic coatings [73, 74–78]. Kinetic dependencies of corrosion currents were obtained by way of graphic processing of alloy polarization curves in inhibited solutions (Fig. 4.6). It was established, that neither zinc phosphate nor bentonite, used singly, does not give desirable anticorrosion effect. However, simultaneously addition of these inhibiting components in the corrosion solution significantly decreases of the alloy destruction. At that, minimal corrosion current is observed in the solution, which contains 0.5 g/l of zinc phosphate Actirox 106 and 0.5 g/l of bentonite. It is within $2.0 \cdot 10^{-6} \ldots 1.3 \cdot 10^{-5}$ mA/cm^2. Basing upon corrosion current results Fig. 4.6), the combination of inorganic inhibitors is commensurable with strontium chromate by its efficiency.

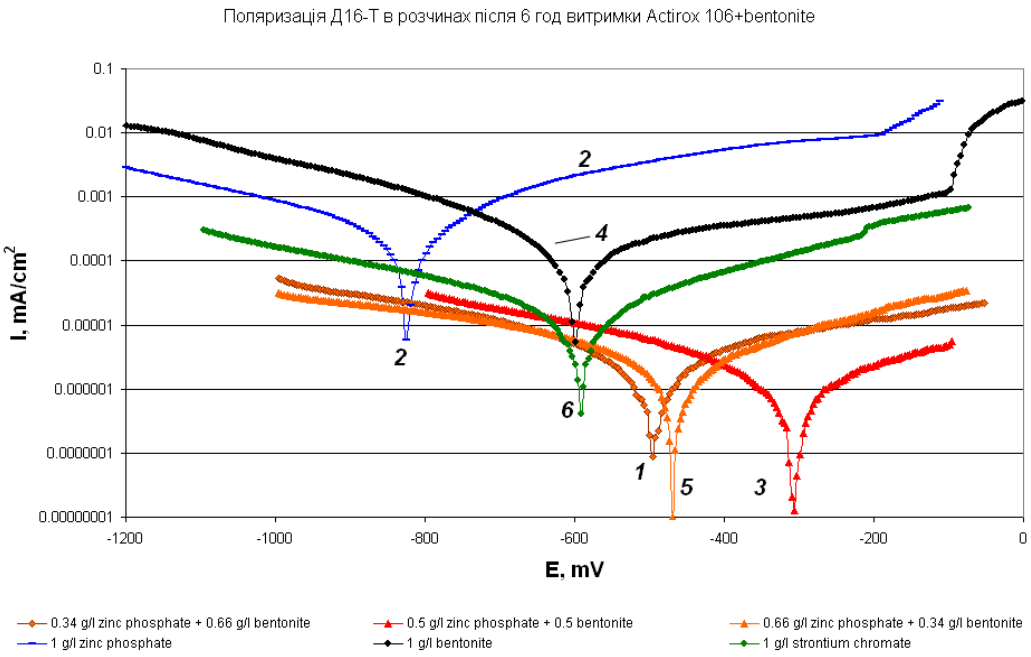

Fig. 4.5. Polarization curves of D16T alloy after 6 hours exposure in acid rain solutions, inhibited: 1) with 0.34 g/l zinc phosphate pigment (Actirox 106) and 0.66 g/l bentonite, 2) with zinc phosphate, 3) with 0.5 g/l zinc phosphate and 0.5 g/l bentonite, 4) with 1 g/l bentonite, 5) with 0.66 g/l zinc phosphate and 0.34 g/l bentonite, 6) with strontium chromate.

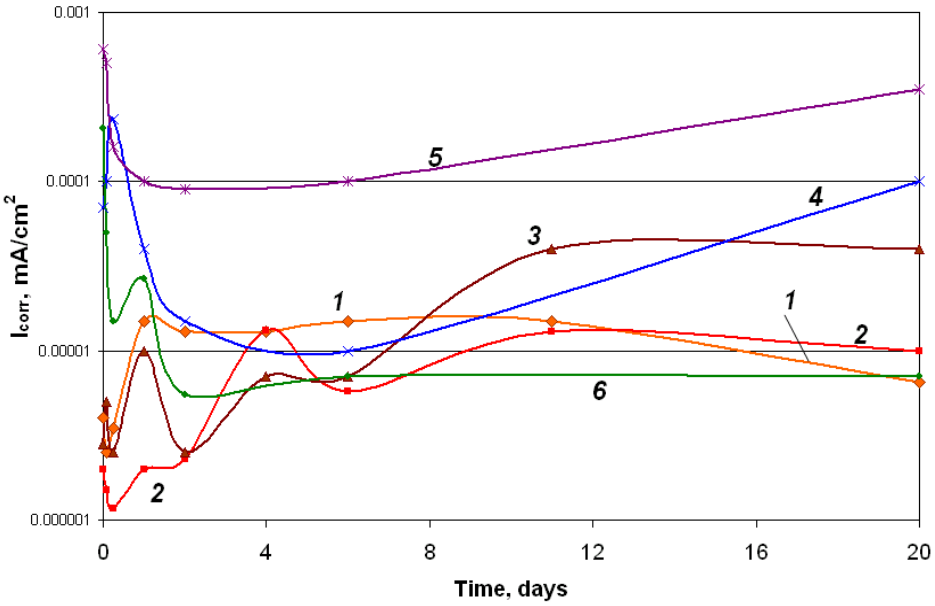

Fig. 4.6. Time dependencies of corrosion current of D16T alloy in acid rain solutions, inhibited: 1) with 0.34 g/l zinc phosphate pigment (Actirox 106) and 0.66 g/l bentonite, 2) with 0.5 g/l zinc phosphate and 0.5 g/l bentonite, 3) with 0.66 g/l zinc phosphate and 0.34 g/l bentonite, 4) with zinc phosphate, 5) with 1 g/l bentonite, 6) with strontium chromate.

Since intermetallic phase is most electrochemical active constituent of aluminum alloy D16T, it was interesting to study chromate-free inhibitors and their blends influence on the intermetallide corrosion. The intermetallide Al_2Cu sample was specially synthesized during fulfillment of the project. The effect of zinc phosphate pigment (Actirox 106), bentonite, ion exchange pigment (Shieldex) and their blends on D16T aluminum alloy corrosion was studied (Fig. 4.7, 4.8, 4.9).

It was established (Fig. 4.9), that zinc phosphate pigment (Actirox 106) addition to corrosion solution makes worse corrosion resistance of aluminum alloy. Probably, this takes place due to rising pH and alloy oxide film dissolution. Calcium ion exchange pigment (Shieldex) practically does not influences alloy corrosion current, comparing with blank acid rain solution without inhibitor. Bentonite, strontium chromate and zinc phosphate/bentonite blend decrease corrosion dissolution of D16T alloy in 6-8 times comparing with uninhibited solution. It should be noted, that zinc phosphate/ion exchange pigment blend provides largest decrease of corrosion current of the aluminum alloy D16T.

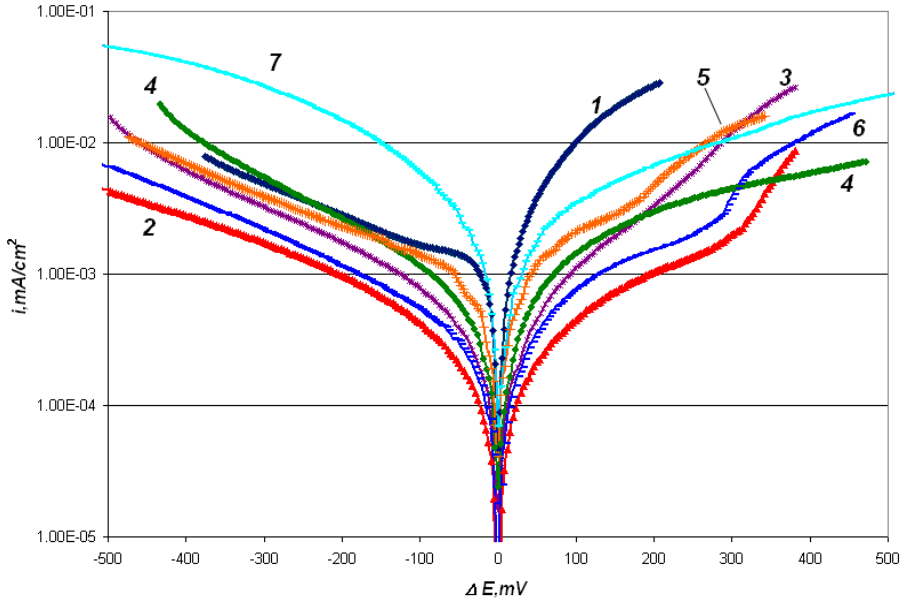

Fig. 4.7. Polarization curves of intermetallic sample after 6 hours exposure in acid rain solutions: 1) without inhibitor, 2) with 0.66 g/l zinc phosphate pigment (Actirox 106) and 0.34 g/l ion exchange pigment, 3) with 0.5 g/l zinc phosphate and 0.5 g/l bentonite, 4) with 1 g/l strontium chromate, 5) with 1 g/l ion exchange pigment, 6) with 1 g/l bentonite, 7) with 1 g/l zinc phosphate.

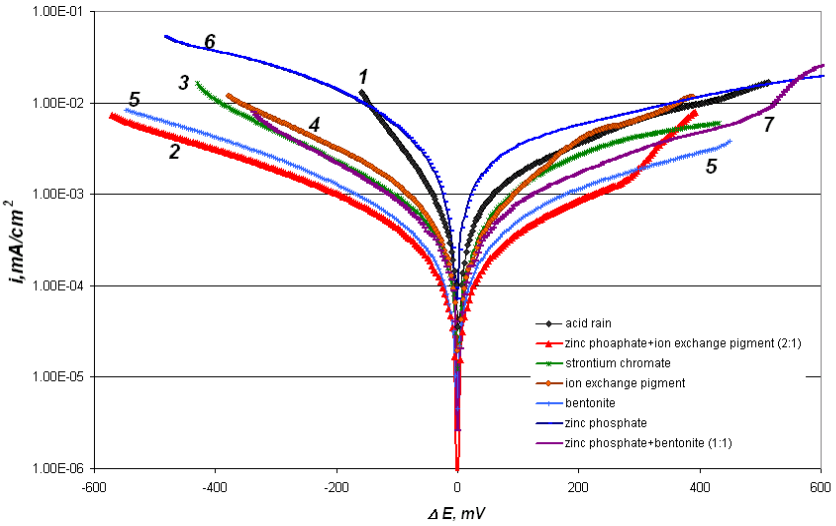

Fig. 4.8. Polarization curves of intermetallic sample after 24 hours exposure in inhibited acid rain solutions: 1) without inhibitor, 2) with 0.66 g/l zinc phosphate pigment (Actirox 106) and 0.34 g/l ion exchange pigment, 3) with 1 g/l strontium chromate, 4) with 1 g/l ion exchange pigment, 5) with 1 g/l bentonite, 6) with 1 g/l zinc phosphate, 7) with 0.5 g/l zinc phosphate and 0.5 g/l bentonite.

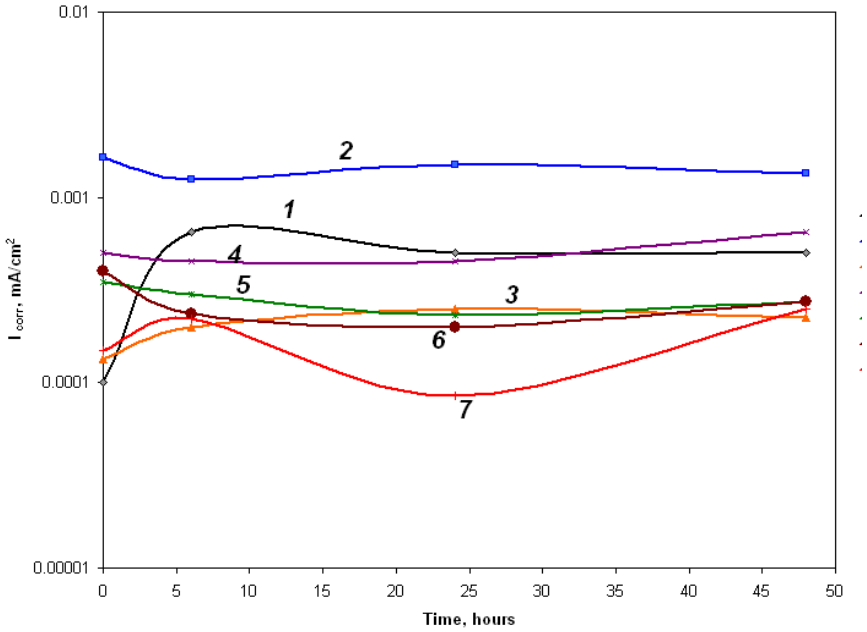

Fig. 4.9. Time dependencies of corrosion current of intermetallic sample in inhibited acid rain solutions: 1) without inhibitor, 2) 1 g/l zinc phosphate (Actirox 106), 3) with 1 g/l bentonite, 4) with 1 g/l ion exchange pigment, 5) with 1 g/l strontium chromate, 6) with 0.5 g/l zinc phosphate pigment (Actirox 106) and 0.5 g/l bentonite, 7) with 0.66 g/l zinc phosphate pigment (Actirox 106) and 0.34 g/l ion exchange pigment.

It was interesting also to estimate corrosion of aluminum as constituent part of the aluminum alloy in the inhibited acid rain solutions. It was established after DC potentiodynamic polarization of aluminum samples in inhibited solutions (Fig. 4.10) and graphical analysis of polarization curves (Fig. 4.11), that three characteristics group of solutions exists, which differ in corrosion activity. The artificial acid rain solution, where corrosion is maximal, can be related to first group. Solutions of single pigments (zinc phosphate, calcium ion exchange silica and bentonite) in acid rain are related to the second group. They have some inhibiting effectiveness. Most effective pigments (zinc phosphate/ion exchange pigment and zinc phosphate/bentonite blends and strontium chromate) can be related to third groups. The last three inhibitors or their blends are very close in their effectiveness and principal possibility exists for substitution of toxic chromate by chromate-free blends.

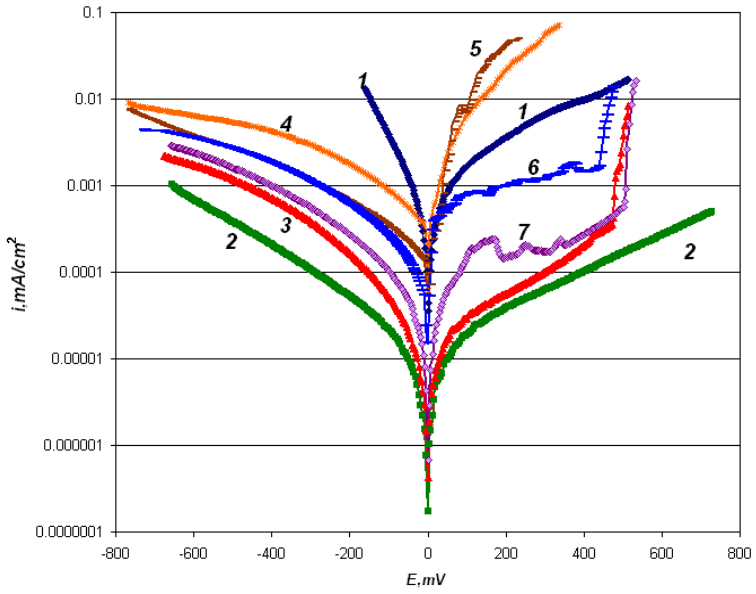

Fig. 4.10. Polarization curves of aluminum sample after 24 hours exposure in inhibited acid rain solutions: 1) without inhibitor, 2) with 1 g/l strontium chromate, 3) with 0.66 g/l zinc phosphate pigment (Actirox 106) and 0.34 g/l ion exchange pigment, , 4) with 1 g/l ion exchange pigment, 5) with 1 g/l bentonite, 6) 1 g/l zinc phosphate (Actirox 106), 7) with 0.5 g/l zinc phosphate pigment (Actirox 106) and 0.5 g/l bentonite,

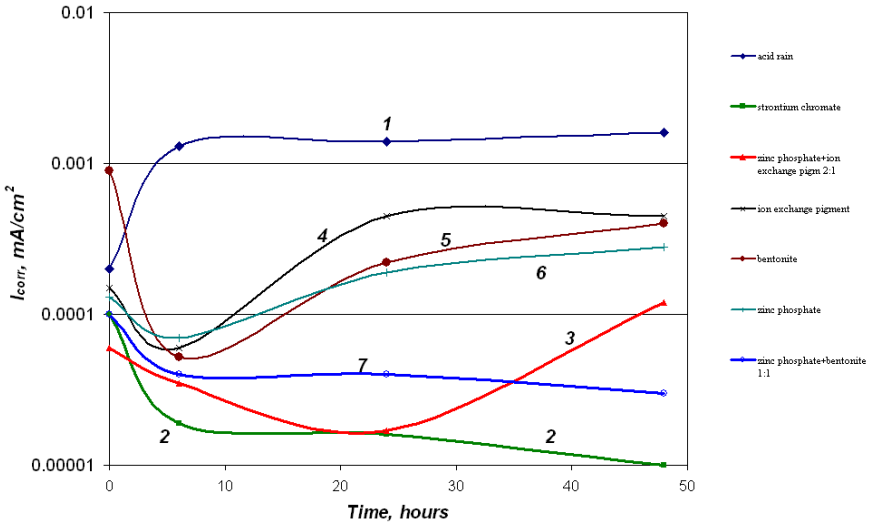

Fig. 4.11. Time dependencies of corrosion current of aluminum sample in inhibited acid rain solutions: 1) without inhibitor, 2) with 1 g/l strontium chromate, 3) with 0.66 g/l zinc phosphate pigment (Actirox 106) and 0.34 g/l ion exchange pigment, 4) with 1 g/l ion exchange pigment, 5) with 1 g/l bentonite, 6) 1 g/l zinc phosphate (Actirox 106), 7) with 0.5 g/l zinc phosphate pigment (Actirox 106) and 0.5 g/l bentonite.

4.3. Electrochemical impedance spectroscopy of D16T alloy in solutions containing phosphate and zeolite blend

It was interesting to study alloy D16T corrosion inhibition by zinc phosphate and zeolite composition. Zeolites constitute a versatile material that has found many technological applications. The employment in paint technology is rather restricted, but zeolites have been used as humidity- and ammonia-adsorbent material in ceiling paints [79] and finishing paints [80]. In this last application, zeolites were exchanged with suitable cations, heated at 350°C, and then mixed with mineral silicate ligands to obtain paints for different substrates with acceptable hiding power. Zeolites exchanged with silver ions were employed in smart hygienic coatings as biocides, due to the ability of silver ions to inhibit vital processes in microorganisms [81]. It was established that combination of zinc phosphate and calcium-containing ion-exchange pigment enables one to inhibit efficiently the local corrosion of an aluminum-copper alloy in a slightly acid medium [82]. Because zeolites are ionic-exchanging materials, it seemed reasonable to study aluminum alloy corrosion inhibition by phosphate/zeolite composition.

The method of electrochemical impedance spectroscopy was used with this aim. Corrosion of aluminum alloy samples was studied in artificial acid rain solution, which contained extracts of zeolite, zinc phosphate (Actirox 106) both single and in compositions. Obtained results are represented as Nyquist plots (Fig. 4.12, 4.13). The working area of samples was 2 cm^2. Impedance dependencies in all cases had appearance of slightly deformed semicircles. Impedance semicircles in the solutions containing extracts of phosphate/zeolite compositions had significantly bigger sizes than in solutions of single pigments. Moreover, the semicircles were not complete, possible due to high measured resistance values.

Special software and electrical equivalent circuit $R_s(Q_{dl}R_{ct})$ were used for fitting of experimental spectra shown. It was established (Fig. 4.14), that resistance of uninhibited acid rain rain and containing ceolite one was in limits of 1000 – 2000 Ohms, and resistance of the solution with zinc phosphate and zeolite composition – in limits of 3000 – 5000 Ohms. Smaller resistance of a corrosion environment can testify about availability of higher concentration of aluminum and and hydrogen ions, indirectly confirming acceleration of aluminum alloy corrosion. It can be supposed using the data that phosphate/zeolite composition significantly decreases of local corrosion of aluminum alloy D16T. However, it is possible to estimate more realistic inhibitor effectiveness from charge transfer resistance kinetic of the alloy. It was established (Fig. 4.15), that the resistance for D16T in the environment inhibited with phosphate/zeolite composition lies

on level of $1 \cdot 10^5$ – $1 \cdot 10^6$ Ohms. This is approximately from one to two orders of magnitude higher than in uninhibited corrosion solution.

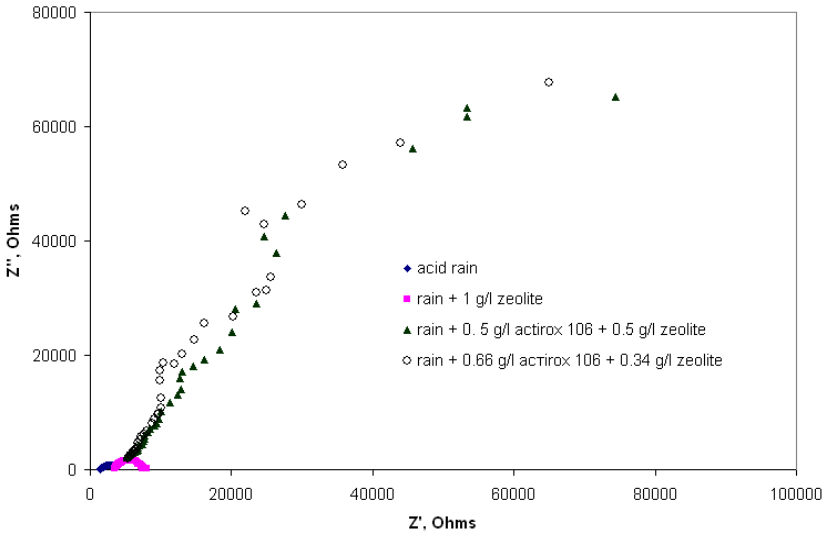

Fig. 4.12. Nyquist impedance diagrams of D16T aluminum alloy after 24 hours exposure in inhibited acid rain solutions.

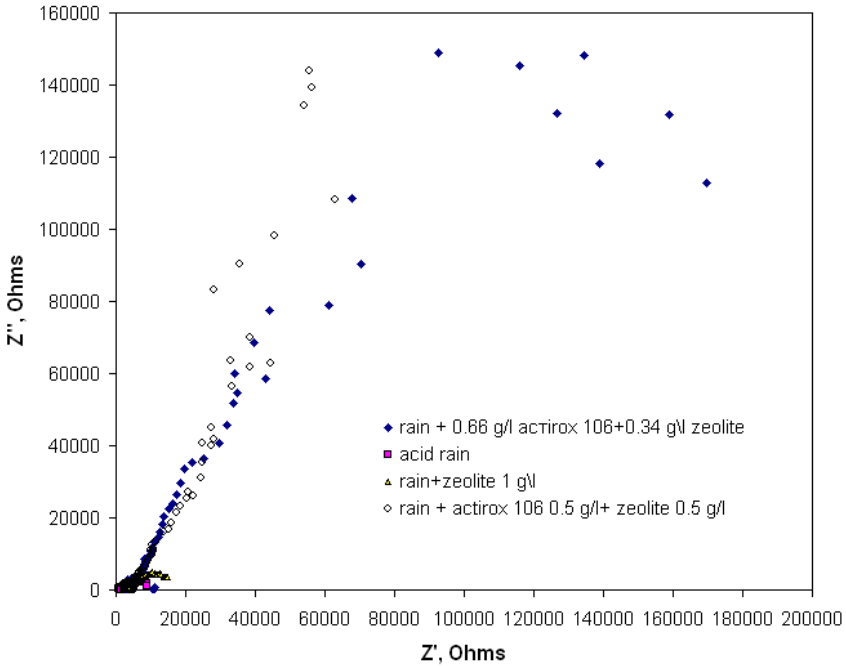

Fig. 4.13. Nyquist impedance diagrams of D16T aluminum alloy after 48 hours exposure in inhibited acid rain solutions.

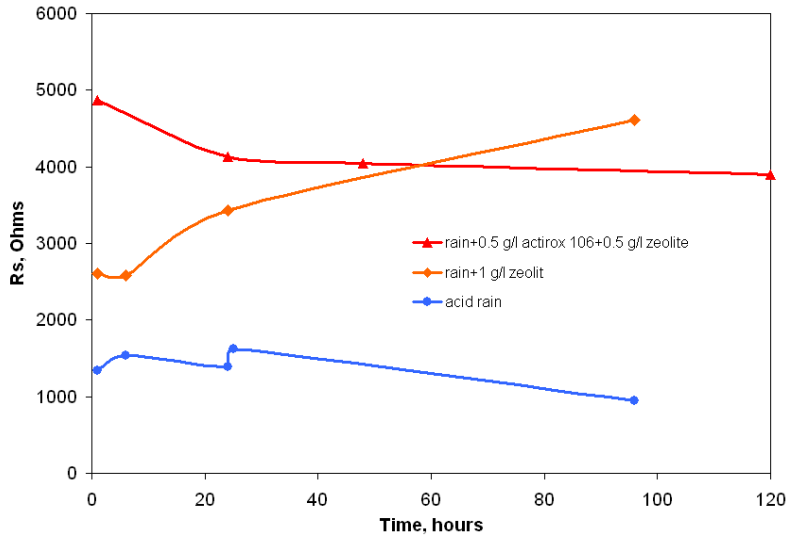

Fig. 4.14. Time dependencies of solution resistance during exposure of D16T alloy in inhibited acid rain.

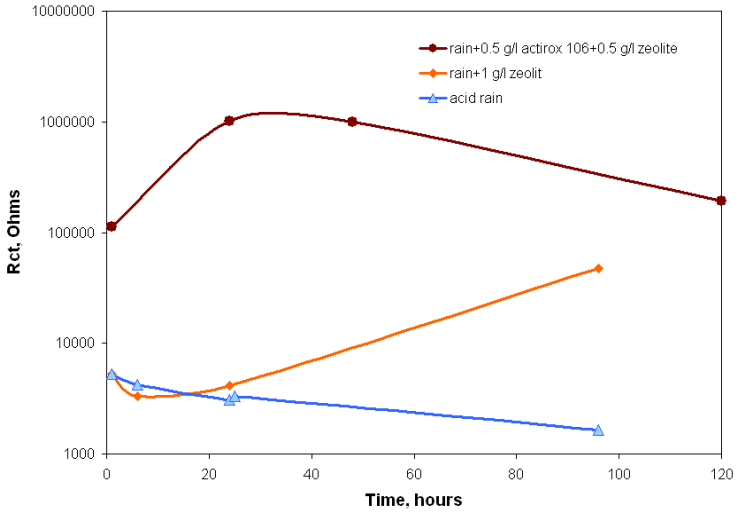

Fig. 4.15. Time dependencies of charge transfer resistance of D16T alloy in inhibited acid rain

Admittance T of constant phase element Q_{dl} (which corresponds to double layer capacitance) is lowest and practically do not changing for the alloy sample in the environment with zinc phosphate/zeolite composition. The admittance of alloy in acid rain solution rises during first day approximately in 10-12 times due to passive film destruction and local corrosion development and further stabilizes on the level of $3 \cdot 10^{-4} – 4 \cdot 10^{-4}$ 1/Ohms (Fig.4.16).

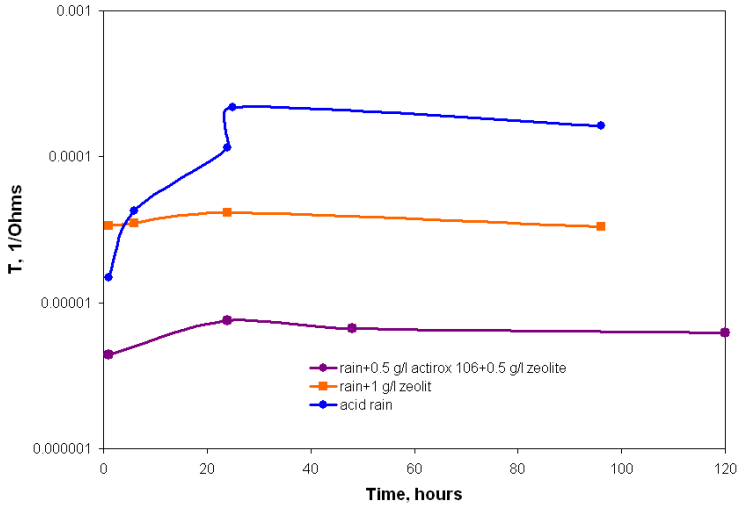

Fig. 4.16. Time dependencies of component P of CPE for D16T alloy in inhibited acid rain

4.4. DC polarization study of D16T alloy in solutions containing phosphate and zeolite blend

The next step in study of effectiveness of phosphate/zeolite composition was DC polarization of D16T alloy in inhibited solutions containing different concentrations of its component (Fig. 4.17, 4.18). It was established that anodic reaction of metal ionization in acid rain solution and zeolite containing solution had higher rate at the beginning of exposure and alloy corrosion was mainly under cathodic control. Ionization of the metal somewhat decreases after 24 hours exposure, possibly due to corrosion product formation. After that anodic currents became identical to cathodic currents. Anodic and cathodic currents essentially decrease at addition of phosphate/zeolite composition into corrosion solution, and pitting potential rises. Minimum anodic and cathode currents are observed at zinc phosphate/zeolite ratio equal to 0.66 g/l/0.34 g/l.

Kinetic dependencies of aluminum alloy corrosion currents in different solutions were obtained by way of graphical extrapolation of tafel slopes on experimental polarization curves (Fig. 4.19). It was established that corrosion currents in uninhibited solution and solution with zeolite increase during exposure in 12-15 times. The phosphate/zeolite composition (0.66/0.34) provides greatest rate of decrease of Al alloy corrosion current in acid rain solution. It should be noted that this occurs at less zinc phosphate content in corrosion solution. A protective film formed on aluminum alloy surface at this concentration can be detected by method of scanning

electron microscopy (Fig. 4.20). The film contains phosphorus (up to 0.25 w.%), zinc (up to 1.9 w.%), calcium (~3 w.%), sulphur, aluminum, oxygen. The mechanism of the film formation needs further investigation. Generally, the film is reasonably effective in corrosion protection of aluminum alloy.

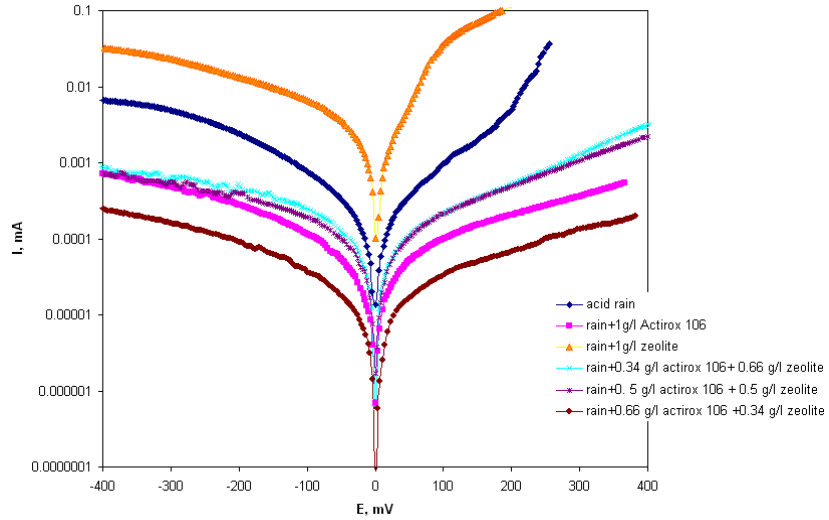

Fig. 4.17. Polarization dependencies of D16T alloys after 3 hours exposure in inhibited acid rain

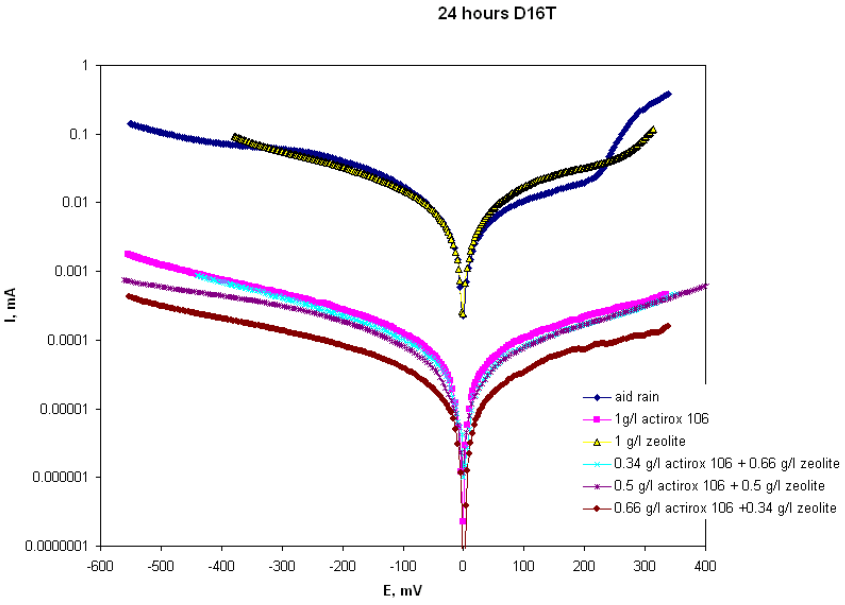

Fig. 4.18. Polarization dependencies of D16T alloys after 24 hours exposure in inhibited acid rain

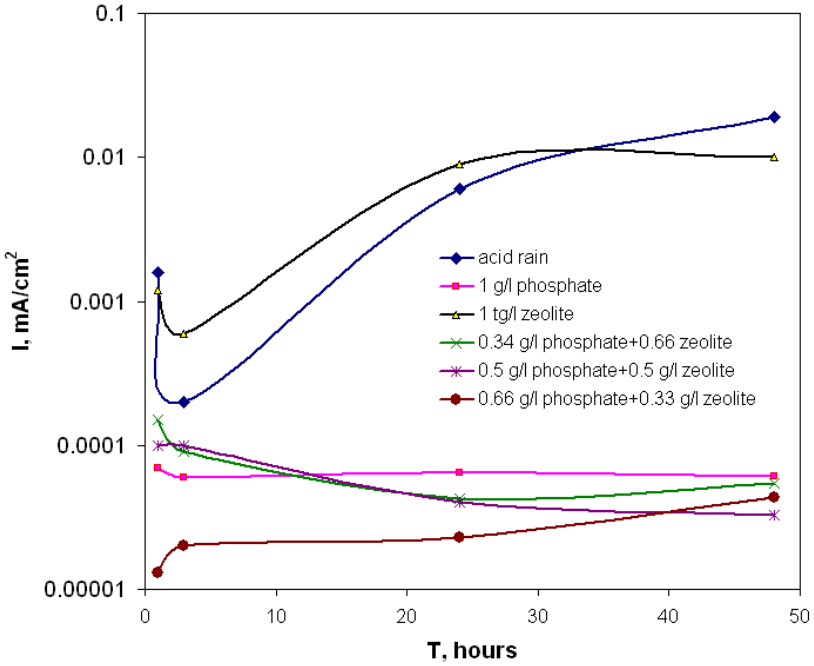

Fig. 4.19. Time dependencies of corrosion current of D16T alloy in inhibited acid rain solutions.

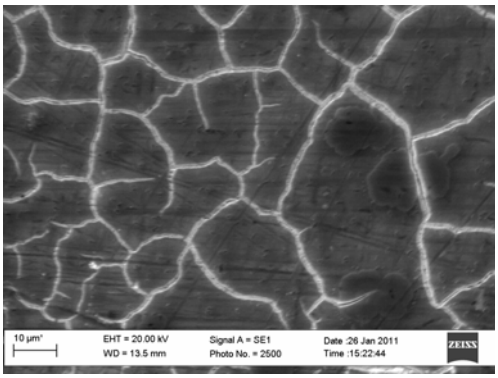

Fig. 4.20. Scanning electron image of surface film on aluminum alloy after its exposure in corrosion solution with phosphate/zeolite composition (phosphate/zeolite ratio - 0.66 g/l/ 0.34 g/l)

4.5. Electrochemical impedance spectroscopy of D16T alloy at cyclic loading in solutions containing phosphate and zeolite blend

Electrochemical impedance spectroscopy is a not destructing method of corrosion study. It is especially important at study of corrosion fatigue of aluminum alloy, because of any polarization can accelerate crack development in the material and falsify results. Aluminum alloy alloy corrosion inhibition at conditions of corrosion fatigue in acid rain solution was studied by

using electrochemical impedance spectroscopy (Fig. 4.21, 4.22). It was established that sizes of impedance semicircles decrease with increase of number of loading cycles. Accordingly both active (Z') and the reactive (Z") components of electrode impedance decrease. However, while these semicircles are complete in uninhibited solution (Fig. 4.21), they are not full in solution inhibited with zinc phosphate/zeolite composition (Fig. 4.22). This indicates strong inhibition of aluminum alloy corrosion.

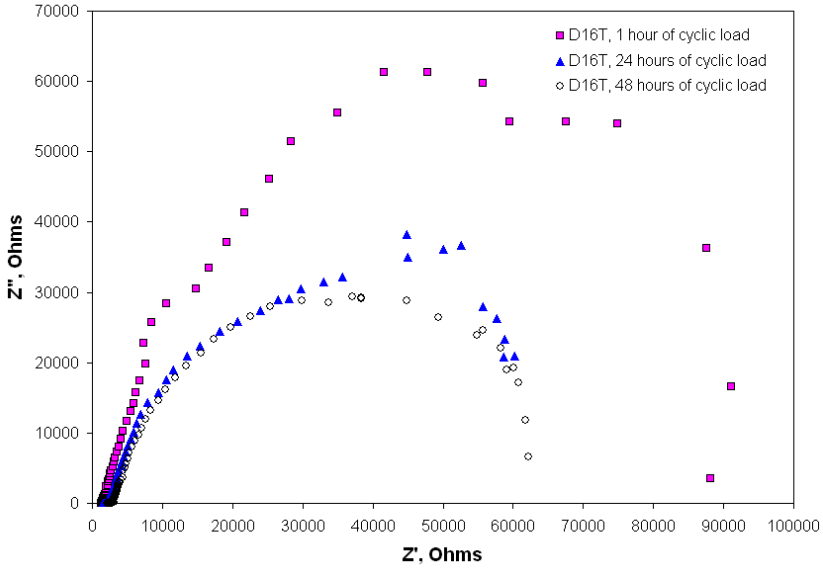

Fig. 4.21. Nyquist impedance diagrams of cyclically loaded aluminum alloy in acid rain solution

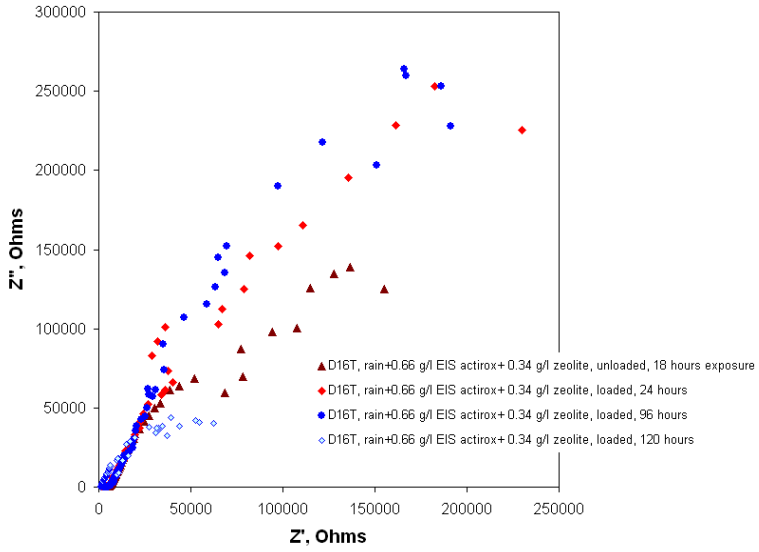

Fig. 4.22. Nyquist impedance diagrams of cyclically loaded aluminum alloy in inhibited acid rain solution

Fitting results of experimental spectra with using electrical equivalent circuit $R_s(Q_{dl}R_{ct})$ are shown in Fig. 4.23 and 4.24. It was established (Fig. 4.23), that resistance of uninhibited environment in electrochemical cell during corrosion fatigue tests is in limits of 1500 – 2500 Ohms, and resistance of solution with zinc phosphate/zeolite composition – in limits of 2000 – 7000 Ohms. Less solution resistance can testify about availability in the solution of higher concentration of hydrogen and aluminum ions, indirectly indicating on acceleration of aluminum alloy corrosion. On the basis of these data, the zinc phosphate/zeolite composition significantly decreases local corrosion of aluminum alloy, can inhibit pitting growth and increase time to corrosion fatigue crack initiation. Charge transfer resistance of aluminum alloy in environment inhibited by zinc phosphate/zeolite composition is on the level of $1.5 \cdot 10^5 – 1 \cdot 10^6$ Ohms, which is approximately in one order of magnitude higher than in uninhibited solution (Fig. 4.24).

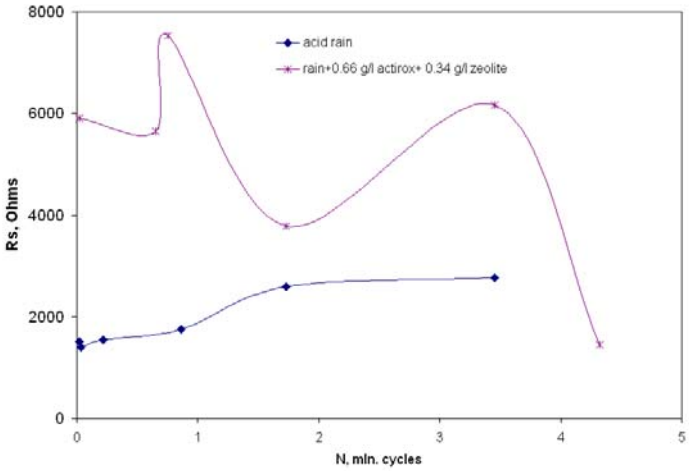

Fig. 4.23. Time dependencies of solution resistance during cyclic loading of D16T alloy in acid rain solutions

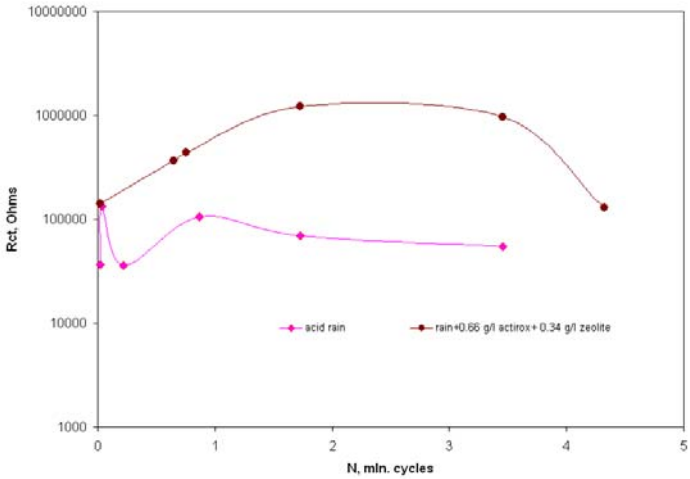

Fig. 4.24. Time dependencies of charge transfer resistance of cyclically loaded aluminum alloy in acid rain solutions

5. STUDY OF AA7075 CORROSION INHIBITION BY PIGMENT BLENDS

Corrosion of aluminum alloy AA7075 was studied in solutions containing filtrates of inhibiting blends – zinc phosphate with Ca-ion exchanged silica, zinc phosphate with bentonite, phosphate with zeolite by method of electrochemical impedance spectroscopy (EIS). Uninhibited acid rain solution and strontium chromate filtrate were used for comparison. The working area of alloy samples was 1 cm^2. It was established (fig. 5.1), that Nyquist impedance dependencies of aluminum alloy AA7075 have form of incomplete semicircles possibly due certain diffusional limitations of corrosion. EIS dependencies of the alloy are approximately on the same level in solutions of inhibited by blends of zinc phosphate/Ca-ion exchanged silica, zinc phosphate/bentonite and zinc phosphate/zeolite. This testifies about similar values of charge transfer resistance. Impedance parameters of the alloy sample in uninhibited acid rain are very low in comparison with samples in inhibited solutions (fig. 5.1).

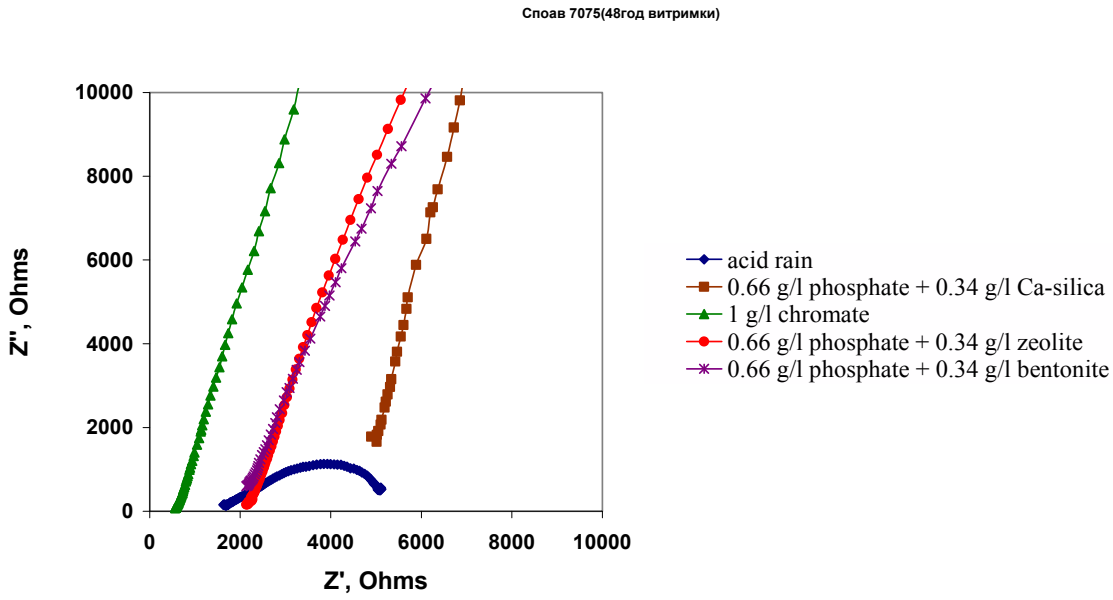

Fig. 5.1 a. Nyquist impedance diagrams of AA7075 aluminum alloy after 48 hours exposure in inhibited acid rain solutions.

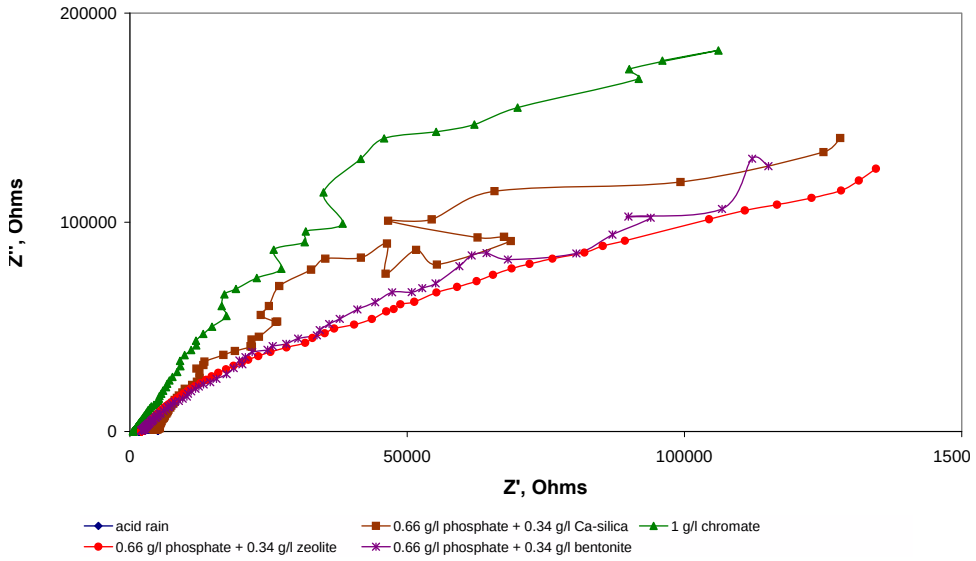

Fig. 5.1 b. Nyquist impedance diagrams of AA7075 aluminum alloy after 48 hours exposure in inhibited acid rain solutions.

The results of potentiodynamic polarization study show (fig. 5.2), that alloy AA7075 corrosion after 48 hours exposure in uninhibited acid rain proceeds with some increase in anodic reaction effectiveness. Both partial reactions of electrochemical corrosion are slowed down in inhibited solutions. Especially it is characteristically for the solution with filtrates of strontium chromate and zinc phosphate/bentonite blend. A current rise is observed at anodic potential of -300 mV on alloy sample immersed in corrosion solution with filtrate of phosphate/Ca-ion exchanged silica blend. This current increase in solutions with phosphate/zeolite and phosphate/bentonite blends occurs at anodic potentials 0 mV and +350 mV respectively. Lowest corrosion currents were detected for alloy AA7075 in chromate containing solution and in solution with filtrate of phosphate/bentonite blend, highest – in uninhibited acid rain.

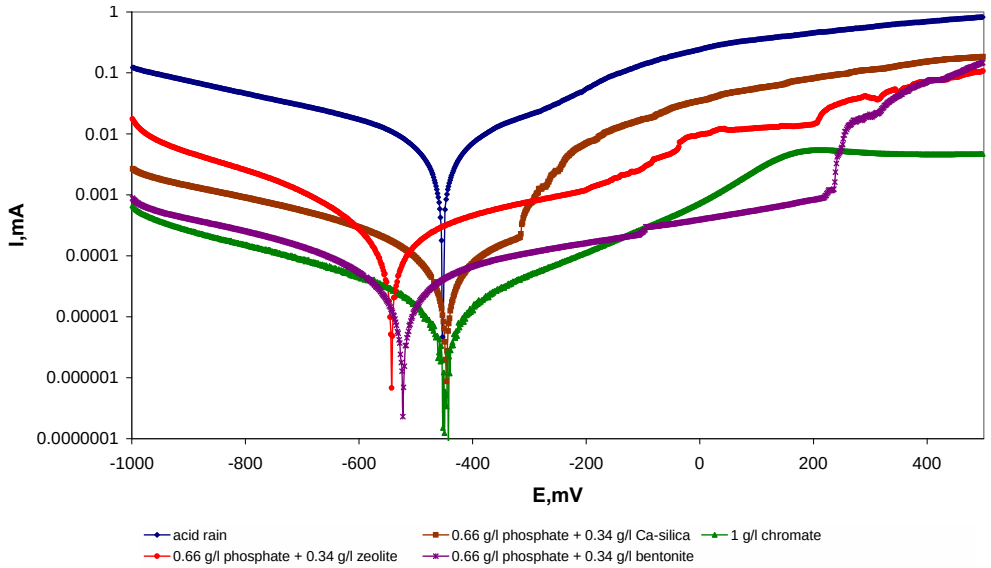

Fig. 5.2. Potentiodynamic polarization dependencies of AA7075 aluminum alloy after 48 hours exposure in inhibited acid rain solutions.

Investigations of aluminum alloy AA7075 surface with the aid of Carl Zeiss Stemi 2000 Stereomicroscope (fig. 5.3) revealed the beginning of local corrosion after 48 hours at absence of an inhibitor in the solution. White and gray corrosion products are clear visible near intermetallic inclusions. The sample exposed to the solution inhibited with blend of zinc phosphate/Ca-ion exchanged silica is in second place. Smallest corrosion is observed on alloy samples in chromate, phosphate/bentonite and phosphate/zeolite solutions.

1 g/l chromate

0.66 g/l phosphate + 0.34 g/l bentonite

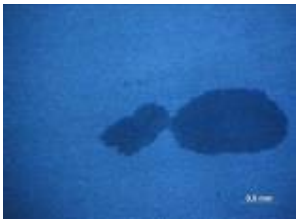

0.66 g/l phosphate + 0.34 g/l zeolite 0.66 g/l phosphate + 0.34 g/l Ca-silica

acid rain

Fig. 5.3. Optical microphotographs of corrosion development on surface of AA7075 alloy after 48 hours exposure in different solutions

6. ELECTROCHEMICAL IMPEDANCE SPECTROSCOPY OF INHIBITED POLYURETHANE COATINGS ON ALUMINIUM ALLOY D16T

Inhibiting pigments - zinc phosphate (Actirox 106), strontium chromate, calcium ion exchange silica (Shieldex CP-4 7394) and zeolite were added in quantity of 3 vol. % to the polyurethane composition. Control polyurethane composition contained 3 vol. % of titanium dioxide. Inhibited compositions after mixing by ultrasonic ultrasonic dispergator were applied on samples of aluminum alloy D16T decreased with Vienna lime. First primer layer had about 40-50 μm thickness. The second uninhibited layer on basis of clear uninhibited composition was applied after hardening of the primer layer. The coating total thickness was about 120 μm. Since inhibiting pigments are designed for metallic substrate protection at paint layer damages, it was used coating samples both undamaged and with artificial defects (through holes of 1 mm diameters). The working area of alloy samples was 6 cm^2.

Electrochemical impedance spectroscopy (EIS) of inhibited coatings on D16T alloy revealed (fig. 6.1), that highest magnitude of impedance was measured for polyurethane coating with chromate free pigment blend. Polyurethane coating with phosphate/zeolite blend has similar protective characteristics to chromate containing one. Coating with blend of zinc phosphate/Ca-ion exchanged silica has something lower impedance parameters. Coatings, inhibited separately by zinc phosphate or zeolite, and uninhibited have smallest sizes of impedance semicircles. This testifies about synergy anticorrosion effect from addition of the phosphate/zeolite composition to polyurethane coating and confirms a possibility for chromate substitution in the primer paint layer.

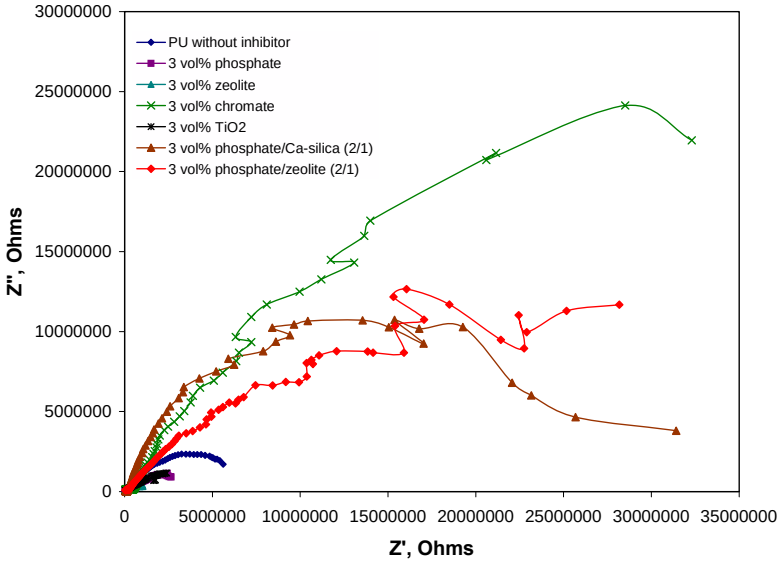

Fig. 6.1. Nyquist impedance plots for D16T alloy with artificially damaged polyurethane coatings after 24 hour exposure in corrosion environment.

Equivalent electrical circuit $\mathbf{R_e(Q_{dl}R_{ct})}$ (fig. 6.2) was used for fitting of experimental data and calculation of electrochemical parameters of coated aluminum alloy samples exposed to aggressive environment. Here $\mathbf{R_e}$ is solution resistance; $\mathbf{Q_{dl}}$ − constant phase element (CPE) related to frequency dependent electrochemical and diffusion processes in double layer on metal and $\mathbf{R_{ct}}$ − charge transfer resistance. Impedance of CPE is described with formula (6.1). Constant phase element is determined by admittance **P** and exponent **n**. In case **n** is equal 1, $\mathbf{Q_{dl}}$ corresponds to capacitance. The parameter **P** represents Warburg impedance when **n** = 0.5. The CPE models heterogeneity of alloy surface in the vicinity of defect caused its local corrosion and surface film formation. Similarly to capacitor, CPE keeps the phase constant at variable frequency but the phase shift differs from 90°. CPE is especially helpful for representing slightly distorted capacitances.

The equivalent circuit (fig. 6.2) is appropriate to this corrosion situation because of investigated polyurethane coatings contain drilled defects. In such way conditions for local underfilm corrosion at defect site were created.

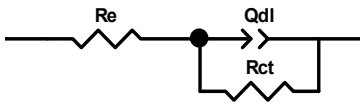

Fig. 6.2. Equivalent electrical circuit for modeling corrosion of epoxy coated aluminum alloy in acid rain solution

$$Z_{Q_{dl}} = \frac{1}{P(j \cdot \omega)^n} \qquad (4.1)$$

where $j = \sqrt{-1}$, ω – angular frequency of AC current

Kinetic dependencies of resistance $\mathbf{R_{ct}}$, and admittance **P** are presented in fig. 6.3, 6.4. Charge transfer resistance (fig. 6.3) is highest for polyurethane coatings containing strontium chromate and chromate-free pigment blend on basis phosphate/zeolite. The resistance is on level of $5 \cdot 10^7 ... 1 \cdot 10^8$ Ohms. Phosphate and zeolite, used separately in the coatings, insignificantly influence charge transfer resistance of the alloy. The blend of phosphate/Ca-ion exchanged silica behaves controversially and did not show stabile protection. Alloy samples with coatings without inhibitor and with addition of single pigments, either phosphate or zeolite do not have high charge transfer resistance.

Component **P** of constant phase element $\mathbf{Q_{dl}}$ during tests is lowest for coating samples with chromate pigment and pigment composition on basis of zinc phosphate and zeolite (fig. 6.4). **P** for them does not exceeds the level of $4{,}0 \cdot 10^{-7}$ 1/Ohms. The sample of aluminum alloy protected by polyurethane coating with phosphate pigment has intermediate admittance. **P** of uninhibited coating is higher and later gradually exceeds the level of $1.0 \cdot 10^{-6}$ 1/Ohms possibly due to under film corrosion development. The parameter **P** has directly proportional dependence from corroding surface area. It can be concluded on basis of kinetic of P that coatings containing titanium dioxide as single filler have worst protective properties.

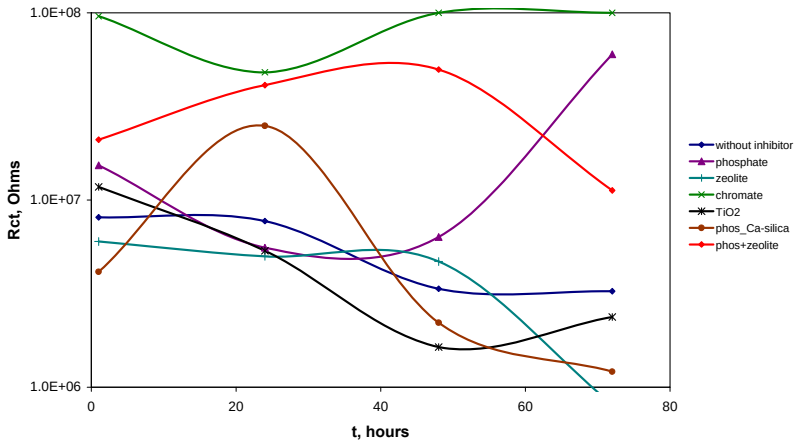

Fig. 6.3. Time dependencies of charge transfer resistance R_{ct} of D16T aluminum alloy with inhibited polyurethane coatings in acid rain solution. Coatings contain phosphate, zeolite, chromate titanium dioxide, blends of phosphate/Ca-ion exchange silica and phosphate/zeolite at 3

3 vol%.

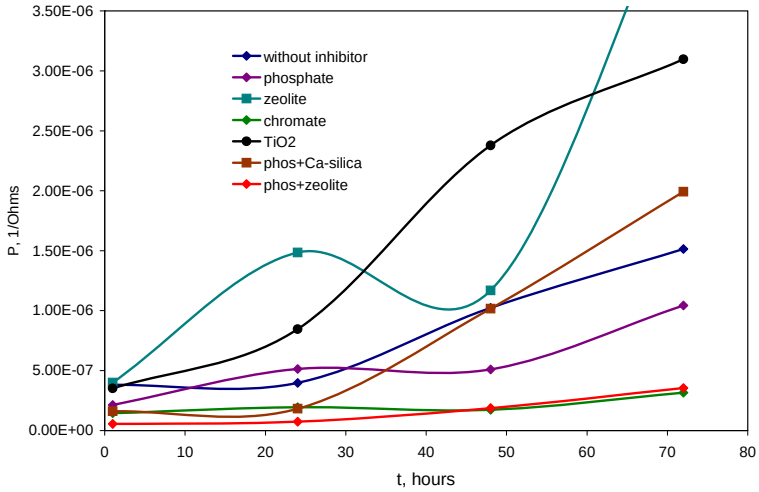

Fig. 6.4. Time dependencies of admittance P of CPE for D16T aluminum alloy with inhibited polyurethane coatings in acid rain solution. Coatings contain phosphate, zeolite, chromate titanium dioxide, blends of phosphate/Ca-ion exchange silica and phosphate/zeolite at 3 vol%.

7. EFFECT OF CORROSION FATIGUE LOADING ON PROTECTIVE PROPERTIES OF INHIBITED POLYURETHANE COATINGS

7.1. EIS of unstressed samples

Samples of aluminum alloy with double-layer polyurethane coatings were preliminary studied without a corrosion-fatigue load. Inhibited polyurethane primer was applied as a first layer and a clear polyurethane lacquer - as a top layer. The total thickness of the coating was 120 ... 150 microns. Primers have been varied by inhibiting pigment composition. The total concentration of inhibiting pigments in the primer coatings was 3 vol. %. The results of studies of protective properties of inhibited polyurethane coatings on aluminum alloy by electrochemical impedance spectroscopy are presented in Fig. 7.1, 7.2. The working area of the sample was 7 cm^2. Coatings contained a through defect (a scratch of 1 cm length). Studies have shown that the impedance characteristics of uninhibited coating at different exposure times are lowest, and inhibited by strontium chromate - highest. Within 48 hours of test impedance module at low frequencies and therefore the charge transfer resistance of the coated sample with chromate inhibitor is highest, followed by the value of the module of impedance for coating with phosphate/zeolites inhibitor blend. Third place has the coating with phosphate / calcium ion exchange pigment. The value for uninhibited coating is relatively very low. It should be noted

close protective properties of coatings inhibited with a mixture of phosphate/ zeolite and chromate containing coating. Also it can be observed a significant decrease of resistance of the electrolyte in the presence in polyurethane coating of chromate inhibitor. This is due to its high solubility and ultimately can cause blistering of coating in corrosive environments. At the same time, the resistance of electrolyte in contact with the coating inhibited by phosphate and zeolite blend after 24 and 48 hours of exposure is the highest, which indirectly indicates a reduction of aluminum ions in corrosion solution and inhibition of corrosion processes.

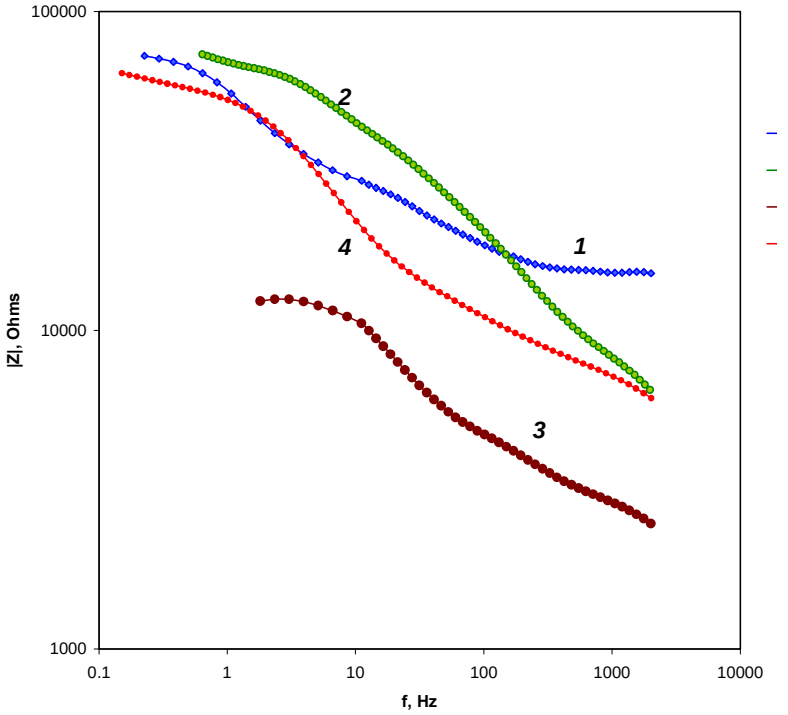

Fig. 7.1. Bode impedance diagrams of aluminum alloy samples with damaged polyurethane coatings after 24 hours of exposure in acid rain solution: 1) polyurethane coating inhibited with zinc phosphate/zeolite blend; 2) polyurethane coating inhibited with strontium chromate; 3) uninhibited polyurethane coating; 4) polyurethane coating inhibited with zinc phosphate/calcium ion exchange silica blend.

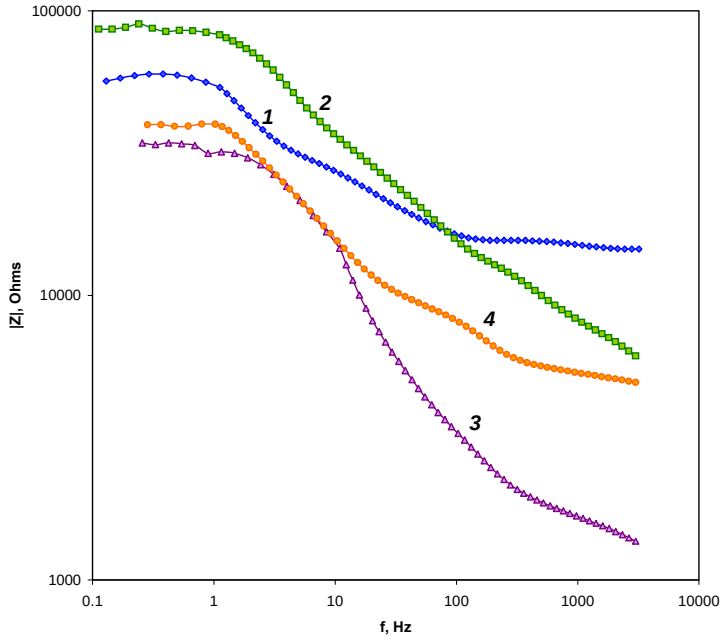

Fig. 7.2. Bode impedance diagrams of aluminum alloy samples with damaged polyurethane coatings after 48 hours of exposure in acid rain solution: 1) polyurethane coating inhibited with zinc phosphate/zeolite blend; 2) polyurethane coating inhibited with strontium chromate; 3) uninhibited polyurethane coating; 4) polyurethane coating inhibited with zinc phosphate/calcium ion exchange silica blend.

7.2. EIS of round samples after corrosion fatigue

EIS spectra of samples with inhibited polyurethane coatings firstly have been obtained on unstressed round samples after 1 hour of exposure in acid rain. After that the samples were cyclically loaded during 24 hours and 48 hours in corrosive environment and studied with electrochemical impedance spectroscopy (Fig. 7.3, 7.4.). Coatings samples were preliminary damaged by a way of drilling of hole in order to simulate penetrating defect and to initiate protective action of inhibitors. The obtained data indicate a significant impact of applied cyclic stress on the protective properties of inhibited and uninhibited polyurethane coatings. Charge transfer resistance of aluminum alloy with polyurethane coatings decreases with increasing of cyclic loading time. It can seen (Fig. 7.4), that chromate containing coating has better protective properties initially in unloaded state, but later after cyclic load the charge transfer resistance of the sample is reduced approximately in 10 times simultaneously with the decrease of resistance of corrosive environment. It is likely that cyclic mechanical stresses accelerate the dissolution and leaching of chromate from polyurethane coating. Polyurethane coating sooner loses protective properties as a result of this dissolution process. Polyurethane coatings inhibited with chromate-free mixtures are comparable or even slightly better in their protective properties with

chromate containing coating under conditions of corrosion fatigue (Fig. 7.4). However, it is necessary for making of final conclusions to carry out further corrosion-fatigue studies of inhibited polyurethane coatings, including those with different concentrations of the same inhibitors.

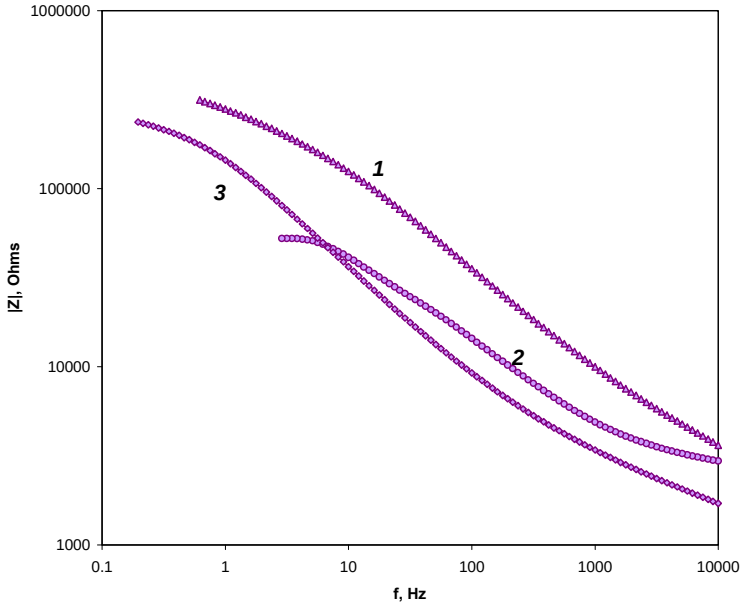

Fig. 7.3. Bode impedance diagrams of aluminum alloy D16T with damaged clear polyurethane coatings after 1 hour (1), 24 hours (2) and 48 hours (3) of cyclic loading in acid rain solution at $\sigma = \pm 75 MPa$.

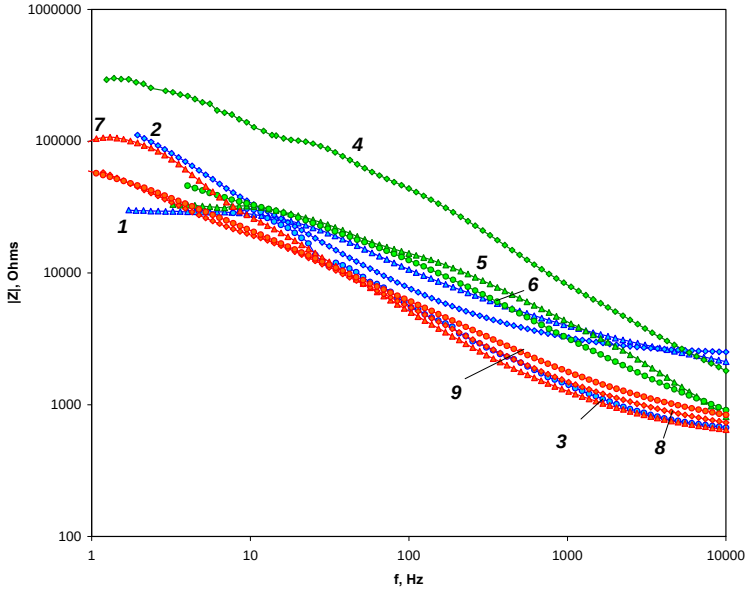

Fig. 7.4. Bode impedance diagrams of aluminum alloy D16T with damaged polyurethane coatings inhibited with phosphate/zeolite blend after 1 hour (2), 24 hours (1) and 48 hours (3); inhibited with strontium chromate after 1 hour (4), 24 hours (5) and 48 hours (6); inhibited with phosphate/calcium containing silica blend after 1 hour (7), 24 hours (8) and 48 hours (9) of cyclic loading in acid rain solution $\sigma = \pm 100 MPa$.

7.3. EIS of flat samples after corrosion fatigue

Corrosion fatigue and impedance study of flat samples of aluminum alloy showed that the presence of chromate inhibitor in polyurethane coating slows down its degradation under cyclic loading in acid rain solution and improves its protective properties (Fig. 7.5). A difference in impedance module between inhibited and uninhibited coatings was about 5-8 times for all frequency range with benefit for inhibited sample after 24 hours of cyclic loading. The sample with uninhibited polyurethane coating fractured after 48 hours of cyclic loading.

Impedance spectra of aluminum alloy with polyurethane coatings were fitted using EIS Spectrum Analyzer [83]. Equivalent circuit $R_e(QR_{ct})$ [83-85] was used, where R_e - resistance of electrolyte in the cell, R_{ct} - charge transfer resistance of the metal, Q - constant phase element. Results of fitting procedure are presented in Fig. 7.6. It can be concluded from these data that decrease of charge transfer resistance is observed for both samples of chromate containing and uninhibited polyurethane coatings with increase of cyclic loading time. This fact most likely may indicate an increase of under paint corrosion area around the through defect in the coating. However, solution resistance in both cases not differs significantly, probably due to hydration of strontium chromate and its leaching from polyurethane coating.

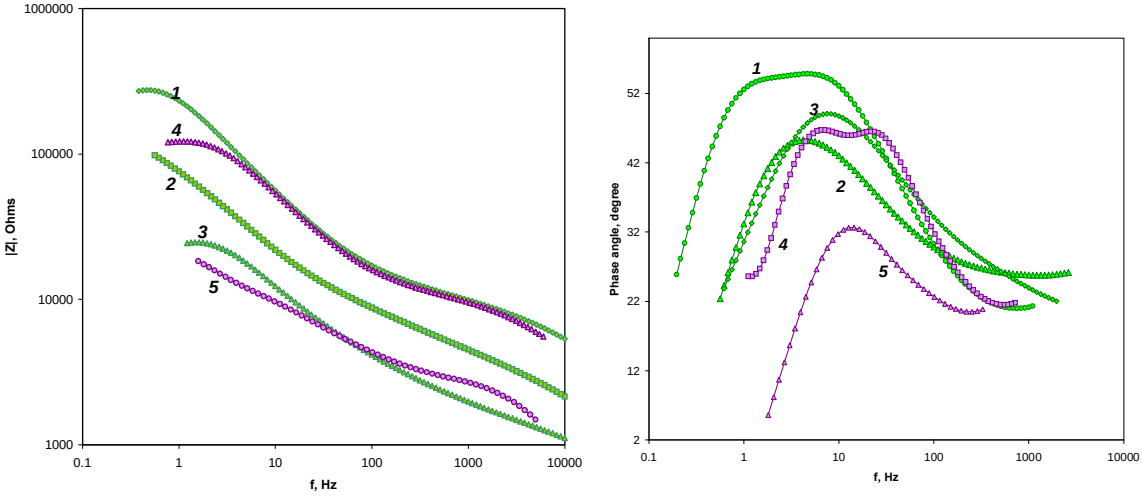

Fig. 7.5. Bode and phase angle diagrams of flat samples of alloy D16T with damaged chromate containing polyurethane coating after 1 hour (2), 24 hours (1) and 48 hours (3) and uninhibited polyurethane coating 1 hour (4) and 24 hours (5) of cyclic loading in acid rain solution $\sigma = \pm 180 MPa$.

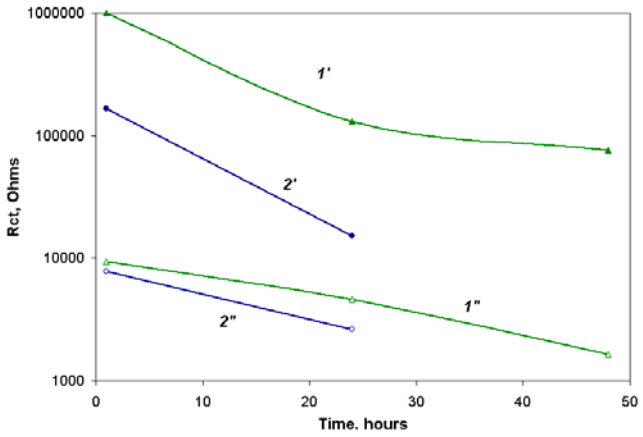

Fig. 7.6. Time dependencies of charge transfer resistance R_{ct} (1', 2') and solution resistance R_e (1", 2") for chromate containing (1',1") and uninhibited polyurethane coatings (2',2").

8. DC POLARIZATION STUDY OF ALUMINIUM ALLOY CORROSION IN ACID RAIN SOLUTION INHIBITED WITH PHOSPHATE/MODIFIED ZEOLITE BLENDS

It was interesting to study of the effect of protection of aluminum alloy from corrosion by addition to acid rain solution of zinc phosphate, zeolite and mixtures thereof. It was investigated two types of inhibiting mixtures – phosphate with Ca-containing and Zn- containing zeolites. Experiments have revealed more larger anodic and cathodic currents on aluminum alloy in uninhibited acid rain solution and the solution containing unmodified natural zeolite (Fig. 8.1, 8.2, 8.3). An addition to corrosive environment of zinc phosphate/Ca-ion exchanged zeolite composition under 2/1 component ratio in the total amount of 1 g/l significantly slows down aluminum ionization and cathode reaction. Pigments due to their inhibiting effectiveness could be placed in next order: By increasing the effectiveness of protective actions inhibiting pigments can ranged as follows: natural zeolite $\prec$ phosphate/Zn-zeolite $\prec$ phosphate/Ca-zeolite. It is possible that calcium ions enter into synergistic interaction with zinc phosphate. A similar effect was observed for calcium containing inhibiting pigment on galvanized steel [86]

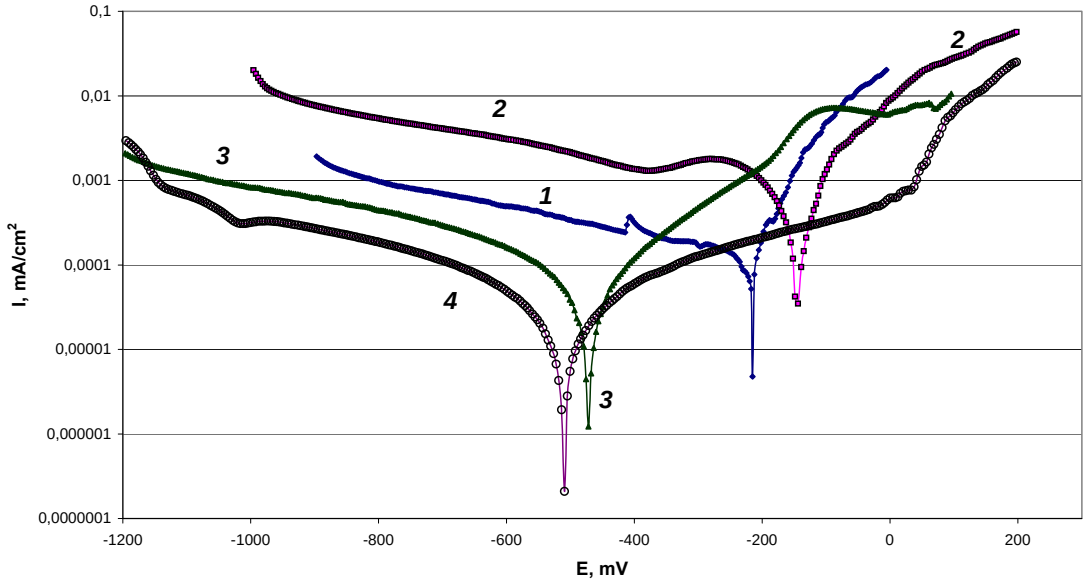

Fig. 8.1. Polarization dependencies of D16T alloy after 3 hours exposure in acid rain solution (1), in acid rain containing 1 g/l natural zeolite (2), 0.66 g/l zinc phosphate and 0.34 g/l Zn-ion exchanged zeolite (3), 0.66 g/l zinc phosphate and 0.34 g/l Ca-ion exchanged zeolite (4).

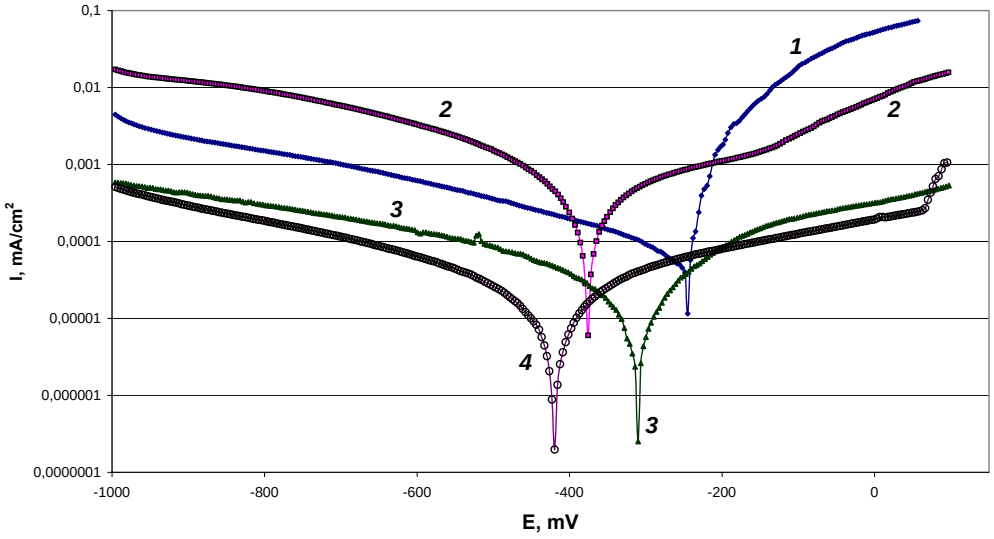

Fig. 8.2. Polarization dependencies of D16T alloy after 24 hours exposure in acid rain solution (1), in acid rain containing 1 g/l natural zeolite (2), 0.66 g/l zinc phosphate and 0.34 g/l Zn-ion exchanged zeolite (3), 0.66 g/l zinc phosphate and 0.34 g/l Ca-ion exchanged zeolite (4).

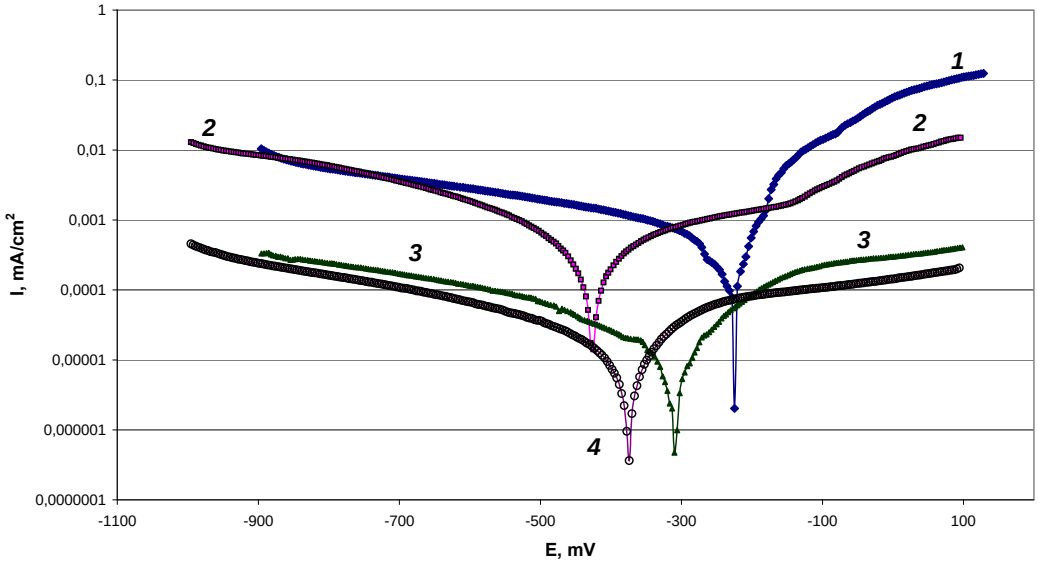

Fig. 8.3. Polarization dependencies of D16T alloy after 48 hours exposure in acid rain solution (1), in acid rain containing 1 g/l natural zeolite (2), 0.66 g/l zinc phosphate and 0.34 g/l Zn-ion exchanged zeolite (3), 0.66 g/l zinc phosphate and 0.34 g/l Ca-ion exchanged zeolite (4).

Graphical calculation of corrosion currents for aluminum alloy in acid rain solutions shows (Fig. 8.4), that corrosion of the alloy in uninhibited environment grows during testing. It is possible that local corrosion develops faster in this case, surface oxide film is destroyed, pittings are generated. Unmodified natural zeolite has some protective properties. Possible, It takes part in ion exchange processes with ions from corrosion environment such as Al^{3+} and H^{+}, releasing calcium ions instead of them. Modified zeolites in mixtures with zinc phosphate relatively well inhibit corrosion of aluminum alloy in this environment. Lowest corrosion currents and metal corrosion were observed in the extract of Ca-zeolite and phosphate blend.

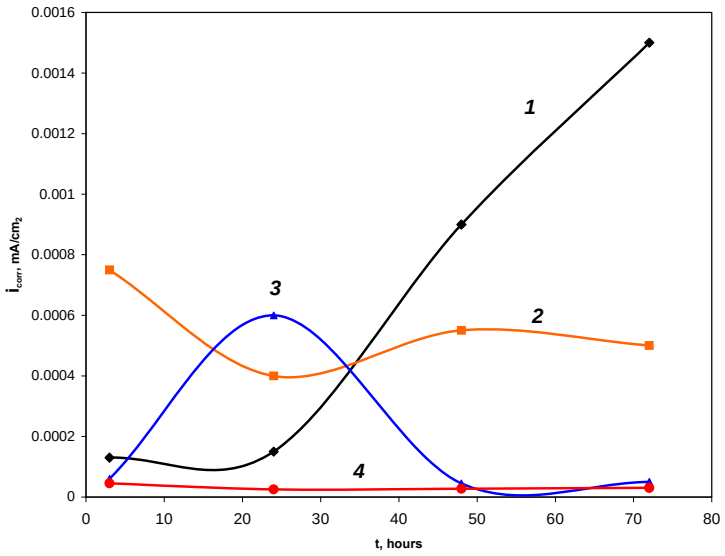

Fig. 8.4. Time dependencies of corrosion current for D16T alloy in acid rain solution (1), in acid rain containing 1 g/l natural zeolite (2), 0.66 g/l zinc phosphate and 0.34 g/l Zn-ion exchanged zeolite (3), 0.66 g/l zinc phosphate and 0.34 g/l Ca-ion exchanged zeolite (4).

9. CYCLIC LOADING EFFECT ON PROTECTIVE PROPERTIES OF POLYURETHANE COATINGS INHIBITED WITH PHOSPHATE/MODIFIED ZEOLITE BLENDS

9.1. Coatings on flat aluminum alloy samples

Electrochemical impedance spectroscopy results obtained for coated aluminum alloy samples under corrosion fatigue conditions testify about significant impact of cyclic loading on protective properties of uninhibited polyurethane coatings. It can be seen from Bode impedance diagrams (Fig. 9.1, 9.2), that, in principle, the tendency of impedance module decreasing is revealed in case both unloaded polyurethane coated samples and alloy samples subjected to cyclic stress over wide frequency diapason of alternating current − from 0.1 to 1000 Hz. The impedance reduction is especially noticeable after 120 hours exposure in corrosion solution. However, comparison of data obtained for the loaded and unloaded samples of aluminum alloy with uninhibited polyurethane coating, shows that their impedance characteristics are lowered more significantly under corrosion fatigue loading. The difference in impedance module between loaded and unloaded samples can make up to 5-7 times.

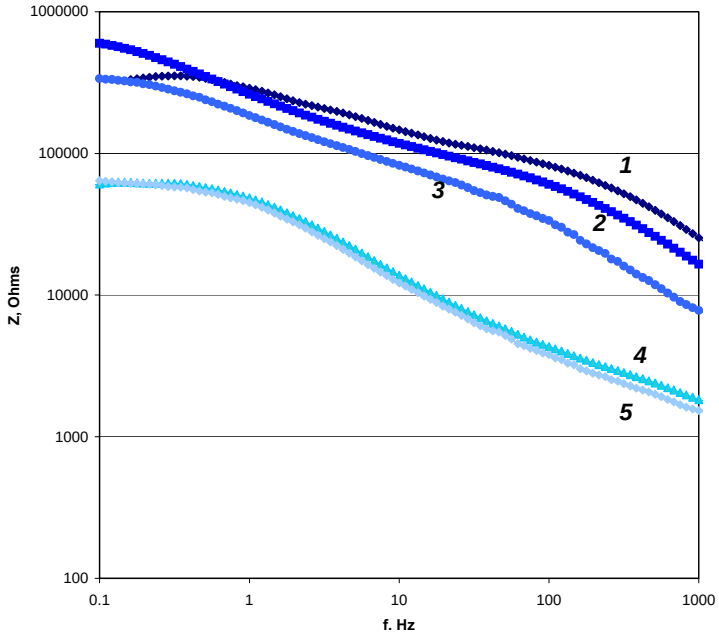

Fig. 9.1. Bode impedance diagrams of D16T alloy flat samples with uninhibited polyurethane coatings after 3 hours (1), 24 hours (2) , 48 hours (3) and 120 hours (4) exposure in acid rain solution.

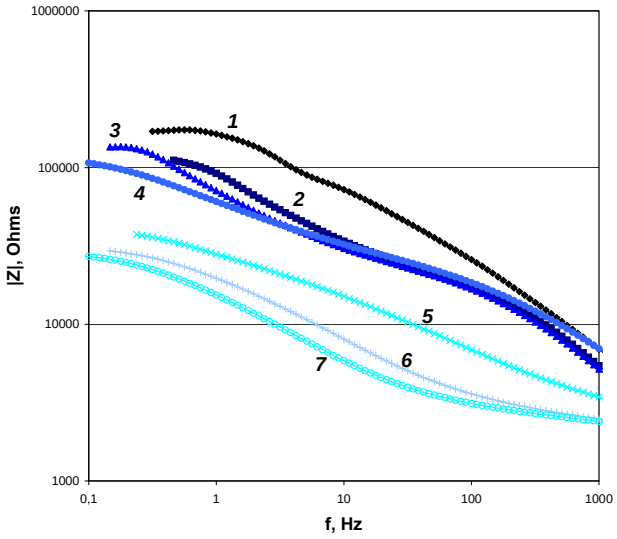

Fig. 9.2. Bode impedance diagrams of D16T alloy flat samples with uninhibited polyurethane coatings after 4.5 hours (1), 24 hours (2), 48 hours (3), 72 hours (4), 120 hours (5), 168 hours (6) and 216 hours (7) of cyclic loading in acid rain solution

The addition of chromate free pigment blend (phosphate/Ca-zeolite) increases impedance

module of protected samples of aluminum alloy, both not stressed and under cyclic loads in corosion environment compared to clear polyurethane coating (Fig. 9.3, 9.4.).

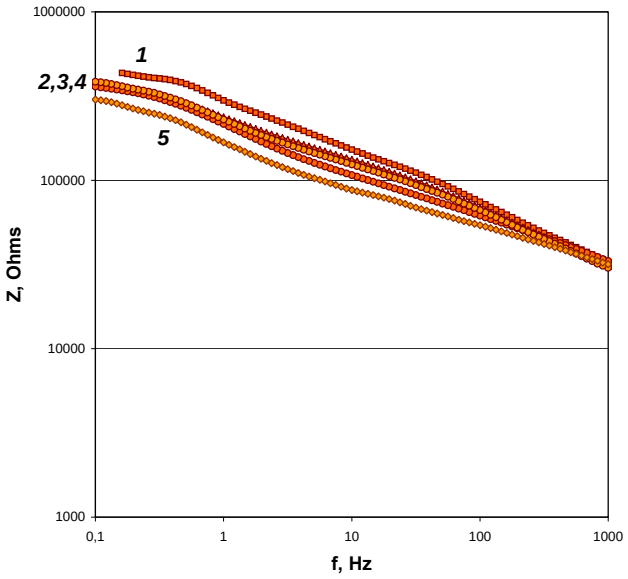

Fig. 9.3. Bode impedance diagrams of D16T alloy samples with polyurethane coatings inhibited by zinc phosphate and Ca-zeolite after 24 hours (1), 48 hours (2), 72 hours (3), 120 hours (4) and 168 hours (5) exposure in acid rain solution.

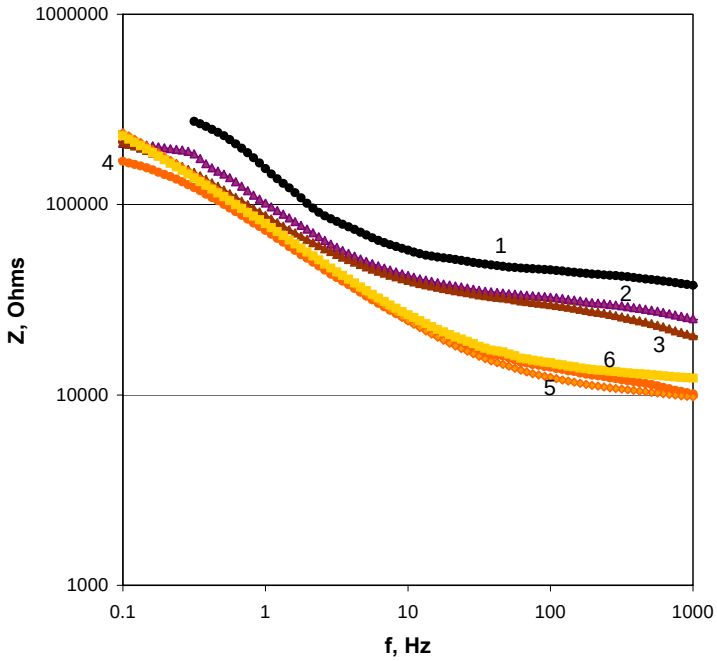

Fig. 9.4. Bode impedance diagrams of D16T alloy samples with polyurethane coatings inhibited by zinc phosphate and Ca-zeolite after 6 hours (1), 24 hours (2), 48 hours (3), 72 hours (4), 112 hours (5) and 144 hours (6) of cyclic loading in acid rain solution.

Impedance spectra of aluminum alloy with polyurethane coatings were fitted using EIS Spectrum Analyzer [83]. Equivalent circuit $R_e(QR_{ct})$ [84,85] was used to model corrosion behavior of aluminum alloy with polyurethane coatings. R_e is resistance of electrolyte in the cell, R_{ct} - charge transfer resistance of the metal, P of Q (constant phase element) represents of double layer capacitance. Results of fitting procedure are presented in Fig. 9.5, 9.6, 9.7. It can be seen from these data, that decrease of charge transfer resistance takes place for both samples of chromate-free containing and uninhibited polyurethane coatings with increase of testing time. This fact most likely indicates an increase of under paint corrosion area around the through defect in the coating. The difference in charge transfer resistance for loaded and unloaded alloy samples alloy with clear polyurethane coatings became minimal after 3 days exposure, and solution resistance not differs significantly (Fig. 9.5, 9.6). Resistance to charge transfer of inhibited alloy sample without loading is highest and after 168 hours exposure is approximately $4.0*10^5$ Ohms. The resistance for inhibited sample under load is reduced within 24 hours of cyclic loading to the level below $2.5\text{-}2.8*10^5$ Ohms, that is higher than values obtained for the aluminum alloy with clear polyurethane coating under conditions of corrosion fatigue. Solution resistance in the cell with placed sample is lowest in case of uninhibited polyurethane coating samples unloaded and under cyclic load (Fig. 9.6), which may indicate about an increase of concentration of metal and hydrogen ions in the solution due to under paint corrosion of aluminum alloy. At the same time solution resistance in case of aluminum alloy with inhibited coating is higher. Time dependence of the phase constant parameter R (double layer capacitance) (Fig. 9.7) correlates with the data of the kinetics of charge transfer resistance and electrolyte resistance.

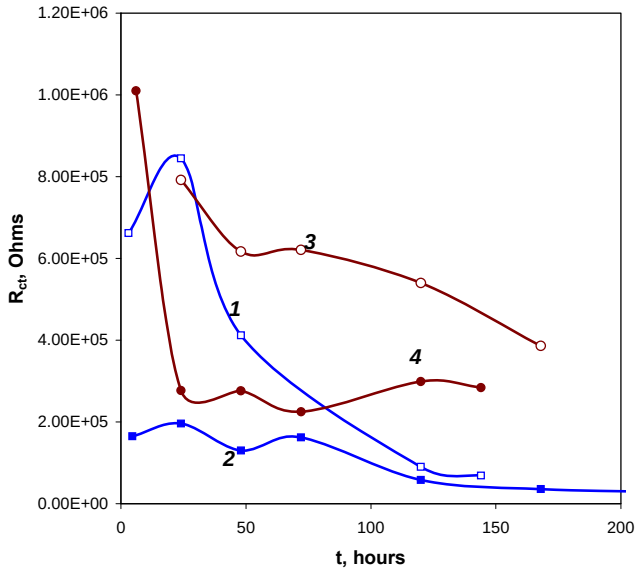

Fig. 9.5. Time dependencies of charge transfer resistance of D16T alloy flat samples with polyurethane coatings uninhibited (1,2); inhibited by zinc phosphate and Ca-zeolite (3,4); without loading (1,3) and under cyclic loading (2,4) in acid rain solution.

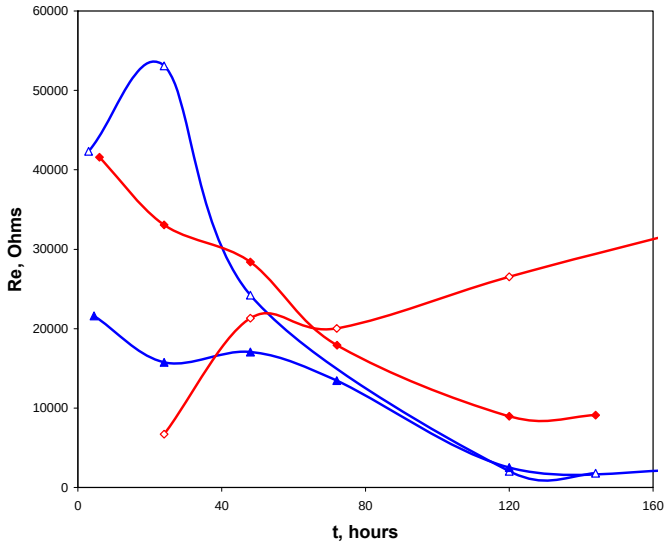

Fig. 9.6. Time dependencies of solution resistance during exposure of coated D16T alloy flat samples in acid rain solution: uninhibited coatings (1,2); inhibited by zinc phosphate and Ca-zeolite (3,4); without loading (1,3) and under cyclic loading (2,4).

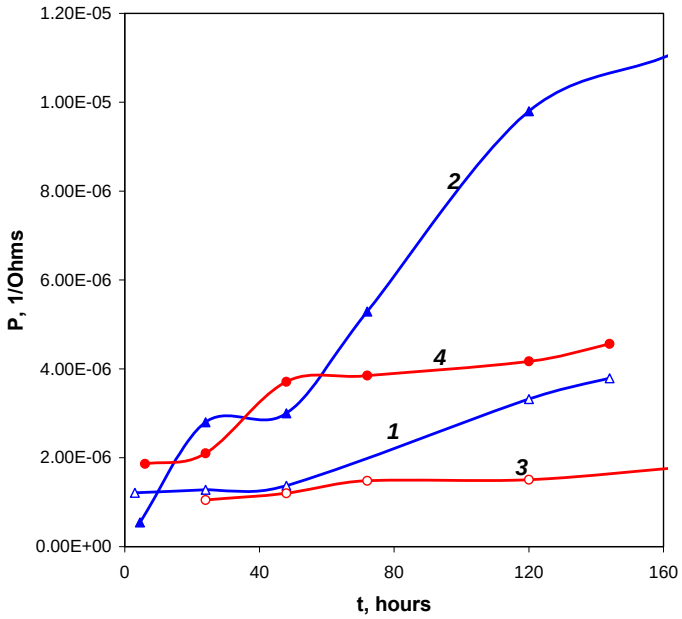

Fig. 9.7. Time dependencies of double layer capacitance (P of Q) of D16T alloy flat samples with polyurethane coatings uninhibited (1,2); inhibited by zinc phosphate and Ca-zeolite (3,4); without loading (1,3) and under cyclic loading (2,4) in acid rain solution.

9.2. Round samples with polyurethane coatings

Round samples tests at stress level of 150 MPa have revealed positive effects of intact undamaged polyurethane coatings on cyclic durability of aluminum alloy in acid rain solution (Fig. 9.8). The polyurethane coating with strontium chromate inhibitor provides highest cyclic endurance of the aluminum alloy in the corrosive environment - approximately 7.5 times greater compared to unprotected sample. The polyurethane coating inhibited by phosphate/Ca-zeolite mixture increases endurance of the alloy for the specified load level approximately in 7.0 times.

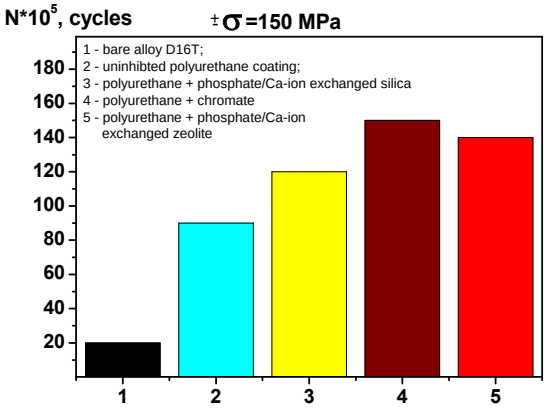

Fig. 9.8. Corrosion endurance diagram for aluminum alloy round samples with polyurethane

coatings: 1 – bare D16T alloy; 2 – uninhibited polyurethane coating; 3 – polyurethane coating + phosphate/Ca-ion exchanged silica; 4 – polyurethane coating + strontium chromate; 5 – polyurethane coatings + phosphate/Ca-ion exchanged zeolite.

9. 3. Influence of chromate-free pigment blend concentration on protective properties of polyurethane coatings

EIS study of aluminum alloy D16T with 1 cm long scratch polyurethane coatings inhibited by different concentrations of phosphate / zeolite blends has showed a greater inhibition effect on the use of Ca-zeolite than Zn-zeolite (fig. 9.9). Addition to polyurethane composition of zinc phosphate/Ca-zeolite blend at 10 mass % concentration provides larger charge transfer resistance of coated aluminum alloy.

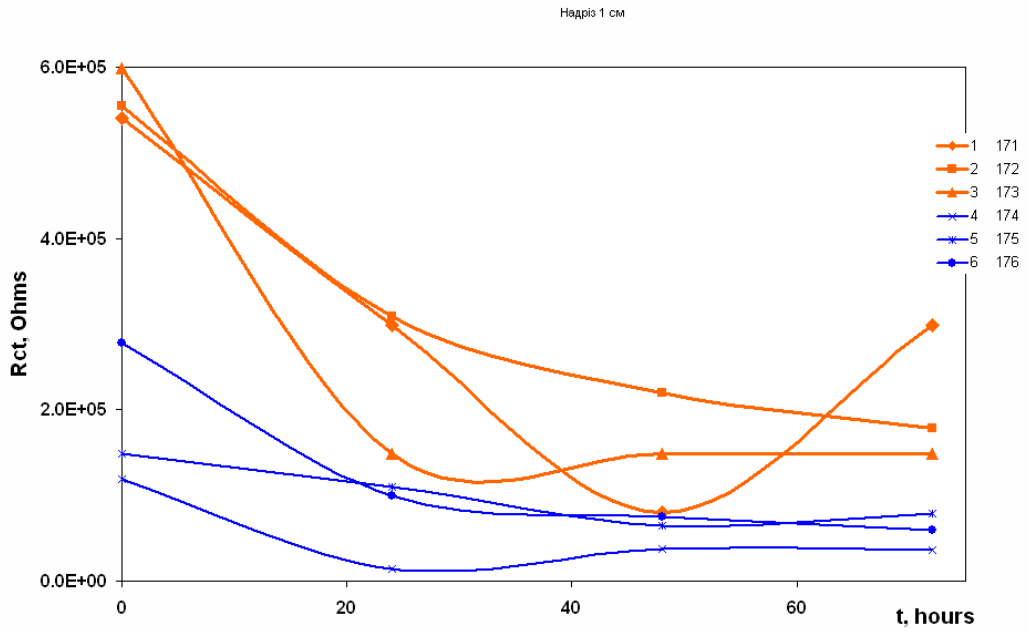

Fig. 9.9. Time dependencies of charge transfer resistance of aluminum alloy samples with polyurethane coatings in acid rain solution: 1) coating inhibited with 5 mass % of blend Ca-zeolite/zinc phosphate; 2) coating inhibited with 10 mass % of blend Ca-zeolite/zinc phosphate; 3) coating inhibited with 15 mass % of blend Ca-zeolite/zinc phosphate; 4) coating inhibited with 5 mass % of blend Zn-zeolite/zinc phosphate; 5) coating inhibited with 10 mass % of blend Zn-zeolite/zinc phosphate; 6) coating inhibited with 15 mass % of blend Zn-zeolite/zinc phosphate. The ratio between zinc phosphate and zeolites in the blends was 2/1 by mass and working area of coated samples - 6.6 cm^2.

CONCLUSIONS

Addition of strontium chromate to acid rain solution increases resistance of aluminum alloy D16T to corrosion fatigue destruction. Fatigue limit of the alloy in inhibited by chromate corrosion environment reaches nearly about 160 MPa after $5.5 \cdot 10^6$ cycles.

Chromate decreases probability of pits initiation, however it accelerates cathodic reaction on mechanically activated surface of aluminum alloy. Chromate layer on aluminum alloy is less strong and less wear resistant than aluminum oxide and zinc phosphate films. Zinc phosphate in contrast to strontium chromate decreases tribocorrosion aluminum alloy in acid rain in 1.5-2 times.

Corrosion current and charge transfer resistance decrease in one-two orders of magnitude for aluminum alloy in acid rain solution with addition of inhibiting composition on basis zinc phosphate and zeolite. The composition significantly inhibits aluminum alloy corrosion under fatigue loading.

The synergism of protective action of the couple "phosphate/ion exchange pigment" is possibly caused by the ion exchange pigment collecting of some undesirable ions from the corrosion solution and releasing of calcium ions, which can than react with phosphate ions.

Investigations of alloy AA7075 corrosion in acid rain solution, inhibited by chromate-free blends of zinc phosphate with bentonite, zeolite and calcium containing pigment have revealed significant increase of an inhibiting effect at combined use of phosphate and other pigments, able to Ca-ion exchange with solution components. Single use of zinc phosphate and these ion exchanged pigments for corrosion inhibition do not provide desired effect.

Charge transfer resistance of aluminum alloy D16T with artificially damaged polyurethane coating inhibited by zinc phosphate/zeolite pigments blend is close to the resistance of aluminum alloy samples with chromate containing polyurethane coatings. This testifies about significant anticorrosion effect from addition of the phosphate/zeolite pigment composition to polyurethane coating and confirms the possibility of chromate substitution in the primer paint layer.

Corrosion fatigue and impedance study of samples of aluminum alloy with polyurethane coatings has showed that the presence of chromate inhibitor slows down degradation of polyurethane coating under cyclic loading in acid rain solution and increases its protective properties. Impedance module of inhibited coating over the entire range of frequencies was greater by 5-8 times compared with uninhibited samples after 24 hours of cyclic load.

Polarization characteristics of the alloy D16T in acid rain solution with added natural zeolite and mixtures of zinc phosphate/calcium modified zeolite and zinc phosphate/zinc modified zeolites were studied. It was established that largest inhibiting effect has the pigment blend containing phosphate and Ca-ion exchanged zeolite.

It was established that addition of phosphate/Ca-zeolite pigment blend improves protective properties of polyurethane coatings at conditions of cyclic loading by inhibition of under paint corrosion of aluminum alloy.

Alloy samples with chromate containing polyurethane coatings had corrosion endurance under cyclic stress level of 150 MPa in about 7.5 times greater than unprotected samples. Polyurethane coating inhibited by phosphate/Ca-zeolite mixture increased endurance of the alloy for the stress level approximately in 7.0 times.

REFERENCES

1. V.S.Syniavski, V.D.Valkov, V.D.Kalinin. Corrosion and Protection of Aluminium Alloys. Moscow, Metallurgia Publisher, 1986.

2. Z.Szklarska-Smialowska. Pitting Corrosion of Aluminum. Corrosion Science, 41 (1999) 1743.

3. G.S. Chen, M. Gao, R.P. Wei, Microconstituent-Induced Pitting Corrosion in Aluminum Alloy Alloy 2024-T3. Corrosion, 52 (1996) - p. 8-15.

4. R.P. Wei, C.M. Liao, M. Gao, A Transmission Electron Microscopy Study of Constituent-Particle-Induced Corrosion in 7075-T6 and 2024-T3 Aluminum Alloys // Metall. Mater. Trans. A, 29A (1998) 1153-1160.

5. Pourbaix, M. Atlas of Electrochemical Equilibria in Aqueous Solutions, NACE Cebelcor, Huston, 1974.

6. Shimizu, K.; Furneaux, R. C.; Thompson, G. E.; Wood, G. C.; Gotoh, A. and Kobayashi, K., On The Nature of "Easy Paths" for The Diffusion of Oxygen in Thermal Oxide Films on Aluminium, Oxidation of Aluminium, 35 (5/6):427-439, 1991.

7. Davis, J. R. et. al, editor, Metals Handbook, Volume 13, pages 104-122 and 583-609. Ninth edition, ASM International, Ohio, 1987.

8. Nisancioglu, K., Corrosion of Aluminium Alloys. Proceedings of ICAA3, volume 3, pages 239-259. Trondheim, 1992. NTH and SINTEF.

9. Scamans, G. M.; Hunter, J. A.; Holroyd, N. J. H.. Corrosion of Aluminum - a New Approach, Proceedings of 8th International Light Metals Congress, pages 699-705. Leoben-Wien, 1987.

10. Hatch, J. E., editor. Aluminium - Properties and Physical Metallurgy, pages 242-264. ASM, Ohio, 1984.

11. Gaute Svenningsen. Corrosion of Aluminium Alloys. The NorLight conference, January 27-28th, Trondheim, 2003. Poster N 9. - www.sintef.no/static/mt/norlight/ seminars/ norlight2003/ Postere/ Gaute%20Svenningsen.pdf.

and

Gaute Svenningsen. Intergranular Corrosion of AA6000-Series Aluminium Alloys. Doctoral thesis, Norwegian University of Science and Technology, April 2005.

12. Golubev A.I.. Corrosion Processes on Real Microelements. Moscow: State Publishing House "Oborongyz", 1963 (in Russian)

13. Q.Y. Wang, N. Kawagoishi, Q. Chen. Effect of Pitting Corrosion on Very High Cycle Fatigue Behavior. Scripta Materialia 49 (2003) 711–716.

14. C. G. Schmidt, J. E. Crocker, J. H. Giovanola, C. H. Kanazawa, D. A. Shockey. Characterization of Early Stages of Corrosion Fatigue in Aircraft Skin. SRI International Report # DOT/FAA/AR-95/108. February 1996. - www.tc.faa.gov/its/worldpac/techrpt/ar99-34.pdf

15. V. S. Sinyavskii. Pitting and Stress Corrosions of Aluminum Alloys; Correlation between

Them. Protection of Metals, Vol. 37, No. 5, 2001, P. 469–478.

16. V. Yu. Vasil'ev, V. S. Shapkin, N. V. Barulenkova, M. V. Antonova, and E. N. Antonova. The Aftereffect of Cyclic Loading on the Corrosion of Aluminum-Based Alloys. Protection of Metals, 2006, Vol. 42, No. 3, P. 209–214.

17. P.S. Pao, S.J. Gill and C.R. Feng. On Fatigue Crack Initiation From Corrosion Pits in 7075-T7351 aluminum alloy. Scripta mater. 43 (2000) 391–396

18. Kimberli Jones and David W. Hoeppner. Prior corrosion and fatigue of 2024-T3 aluminum alloy. Corrosion Science. Volume 48, Issue 10, October 2006, P. 3109-3122.

19. Mechanism of Corrosion and Corrosion Fatigue of 2024-T3 Aluminum Alloy in Hydrochloric Acid Solutions by Kowal, Krzysztof A., Ph.D. Thesis, University of Pennsylvania, 1996, 284 pages

20. Corrosion Fatigue Strength of Drill Pipes from Aluminum Alloys / A.V. Karlashov, A.N. Yarov, K.M. Gylman and others// Moscow: Nadra Publisher, 1977. - 183 p. (in Russian)

21. V.I. Pokhmurskii, M.S. Khoma. Corrosion Fatigue of Metals and Alloys. – Lviv; Spolom Publisher, 2008. – 304 p. (in Ukrainian)

22. Glikman L.A. Corrosion Fatigue Strength of Metals. – Moscow: Mashgyz Publisher, 1955. – 80 p. (in Russian).

23. Constructional Strength of Aerospace Alloys // C.V. Serencen, E.V. Giacintov, V.P. Kogaev, M.N. Stepnov. Moscow: Oborongyz Publisher. 1962. – 101 p. (in Russian)

24. V.V. Gerasymov. Corrosion of Aluminum and Its Alloys. Moscow: Publishing House "Metallurgy", 1967. p. 114. (in Russian).

25. Influence of pH on Cyclic Strength of Aluminum Alloy B95 / Bolshakova H.S., Balezyn S.A., Romanov V.V. // Fiziko-Khimichna Mechamika Materialiv. 1972 № 4. – P. 100-102. (in Russian).

26. Ruiz J., Elices M. The Role of Environmental Exposure in the Fatigue Behaviour of An Aluminium Alloy // International Journal of Fatigue. – 2003. –Vol. 39, № 12. – P. 2117-2141.

27. Ruiz J., Elices M. Environmental Fatigue in a 7000 Series Aluminium Alloy // International Journal of Fatigue – 1996. –Vol. 38, № 10. – P.1815-1837.

28. V.U. Ustiancev, V.S. Siniavski. Dependece of Stress Corrosion of Aluminum Alloys from Chloride Ion Concentration, Environment pH and Temperature // Fiziko-Khimichna Mechamika Materialiv. – 1972. – № 1. – P. 62-66. (in Russian).

29. I.M. Zin, R.L. Howard, S.J. Badger, J.D. Scantlebury, S.B. Lyon. The Mode of Action of Chromate Inhibitor in Epoxy Primer on Galvanized Steel. Progress in Org. Coatings, 33 (1998) 203.

30. J. Vander Kloet, W. Schmidt, A.W. Hassel, M. Stratmann. The Role of Chromate in Filiform Corrosion Inhibition // Electrochimica Acta 48 (2003) 1211 -1222.

31. G.S. Frankel and R.L. McCreery. Inhibition of Al Alloy Corrosion by Chromates. The Electrochemical Society Interface, Winter, 2001. – P. 34-38.

32. R.L.Cook, Jr. and S.R.Taylor. Pigment-Derived Inhibitors for Aluminum Alloy 2024-T3 // Corrosion, 56 (2000) P. 321.

33. Santi Chrisanti. The Application of Ion-Exchenged Clay as Corrosion Inhibiting Pigments in Organic Coatings. Dissertation Presented in Partial Fulfillment of the Requirements for the Degree Doctor of Philosophy in the Graduate School of The Ohio State University. 2008. 251 p.

34. M. J. Loveridge, H. N. McMurray and D. A. Worsley. Chrome Free Pigments for Corrosion Protection in Coil Coated Galvanised Steels // Corrosion Engineering, Science and Technology 2006 VOL 41 NO 3. - P. 240-248.

35. Geraint Williams and H. Neil McMurray. Anion-Exchange Inhibition of Filiform Corrosion on Organic Coated AA2024-T3 Aluminum Alloy by Hydrotalcite-Like Pigments // Electrochemical and Solid-State Letters, 6 (3) B9-B11 (2003).

36. Fletcher, T. Ion-exchange Pigments for Anti-Corrosion Coatings. European Coatings J. Volume 9, 1991, Pages 553-558+561.

37. M. Kendig, M. Cunningham, S. Jeanjaquet, and D. Hardwick. Role of Corrosion Inhibiting Pigments on the Electrochemical Kinetics of a Copper-Containing Aluminum Alloy // J. Electrochem. Soc., Vol: 144, No. 11, November 1997. – P. 3721 – 3727.

38. Atwood, S.C.J.. Corrosion and Coatings. JOCCA, 75, (4) 1992, P. 128-134.

39. Wheat N. Protection Since The Lost Ark. A Review of Primers and Barrier Coatings for Steelwork. Protective Coatings Europe, 3, (6), 1998, P. 24-30.

40. Barraclough, J. and Harrison, J.B. New Leadless Anti-Corrosive Pigments. JOCCA, 48, 1965, P. 341-355.

41. Mayne, J.E.O. New Leadless Anti-Corrosion Pigments. Discussion. JOCCA, 48, 1965, P. 352-356.

42. Goldie, B.P.F. and Othen, D.G. Corrosion Control by Surface Coatings; the Use of Chemical Inhibitors. In: Chemical Inhibitors for Corrosion Control, Ed. B.G.Clubley, Roual Society of Chemistry, Athenaeum Press Ltd., Newcastle-u-Tyne, 1990, P. 121-133.

43. Romagnoli,R. and Vetere,V.F. Heterogeneous Reaction Between Steel and Zinc Phosphate. Corrosion, 51, (2), 1995, P. 116-123.

44. Burkill, J.A. and Mayne, J.E.O. The Limitations of Zinc Phosphate as An Inhibitive Pigment. JOCCA, 71, (9), 1988, P. 273-275,285.

45. Clay, H.F. and Cox, J.H. Chromate and Phosphate Pigments in Anti-Corrosive Primers. JOCCA, 56, 1973, P. 13-16.

46. Amirudin, A., Barreau,C., Hellouin, R. and Thierry,D. Evaluation of Anti-Corrosive Pigments by Pigment Extract Studies, atmospheric Exposure and Electrochemical Impedance Spectroscopy. Progress in Organic coatings, 25, 1995, P. 339-355.

47. Morcillo, M. and Mateo, M.P. Behavior of Anticorrosive Paints Formulated with Non Toxic Pigments. European Coatins Journal, (4), 1988, P. 270-282.

48. Electrochemical and XPS Study of Corrosion Inhibition in Al-Cu Alloy with Anti-Corrosion Pigments // S.B. Lyon, I.M. Zin, J. Walton, V.I. Pokhmurskii, M.B. Ratushna, Yu.I. Kuznetsov, E. Kalman, M.D. Sakhnenko. EUROCORR 2007, Freiburg, Germany, Proceedings Paper N-1404, September 9-13 (2007).

49. F.G. Hamel, J. Blain, J. Masounave. The Effect of a Polymeric Coating on the Corrosion-Fatigue of a Suction Roll Alloy // Canadian Metallurgical Quarterly, 29 (1) (1990) 81.

50. T.N. Kalichak, V.I.Pokhmurskii. Influence of Galvanic and Organic Coatings on Fatigue Life of Martensitic Stainless Steel // Fizyko-Ximichna Mechanica Materialiv (translated into English as Soviet Materials Science, 8 (1972) 394.
(in Russian)

51. M.K. Khani and D. Dengel. Improvement of The Corrosion Fatigue Behavior of Steels by Paint Coating. Materials and Corrosion-Werkstoffe und Korrosion, 48(7) (1997) 414-419.

52. The Effect of Inhibiting Pigments on Corrosion and Environmentally Assisted Cracking of Mild Steel / V.I.Pokhmurskii, I.M.Zin, L.M.Bily, M.B.Ratushna // Proceedings of Intern. conf. SCIENCE & ECONOMY New challenges “Corrosion-2005”. Vol. III – Warsawa, Poland. – 8-10 June 2005. - Inzyneria powierzchni (Surface Engineering). — 2A’.- 2005. – P.177-181.

53. Corrosion of Aluminum and Aluminum Alloys. Ed. J.R. Davis. ASM Internatioanal. 1999.

54. US Patent 4,327,152. R.N. Miller, R.L. Smith. Protective Coating to Retard Crack Growth in Aluminium Alloy. Apr. 27, 1982.

55. Protection of Aluminium Alloys Against Corrosion Fatigue Cracking, Erosion Corrosion and Microbiologicall-Induced Corrosion. W.J. van Ooij, A. Seth, T. Mugada and others // NorLight

Conference, 17 October, 2006. www.sintef.no/static/mt/norlight/ICEPAM/06-van-Ooij_Cincinnati.pdf

56. US patent 7482421. Wim Van Ooij, Anuj Seth, Matthew B. Stacy, Superprimer. 01.27.2009.]

57. X.F. Liu, S.J. Huang, H.C. Gu. The Effect of Corrosion Inhibiting Pigments on Environmentally Assisted Cracking of High Strength Aluminum Alloy// Corrosion Science 45 (2003) – P. 1921–1938.

58. X.F. Liu, S.J. Huang, H.C. Gu. Crack Growth Behaviour of High Strength Aluminium Alloy in 3.5%NaCl Solution with Corrosion Inhibiting Pigments. International Journal of Fatigue 24 (2002) 803–809.

59. J.S. Warner, S. Kim, R.P. Gangloff. Molybdate Inhibition of Environmental Fatigue Crack Propagation in Al–Zn–Mg–Cu. International Journal of Fatigue. (2009). – in Press.

60. B. Davo, A. Conde, J.J. de Damborenea. Inhibition of Stress Corrosion Cracking of Alloy AA8090 T-8171 by Addition of Rare Earth Salts // Corrosion Science 47 (2005) - P. 1227–1237.

61. GOST 4784-97. Aluminum and alloys deformed. Brands. Moscow: Standard Publisher. 2001. p. 12.

62. S.J.Haneef, C.Dickinson, J.B.Johnson, G.E.Thompson, G.C.Wood, Effects of Air Pollution on Historic Buildings and Monuments and the Scientific Basis for Conservation: Environmental Test Box Studies, European Cultural Heritage Newsletter on Research N2 (1988) 13–21.

63. G.O. Ilevbare, J.R. Scully, J. Yuan, and R.G. Kelly. Inhibition of Pitting Corrosion on Aluminum Alloy 2024-T3: Effect of Soluble Chromate Additions vs Chromate Conversion Coating. Corrosion. 2000. - Vol. 56, No. 3. - P. 227 – 242

64. AFOSR Multidisciplinary University Research Initiative. Mechanism of Al Alloy Corrosion and the Role of Chromate Inhibitors. Air Force Office of Scientific Research. Contract No. F49620-96-1-0479. Final Report. December 1, 2001. http://www.mse.eng.ohio-state.edu/~bruedigam/MURIreport.pdf

65. M. Kabasakaloglu, H. Aydin and M.L. Aksu. Inhibitors for protection of aerospace aluminum alloy. Materials and Corrosion. – 1997. – V.48. - P. 744-754.

66. V.I. Pokhmurskii, M.S. Khoma. Corrosion Fatigue of Metals and Alloys. – Lviv; Spolom Publisher, 2008. – 304 p. (in Ukrainian)

67. Kerner Z. and Pajkosy T. Impedance of rough capacitive electrodes: the role of surface disorder // Journal oj Electroanalytical Chemistry. – 1998. – 448.- P.139-142.

68 8. Burkill J.A. and Mayne J.E.O. The limitations of zinc phosphate as an inhibitive pigment

// JOCCA. – 1988. – **71**, N9. – P. 273-275,285.

69 9. Clay H.F. and Cox J.H. Chromate and phosphate pigments in anti-corrosive primers // JOCCA. – 1973. - **56. –** P. 13-16.

70. J.Quitmeyer. Grasping the phosphate coating process // www.metalfinishing.com – September, 2006. – P.47-50

71. R.B. Waterhousea. The formation, structure, and wear properties of certain non-metallic coatings on metals. Wear. Volume 8, Issue 6, November-December 1965, Pages 421-447.

72 . F.W.Eppensteir, M.R.Jenkins, Chromate Conversion Coatings, Metal Finishing 105 (N10) (2007) 413–424.

73. S.Chrisanti. The application of ion-exchanged caly as corrosion inhibiting pigments in organic coatings. Dissertation in partial fulfillment of the requirements for the degree Doctor of Phylosophy. The Ohio State University. 2008.

74. Sibel Tunali Akar, Tamer Akar, Zerrin Kaynak, Burcu Anilan, Ahmet Cabuk, Ozge Tabak, Temir A. Demir, Tefik Gedikbey. Removal of copper(II) ions from synthetic solution and real wastewater by the combined action of dried Trametes versicolor cells and montmorillonite // Hydrometallurgy 97 (2009) 98–104.

75. E. Eren, B. Afsin. An investigation of Cu(II) adsorption by raw and acid-activated bentonite: A combined potentiometric, thermodynamic,XRD, IR, DTA study / Journal of Hazardous Materials 151 (2008) 682–691.

76. Erdal Eren. Removal of copper ions by modified Unye clay, Turkey // Journal of Hazardous Materials 159 (2008) 235–244.

77. Noemi M. Nagy, Jozsef Konya, Zita Urbin. The competitive exchange of hydrogen and cobalt ions on calcium-montmorillonite // Colloids and Surfaces. A: Physicochemical and Engineering Aspects 121 (1997) 117-124.

78. Sorina-Alexandra Garea, Horia Iovu. New epoxy coating systems which contain multipurpose additives based on organophilic montmorillonite // Progress in Organic Coatings 56 (2006) 319–326.

79. Del Amo. B, Deyá, C, Zalba, P. Zeolitic Rock as a New Pigment for Ceiling Paints. Influence of the Pigment Volume Concentration. Micropor. Mesopor. Mater., 84 353 (2005)

80. Columbia Pineda, R, Rodriguez Fuentes, G, Victorero Rodriguez, A, Prieto Valdés, JJ. Utilizaciyn de zeolitas modificadas en la obtención de recubrimientos de zeosil. "Zeolitas'91", Memorias de la 3^{o} Conferencia Internacional sobre Ocurrencia, Propiedades y Usos de las Zeolitas naturales, p. 21, La Habana, 9-12 de abril de (1991).

81. Cowan. MM, Abshire, KZ, Houk, SL, Evans, SM, "Antimicrobial Efficacy of a Silver-Zeolite Matrix Coatings on Stainless Steel". Ind. Microbiol. Biotechnol, 30 102 (2003).

82. I. M. Zin', S. B. Lyon, L. M. Bilyi and M. B. Tymus'. Specific features of the corrosion inhibition of an aluminum alloy by a nonchromate pigment mixture. Materials Science. – 2008. - V. 44, N 5.- P. 638-645.

83. Potentiodynamic electrochemical impedance spectroscopy. G. A. Ragoisha and A. S. Bondarenko. Electrochim. Acta. 50 (2005) 1553-1563.

84. B.A. Boukamp, 'Computer assisted analysis of impedance data of electrochemical systems', Proc. of 9th European Congress on Corrosion, (Jaarbeurs Congress Centre / Nederlands Corrosion centre, Utrecht, 1989) FU252.

85**.** Boukamp, B.A. Equivalent Circuit. Version 3.97, Faculty of Chemical Technology, University of Twente, May 1989.

86. I.M. Zin, S.B. Lyon, V.I. Pokhmurskii. Corrosion Science 45 (2003) 777–788.

List of Symbols, Abbreviations, and Acronyms

E_{ocp} or OCP – open circuit potential, mV

$\pm\sigma$ – cyclic stress, MPa

σ_{-1} – fatigue limit, MPa

σ_{-1c} – corrosion fatigue limit, MPa

i – corrosion current, mA/cm^2

E_{pol} – polarization potential, mV

I_{pol} – polarization current, mA

D16T –brand of commercial aluminum alloy

A7075 - brand of commercial aluminum alloy

EIS − electrochemical impedance spectroscopy

AE − a platinum auxiliary electrode

RE − reference electrode

R_e − solution resistance, Ohms

Q_{dl} − constant phase element

R_{ct} − charge transfer resistance, Ohms

Z − impedance, Ohms